

NASA CR 181684

# NASA Contractor Report 181684

NASA-CR-181684  
19880016057

## A LOW SPEED WIND TUNNEL INVESTIGATION OF REYNOLDS NUMBER EFFECTS ON A 60-DEG. SWEPT WING CONFIGURATION WITH LEADING AND TRAILING EDGE FLAPS

Dhanvada M. Rao and Keith D. Hoffer

Vigyan Research Associates, Inc.  
Hampton, Virginia

FOR REFERENCE

NOT TO BE TAKEN FROM THIS ROOM

Contract NAS1-17919  
August 1988

LIBRARY COPY

AUG 5 1988

LANGLEY RESEARCH CENTER  
LIBRARY NASA  
HAMPTON, VIRGINIA



National Aeronautics and  
Space Administration

Langley Research Center  
Hampton, Virginia 23665



NF00901

**A LOW SPEED WIND TUNNEL INVESTIGATION  
OF REYNOLDS NUMBER EFFECTS ON A 60-DEG.  
SWEPT WING CONFIGURATION WITH LEADING  
AND TRAILING EDGE FLAPS**

**Dhanvada M. Rao and Keith D. Hoffer  
Vigyan Research Associates, Inc.  
Hampton, Virginia**

**ABSTRACT**

A low-speed wind tunnel test was performed to investigate Reynolds number effects on the aerodynamic characteristics of a supersonic cruise wing concept model with a 60 deg. swept wing incorporating leading-edge and trailing edge flap deflections. The Reynolds number ranged from  $0.3 \times 10^6$  to  $1.6 \times 10^6$ , and corresponding Mach numbers from .05 to 0.3 . The objective was to define a threshold Reynolds number above which the flap aerodynamics basically remained unchanged, and also to generate a data base useful for validating theoretical predictions of the Reynolds number effects on flap performance. This report documents the test procedures used and the basic data acquired in the investigation.

## Introduction

The application of leading and trailing edge flaps to enhance subsonic maneuverability of supersonic cruise fighter concepts has attracted considerable interest in recent years. Recent NASA Langley experimental and theoretical evaluations of the flap benefits on cranked and delta-type planforms have indicated substantial performance gains (refs. 1 and 2). Future fighter designs most likely will exploit flap technology in order to maximize subsonic maneuverability without compromising supersonic efficiency.

The considerable existing data base of flap characteristics is derived mainly from two-dimensional studies, and also is primarily applicable to relatively thick wing sections with appreciable leading-edge radius which promote attached flow. For thin, highly swept wings representative of supersonic cruise fighters, fully attached flow is not a realistic goal. During this decade, significant research efforts have led to a new approach towards leading edge flap design for wings which can experience significant three-dimensional flow separation by applying vortex flow management concepts (ref. 3). In the "vortex flap" approach, leading edge separation at maneuvering lift coefficients is controlled by means of a suitably configured flap so that the separation is confined as far as possible to the flap itself. Although a fully attached flow is not possible under these conditions, performance levels corresponding to attached flow can be approached because the vortex-induced suction pressures acting on the entire flap surface create a thrust force which largely compensates for the loss of attached-flow suction near the wing leading edge. Because flow separation can be expected to increase at lift coefficients on either side of design conditions, this type of flap encounters a wide spectrum of attached, separated and mixed flows and therefore is likely to exhibit rather different Reynolds number effects from those of conventional flaps. This is also true for trailing edge flaps operating in the complex three-dimensional flow field of highly swept wings.

The present investigation was undertaken to obtain data on the Reynolds number sensitivity of leading-edge and trailing-edge flaps on a supersonic-cruise wing concept model. Using the test model of reference 1, suitably modified to reduce model weight while preserving its geometry, force and moment tests were performed at various Reynolds numbers. This report documents the test procedures, data obtained, and the main conclusions.

### Symbols and Abbreviations

- b - span (18.4 inches)
- $C_A$  - axial force coefficient, Axial force/qS
- $C_l$  - rolling moment coefficient, Rolling moment/qSb
- $C_N$  - normal force coefficient, Normal force/qS
- $C_n$  - yawing moment coefficient, Yawing moment/qSb
- $C_m$  - pitching moment coefficient, Pitching moment/qS(mac)
- $C_y$  - side force coefficient, Side force/qS
- Mach - test section Mach number
- q - test section dynamic pressure (lbs/ft<sup>2</sup>)
- $Rn_{mac}$  - Reynolds number based on mac
- S - Wing area, 1.0379 ft<sup>2</sup>
- $\alpha$  - angle of attack, (deg)
- LEI - Inboard leading edge flap deflection, deg (positive leading edge down)
- LEO - Outboard leading edge flap deflection, deg (positive leading edge down)
- mac - Mean aerodynamic chord, 0.8150 ft
- TEI - Inboard trailing edge flap deflection, deg (positive trailing edge down)
- TEO - Outboard trailing edge flap deflection, deg (positive trailing edge down)

### Experimental Details and Data Reduction

The test model (fig. 1) represents a supersonic cruise wing concept with a

highly swept delta planform incorporating camber and twist, attached to a generic fuselage (see ref. 1 for a complete geometrical description). The wing was provided with interchangeable segmented leading-edge and trailing-edge flaps allowing various combinations of flap angles to be set. This metal model had previously been tested in the NASA Langley 7 x 10 foot High Speed Tunnel at a minimum mac Reynolds number of 1.6 million corresponding to free-stream Mach 0.3 number and dynamic pressure of 125 psf. The objectives in the present study, conducted in the 7.75 x 11.04 foot Glenn L. Martin Wind Tunnel at the University of Maryland, were to duplicate the NASA Langley test data at identical freestream conditions as a check case followed by tests at reduced mac Reynolds numbers to study the influence on basic flap characteristics. This was done by reducing the flow velocity in the tunnel test section. Variation of Mach number and dynamic pressure versus Reynolds number for the Glenn Martin tunnel are shown in figure 2.

In the present test, the sting-supported model was oriented at a  $90^\circ$  roll angle, and the floor turntable was rotated to vary the angle of attack. The model weight acted perpendicularly to the aerodynamic normal force, posing an unusual constraint in the selection of internal balances which are generally designed to have a normal force capacity several times greater than the side force. To aid in the balance selection process, the model weight was reduced by partial substitution of rigid foam and fiberglass composite parts fabricated in molds taken from the original components. The steel wing and flap parts were retained in order to ensure geometrical fidelity. The substituted components (see figure 1) reduced the model weight by 16 lbs giving a weight of 24 lbs for the current test. Carborundum grit of size #120 was applied to the wing upper surface (as indicated in fig. 1) to fix boundary layer transition as in the NASA Langley test. In view of the small blockage of the model and its support system, no wall corrections were applied.

In consideration of the anticipated loads across the dynamic pressure range

of the Glenn Martin tunnel, and the availability of strain gage balances at NASA Langley, two balances having an identical sting attachment were selected. For test Reynolds numbers of 0.6 million and lower (where the model weight exceeded the normal force) Langley balance #827A was employed with its 'normal force' beams oriented in the vertical plane supporting the model weight; the aerodynamic normal force was thus measured by the more sensitive side force beams. Also, the balance moment center was placed closer to the mean position of the aerodynamic center than in reference 1 in order to keep the model pitching moments within the balance yawing moment limits. The maximum loads and stated accuracies for this balance are shown in table I.

For tunnel test runs at and above Reynolds number  $1.17 \times 10^6$ , Langley balance #2031 was rolled  $90^\circ$  with the model the side-force beams therefore supporting the model weight. The load range and accuracies for this balance are shown in table II.

The  $90^\circ$  roll orientation of the model precluded the use of gravity-referenced instruments (e.g. accelerometers or liquid-level sensors) normally employed to measure the true angle of attack in the presence of support deflection. Therefore, an  $\alpha$ -correction due to aerodynamic load had to be established initially. The model in the tunnel test section was loaded by weight via a pulley arrangement applying forces and moments in the horizontal plane. The angular deflection at the forward tip of the balance was measured via an optical-quality mirror, a transit and a scale. This procedure was repeated for the two separate balances employed for the test.

A tunnel flow-angularity correction to angle of attack was obtained by testing the basic model configuration rolled  $180^\circ$  from the normal test orientation. A photograph of the model set-up in the test section is presented in figure 3. The test matrix is shown in table III. The flap angle designation follows reference 1. The data is listed in tabular form in the Appendix.

A preliminary check of the Glenn Martin test data against NASA Langley 7 x 10 foot tunnel data at identical free-stream conditions (fig. 4) indicated a consistent deviation, which was particularly noticeable in the cases with the trailing-edge flaps deflected. The suspected cause was a shift in angle of attack due to inadequate correction of the Glenn Martin data. An attempt to establish an independent angle of attack correction was made using an analytical model of the support system (fig. 5). To the angular deflection computed from this model was added an end-slope increment due to balance bending (per data furnished by NASA Langley). This alternate correction to the angle of attack improves the comparison with NASA Langley data (fig. 6); however, a residual discrepancy is apparent in the cases with trailing edge flap deflection.

In order to verify that the indicated discrepancy in figure 4 and 6 was due only to suspected erroneous angle-of-attack measurements of the present test, the two data sets are replotted in figure 7 as  $C_A$  versus  $C_N$  thus, removing the angle-of-attack as a variable. Note that the tare corrections applied to balance-axis (body axis) aerodynamic coefficients ( $C_A$ ,  $C_N$  and  $C_m$ ) are independent of angle of attack because of the  $90^\circ$  roll orientation of the model. Agreement between the two data sets for all six cases (fig. 7) therefore validates the accuracy of the balance measurement of this test.

In order to avoid any uncertainties relating to the angle of attack, the Glenn Martin tunnel test data are presented in terms of balance axis coefficients. While aircraft performance estimates require aerodynamic coefficients relative to wind axes, the Reynolds number effects on wing/flap aerodynamics (the primary objective of this study) are as clearly revealed by the balance axis coefficients. Indeed, the chord force ( $C_A$ ) provides a more direct measure of leading-edge flap thrust characteristics than  $C_D$  (ref. 4). Therefore, the lack of  $C_L$  and  $C_D$  in the present data does not detract from the usefulness of the data for the study of Reynolds

number effects and for code verification purposes.

Supplementary oil-flow visualization test were performed on the  $20^\circ/20^\circ/0^\circ/0^\circ$  flap configuration of the model in the Vigyan 3 ft x 4 ft low speed wind tunnel. The object was to observe the viscous flow effects related to leading edge flaps at low Reynolds numbers.

### Results and Discussion

Coefficients of axial force and normal force obtained in the Glenn Martin tests are plotted one against the other in figure 8. Generally, in all the test cases a rapid improvement is indicated in the axial thrust (i.e. a reduction in  $C_A$  for a given normal force) with increasing Reynolds numbers between  $0.3 \times 10^6$  and  $0.6 \times 10^6$ , beyond which the axial versus normal force characteristics remain essentially unchanged indicating the flap effectiveness to be no longer sensitive to Reynolds number. The above trend is also generally true of pitching moment characteristics, as shown in figure 9. With the trailing edge flap also deflected, the Reynolds number effect appears to be somewhat more pronounced; nonetheless, the pitching moment characteristics become essentially independent of Reynolds number above  $1.17 \times 10^6$ .

The variation with Reynolds Number of the axial force characteristics at constant normal force coefficients are shown in Figure 10. These results consistently indicate the leading edge thrust characteristics to become invariant with Reynolds number above  $Rn_{mac} = 0.6 \times 10^6$ .

Selected photographs of oil flow tests performed in the Vigyan tunnel at angles of attack  $6^\circ$  and  $12^\circ$ , and  $q=4$  psf and 20 psf for each  $\alpha$ , are presented in figure 11. The leading-edge flap deflection was set at 20 deg. for both inboard and outboard segments; the trailing-edge flap was undeflected. The junction between the right-hand leading edge flap segments was left unsealed permitting the gap flow



effects to be seen directly in comparison with the sealed left-wing.

The photographs indicate that the flow on the flap itself is predominantly attached while separation occurs along the hinge-line. At  $\alpha = 6^\circ$ , this separation is relatively mild all along the wing span. Increasing Reynolds number tends to shrink the hinge-line separation bubble; also chordwise streaks appear on the wing which are believed to indicate small-scale streamwise vortices embedded in attached flow. At  $\alpha = 12^\circ$  each wing panel is dominated by a large scale vortex which is presumed to represent the rolling up of hinge-line separation. A second co-rotating vortex originates from the unsealed flap junction which tends to push the apex vortex further inboard. Also, the hinge-line separation bubble develops discrete vortex structures.

### Conclusions

A low speed wind tunnel investigation was conducted to determine the effect of Reynolds number variations on the basic aerodynamic characteristics of a  $60^\circ$  swept wing configuration with leading and trailing edge flaps. The Reynolds number ranged from  $0.3 \times 10^6$  to  $1.6 \times 10^6$ . The axial force versus normal force characteristics at a Reynolds number of  $1.6 \times 10^6$  were in good agreement with data obtained at comparable free-stream conditions in the NASA Langley 7 x 10 foot high speed tunnel. These basic aerodynamic characteristics were sensitive to Reynolds numbers in the range  $0.3 \times 10^6$  to  $0.6 \times 10^6$ , above which they were found to be relatively unaffected. In addition to providing a threshold Reynolds number as a guide to reliable sub-scale testing with respect to flap aerodynamics on highly swept wing configurations, the data acquired in this investigation may be useful for validating analytical methods attempting to predict flap Reynolds number effects.

## References

1. Reibe, G. D., and Fox, C. H., Jr. "Subsonic Maneuver Capability of a Supersonic Cruise Fighter Concept", NASA TP 2642, 1987.
2. Campbell, B. A., Hom, K. W. and Huffman, J. K., "Investigation of Subsonic Maneuver Performance of a Supersonic Fighter Cranked Wing", NASA TP 2687, 1987.
3. Rao, D. M., "Leading-Edge 'Vortex Flaps' for Enhanced Subsonic Aerodynamics of Slender Wings", ICAS-80-13.5, 1980.
4. Kuchemann, D.: "The Aerodynamic Design of Aircraft", Pergamon Press, 1978. PP. 63.

TABLE I - NASA Langley Balance #2031 Loads and Accuracies

BALANCE COMPONENT	MAXIMUM LOAD (lbs) or MOMENT (in-lbs)	ACCURACIES (±)					
		LOAD (lbs or in-lbs)	FORCE AND MOMENT COEFFICIENTS AT A GIVEN REYNOLDS NUMBER				
			0.30 MILLION	0.43 MILLION	0.60 MILLION	1.17 MILLION	1.60 MILLION
NORMAL	160	0.80	0.1924	0.0962	0.0481	0.0120	0.0062
AXIAL	30	0.15	0.0361	0.0180	0.0090	0.0023	0.0012
SIDE	50	0.25	0.0601	0.0301	0.0150	0.0038	0.0019
PITCHING MOMENT	300	1.50	0.3812	0.2127	0.1064	0.0266	0.0135
ROLLING MOMENT	30	0.15	0.0381	0.0213	0.0106	0.0027	0.0014
YAWING MOMENT	50	0.25	0.0635	0.0355	0.0177	0.0044	0.0023

TABLE II - NASA Langley Balance #827A Loads and Accuracies

BALANCE COMPONENT	MAXIMUM LOAD (lbs) or MOMENT (in-lbs)	ACCURACIES (▲)					
		LOAD (lbs or in-lbs)	FORCE AND MOMENT COEFFICIENTS AT A GIVEN REYNOLDS NUMBER				
			0.30 MILLION	0.43 MILLION	0.60 MILLION	1.17 MILLION	1.60 MILLION
NORMAL	40	0.200	0.0481	0.0240	0.0120	0.0030	0.0015
AXIAL	7	0.035	0.0084	0.0042	0.0021	0.0005	0.0003
SIDE	20	0.100	0.0240	0.0120	0.0060	0.0015	0.0008
PITCHING MOMENT	80	0.400	0.1017	0.0567	0.0284	0.0071	0.0036
ROLLING MOMENT	15	0.075	0.0191	0.0106	0.0053	0.0013	0.0007
YAWING MOMENT	60	0.300	0.0762	0.0425	0.0213	0.0053	0.0027

TABLE III - Glenn Martin Tunnel Test Matrix Showing Run Numbers

FLAP DEF. (DEG.)				REYNOLDS NUMBER ( x 10 <sup>-6</sup> )				
LEI	LEO	TEI	TEO	0.30	0.43	0.60	1.17	1.60
0	0	0	0	③⑤	③⑥	⑥ ③⑦	⑦ ⑧	⑤
0	0	15	12	③②	③③	③④	⑨	⑩
20	20	0	0	②③ ②⑧ ③⑧	②⑥ ③⑨	②④ ②⑤ ②⑦ ④①	⑬	⑭
20	20	15	12	②⑨	③①	③①	⑪	⑫
15	20	0	0	②①		②②	⑮	⑯
15	20	15	12	②①		⑮	⑰	⑱

NASA Langley → ○ - 827A ; □ - 2031  
balance designation

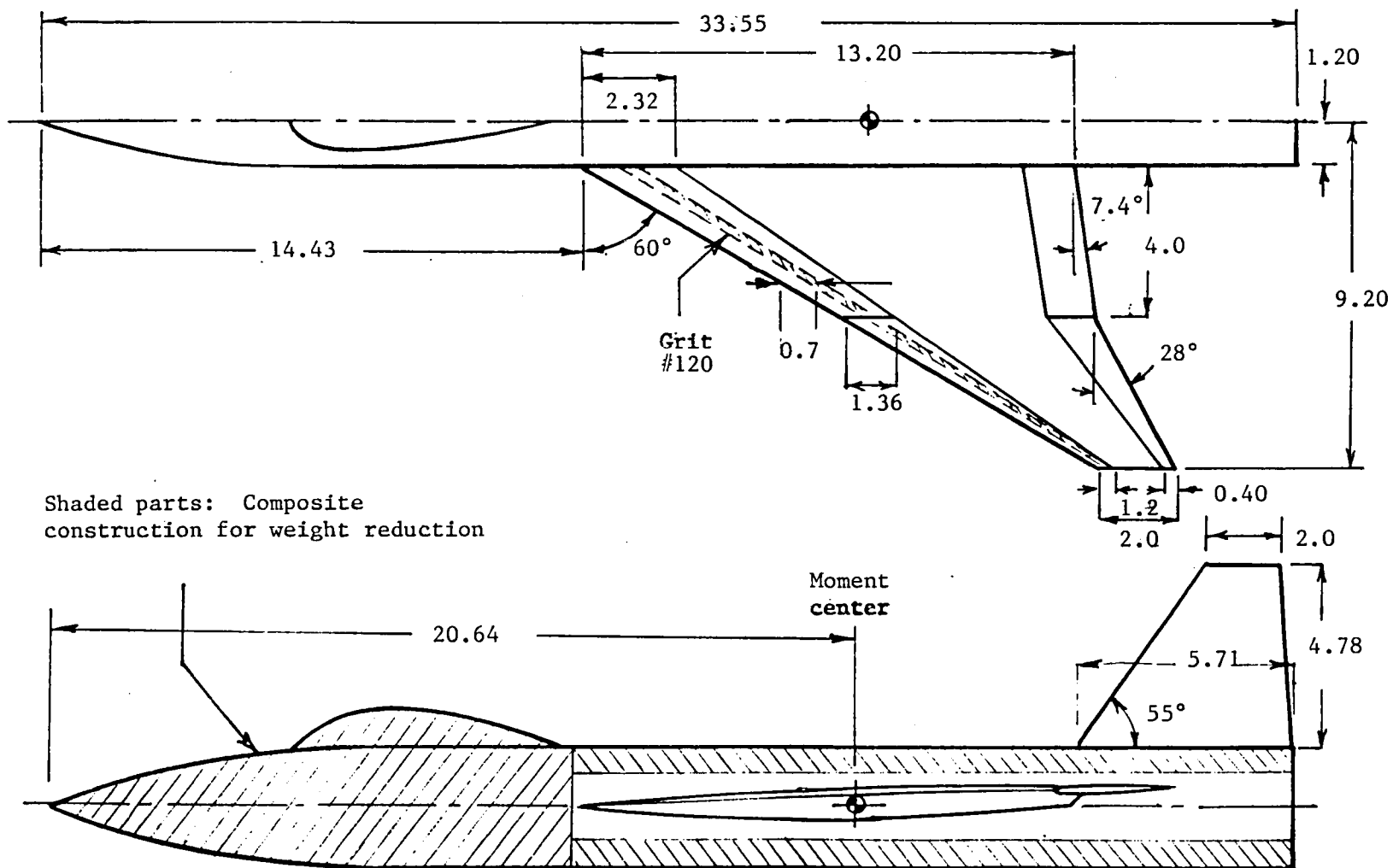


Figure 1. Geometric Description of wind tunnel test model.  
All linear dimensions in inches.

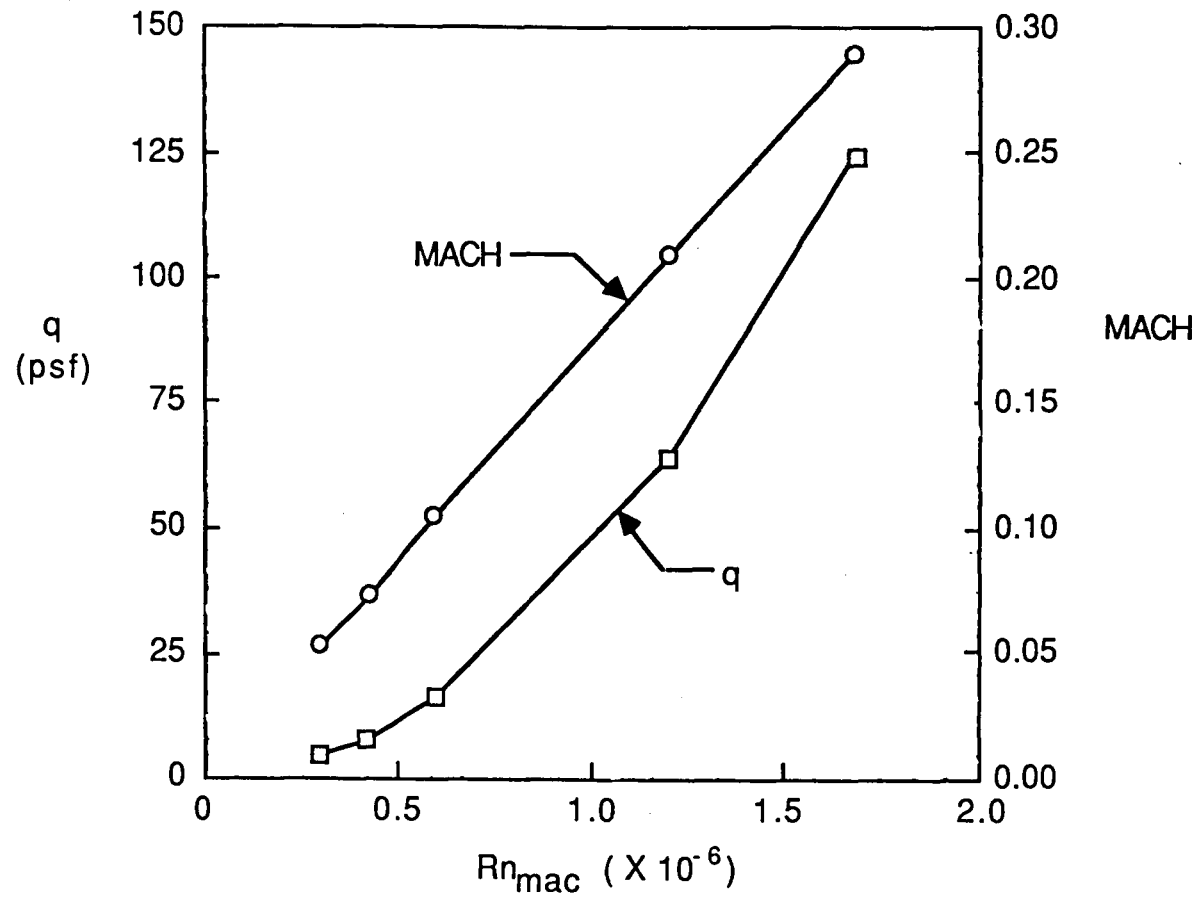


Figure 2. Glenn Martin Wind Tunnel free stream conditions.

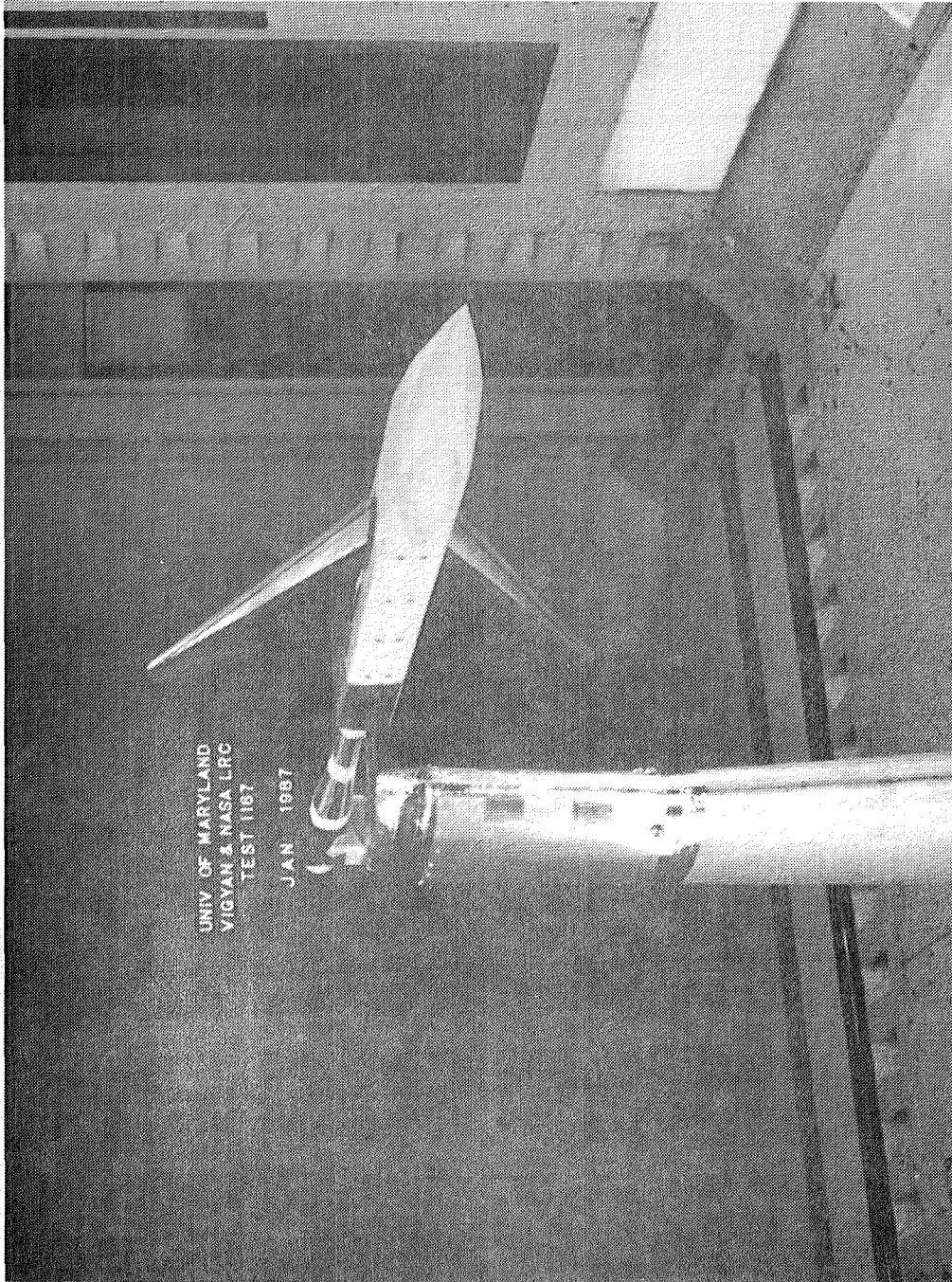
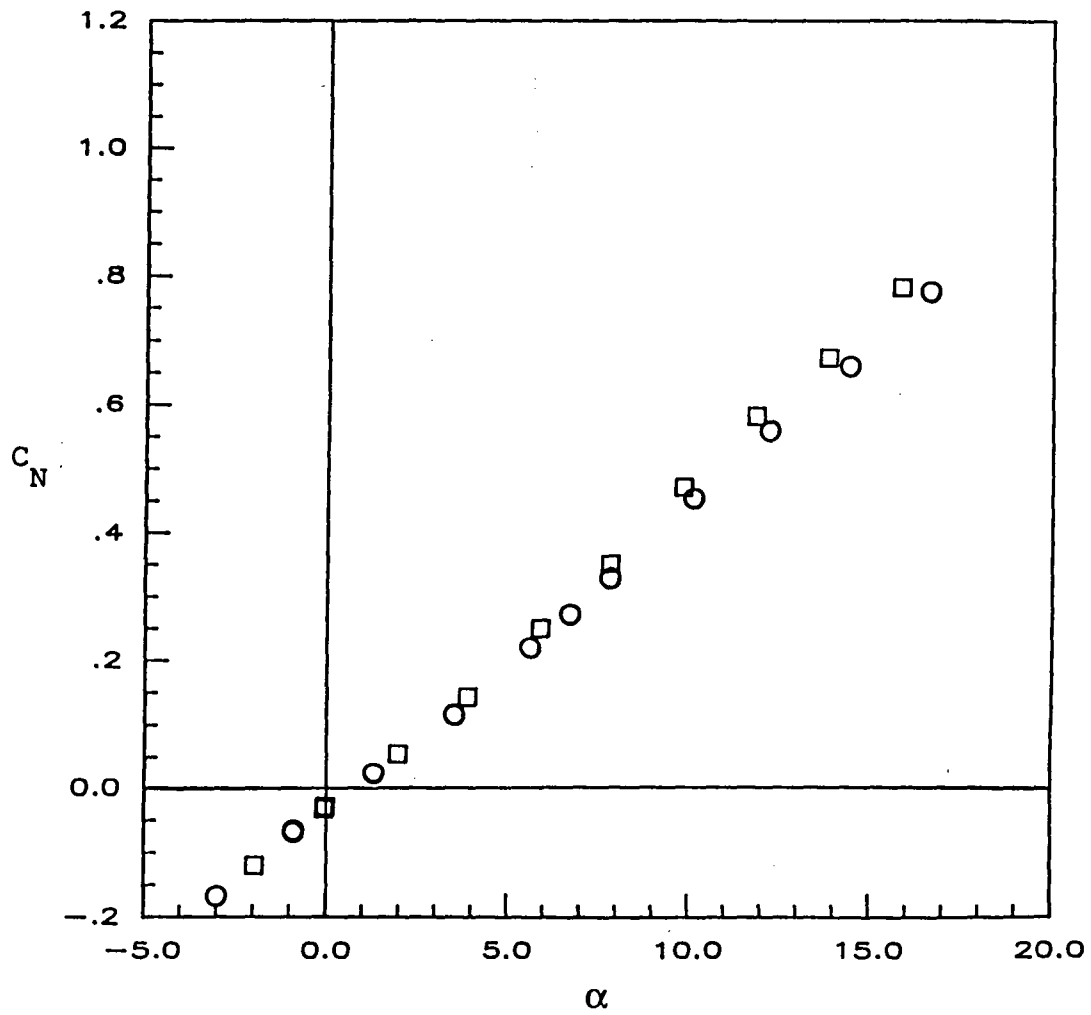


Figure 3. Photograph of Model set up.



FLAP SETTINGS			
LEI	LEO	TEI	TEO
0	0	0	0

WIND TUNNEL	
○	GLENN MARTIN
□	LANGLEY 7 X 10

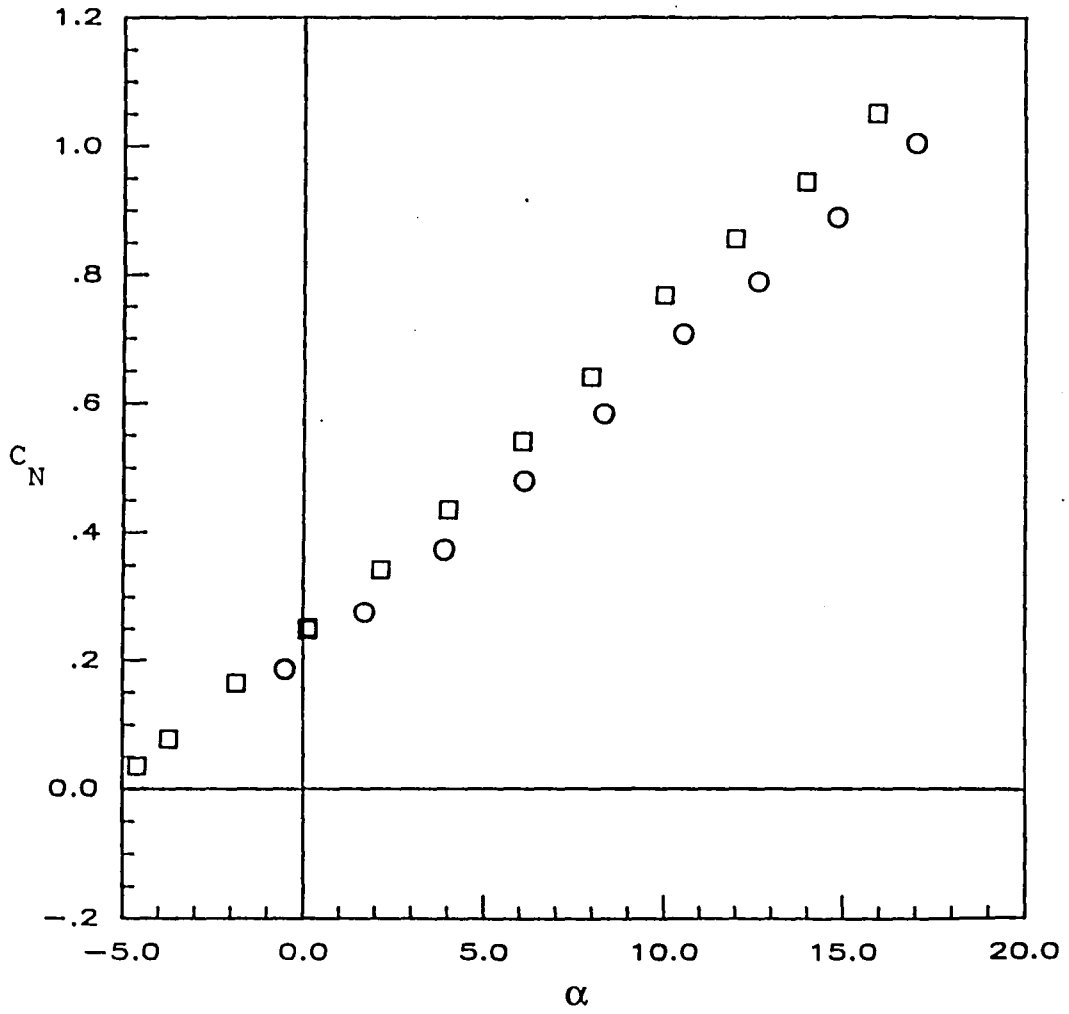


A. Flaps undeflected (basic configuration)

Figure 4. Normal force characteristics compared with NASA Langley data at  $Rn_{mac} = 1.6 \times 10^6$ , angle of attack correction from static loading.

FLAP SETTINGS			
LEI	LEO	TEI	TEO
0	0	15	12

WIND TUNNEL	
○	GLENN MARTIN
□	LANGLEY 7 X 10

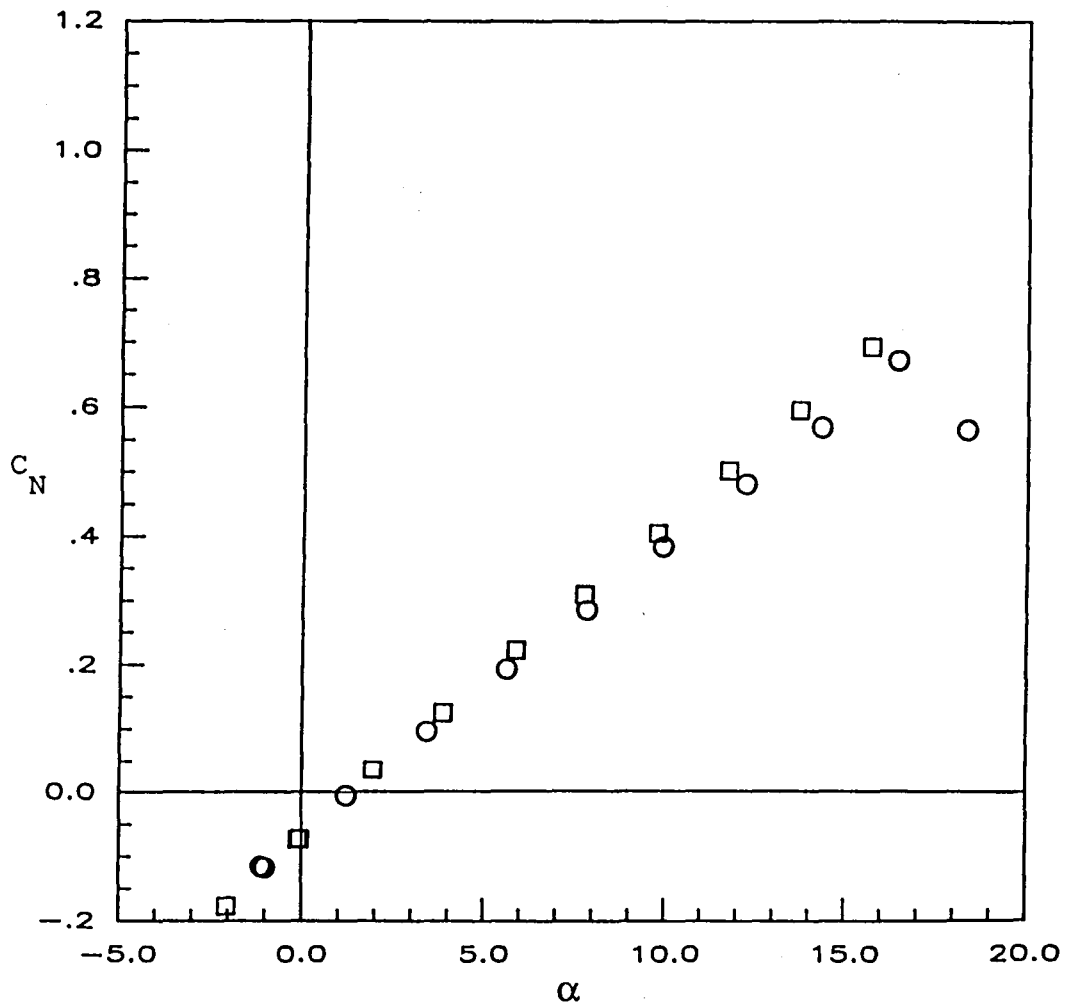


B. Trailing edge flaps only

Figure 4. continued

FLAP SETTINGS			
LEI	LEO	TEI	TEO
15	20	0	0

WIND TUNNEL	
○	GLENN MARTIN
□	LANGLEY 7 X 10

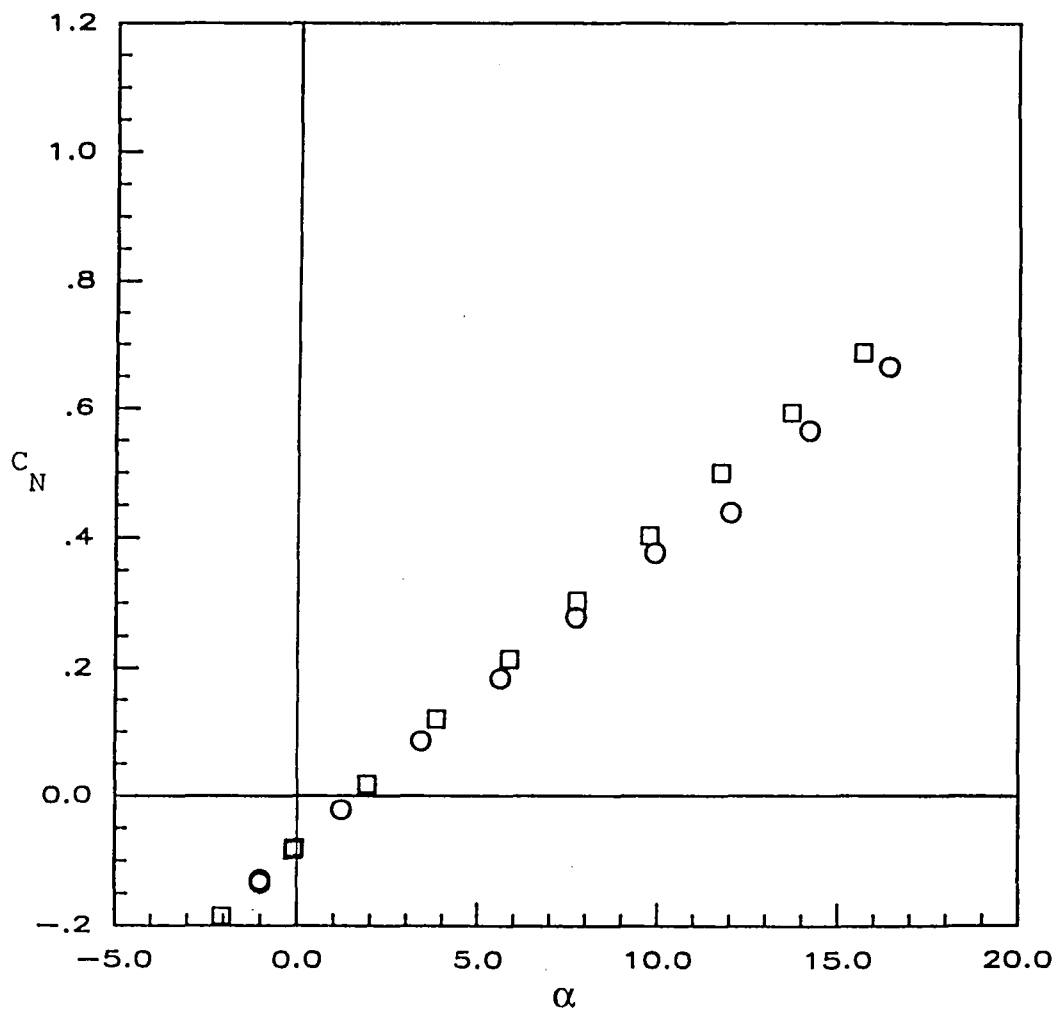


C. Leading edge flaps only

Figure 4. continued

FLAP SETTINGS			
LEI	LEO	TEI	TEO
20	20	0	0

WIND TUNNEL	
○	GLENN MARTIN
□	LANGLEY 7 X 10

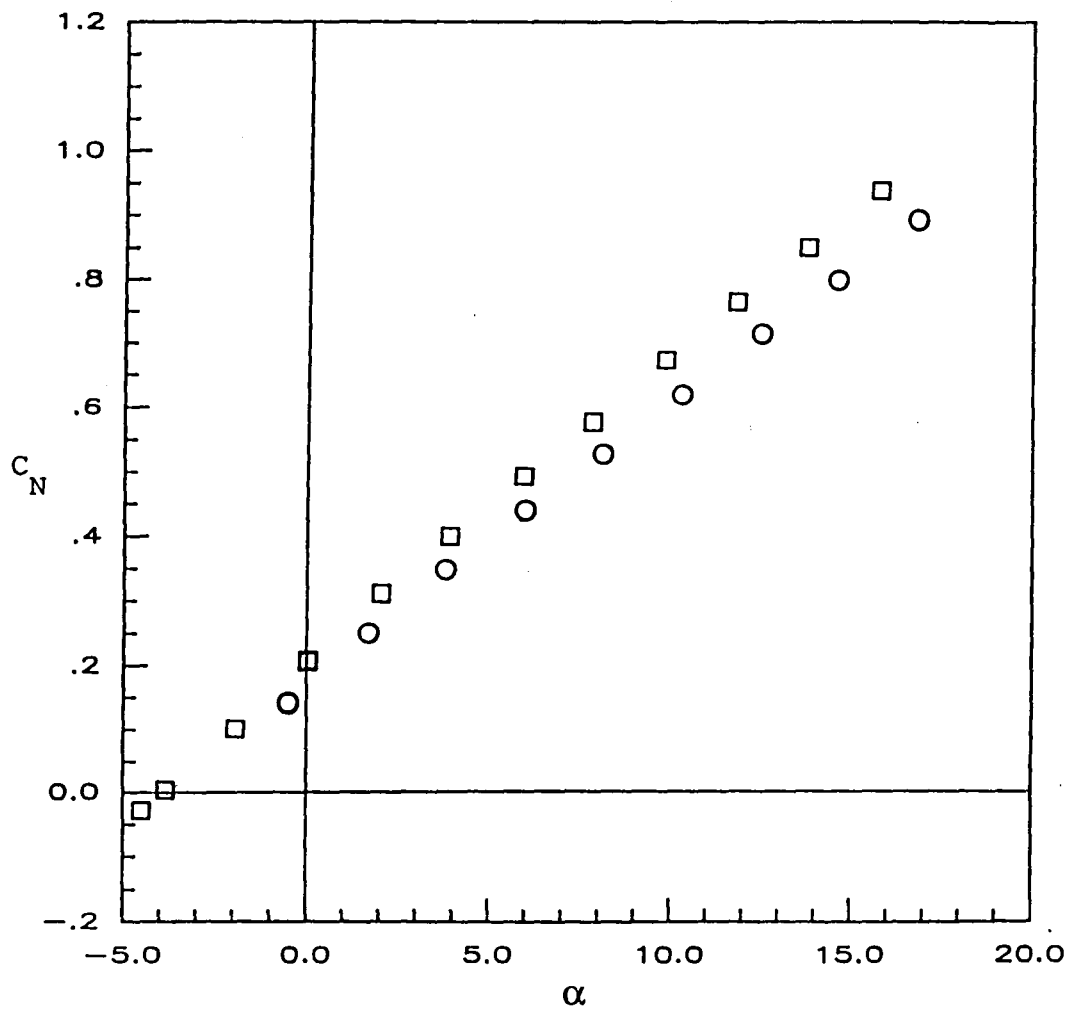


D. Leading edge flaps only

Figure 4. continued

FLAP SETTINGS			
LEI	LEO	TEI	TEO
15	20	15	12

WIND TUNNEL	
○	GLENN MARTIN
□	LANGLEY 7 X 10

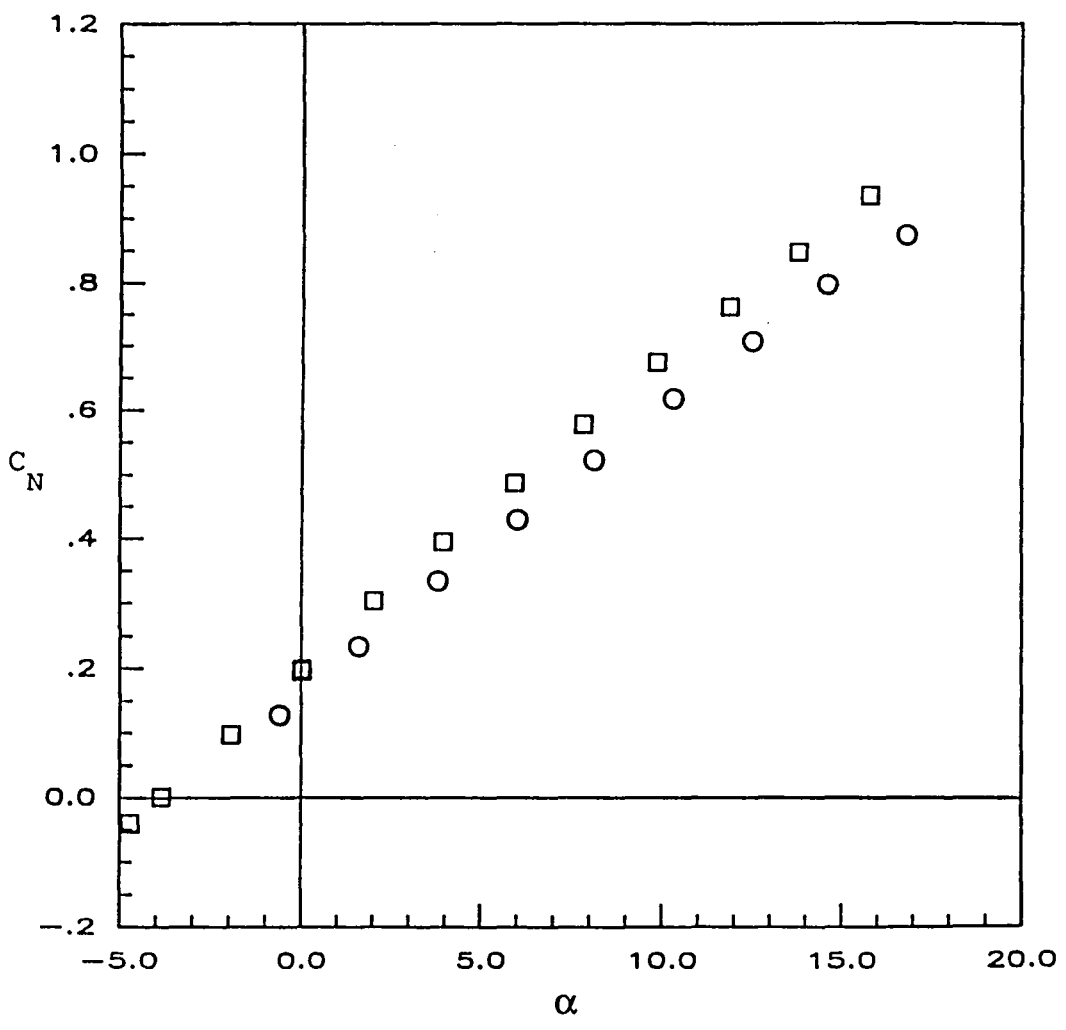


E. All flaps deflected

Figure 4. continued

FLAP SETTINGS			
LEI	LEO	TEI	TEO
20	20	15	12

WIND TUNNEL	
○	GLENN MARTIN
□	LANGLEY 7 X 10



F. All flaps deflected

Figure 4. concluded

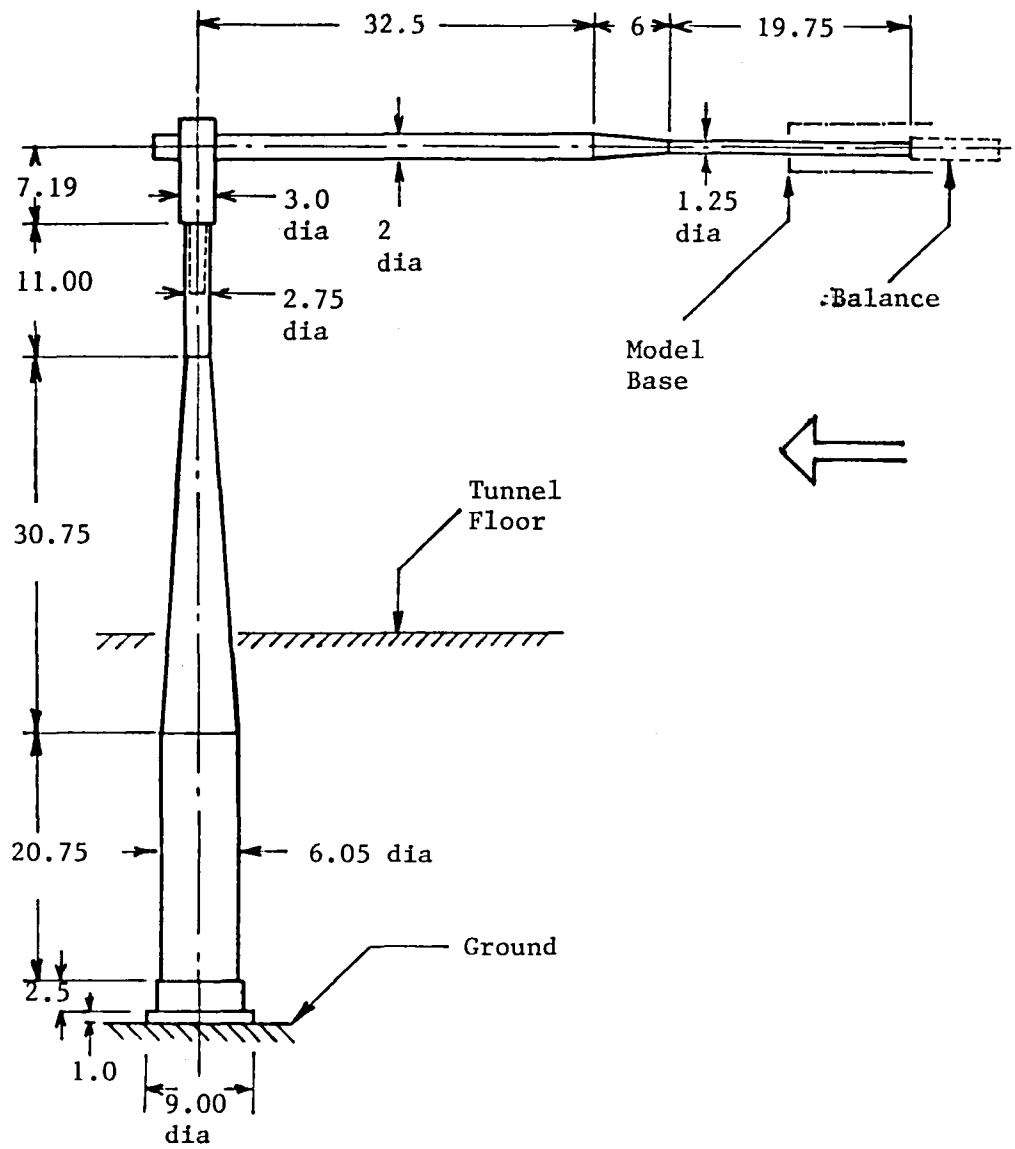
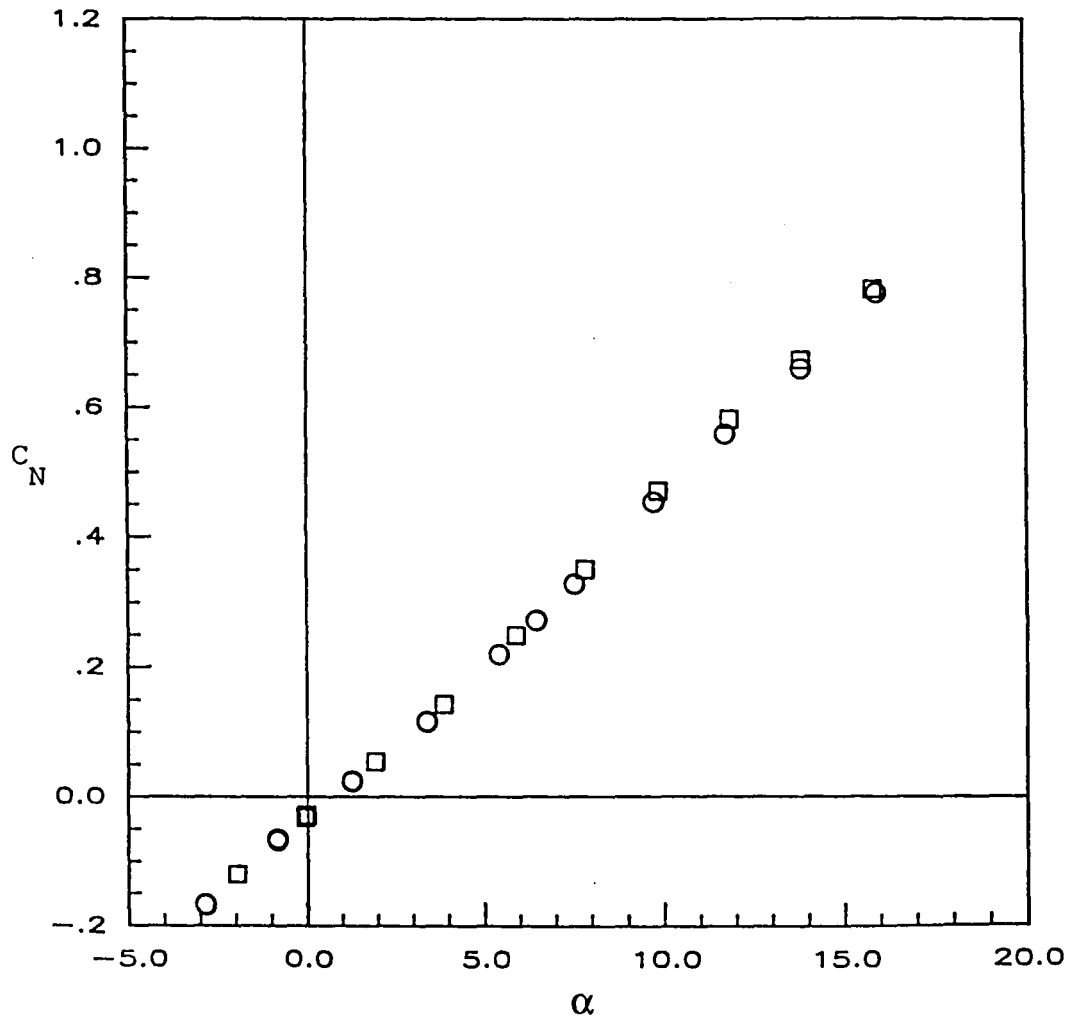


Figure 5. Analytical model used to calculate support system deflection for angle of attack correction. All linear dimensions in inches.

FLAP SETTINGS			
LEI	LEO	TEI	TEO
0	0	0	0

WIND TUNNEL	
○	GLENN MARTIN
□	LANGLEY 7 X 10



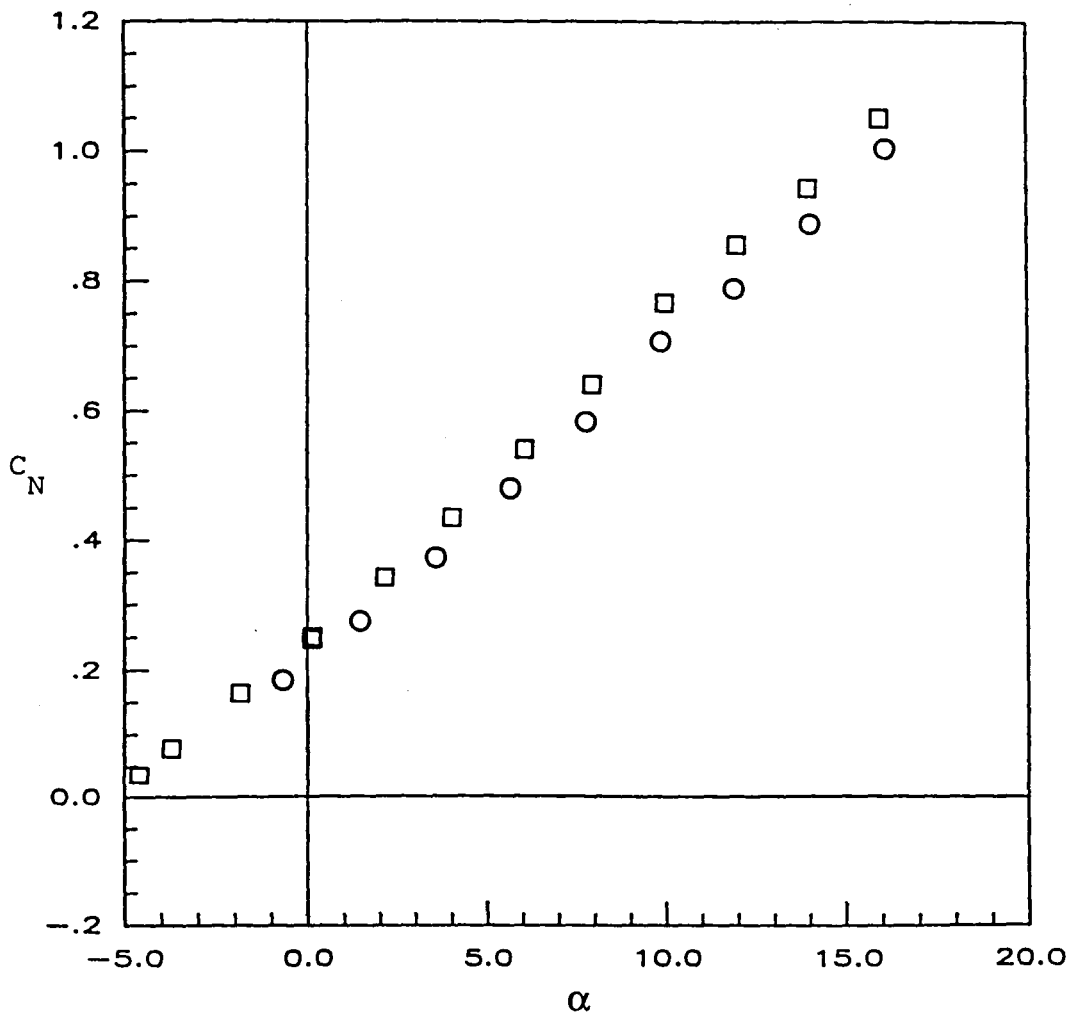
A. Flaps undeflected (basic configuration)

Figure 6. Normal force characteristics compared with NASA Langley data at  $Rn_{mac} = 1.6 \times 10^6$ , angle of attack correction from calculated support deflection



FLAP SETTINGS			
LEI	LEO	TEI	TEO
0	0	15	12

WIND TUNNEL	
○	GLENN MARTIN
□	LANGLEY 7 X 10

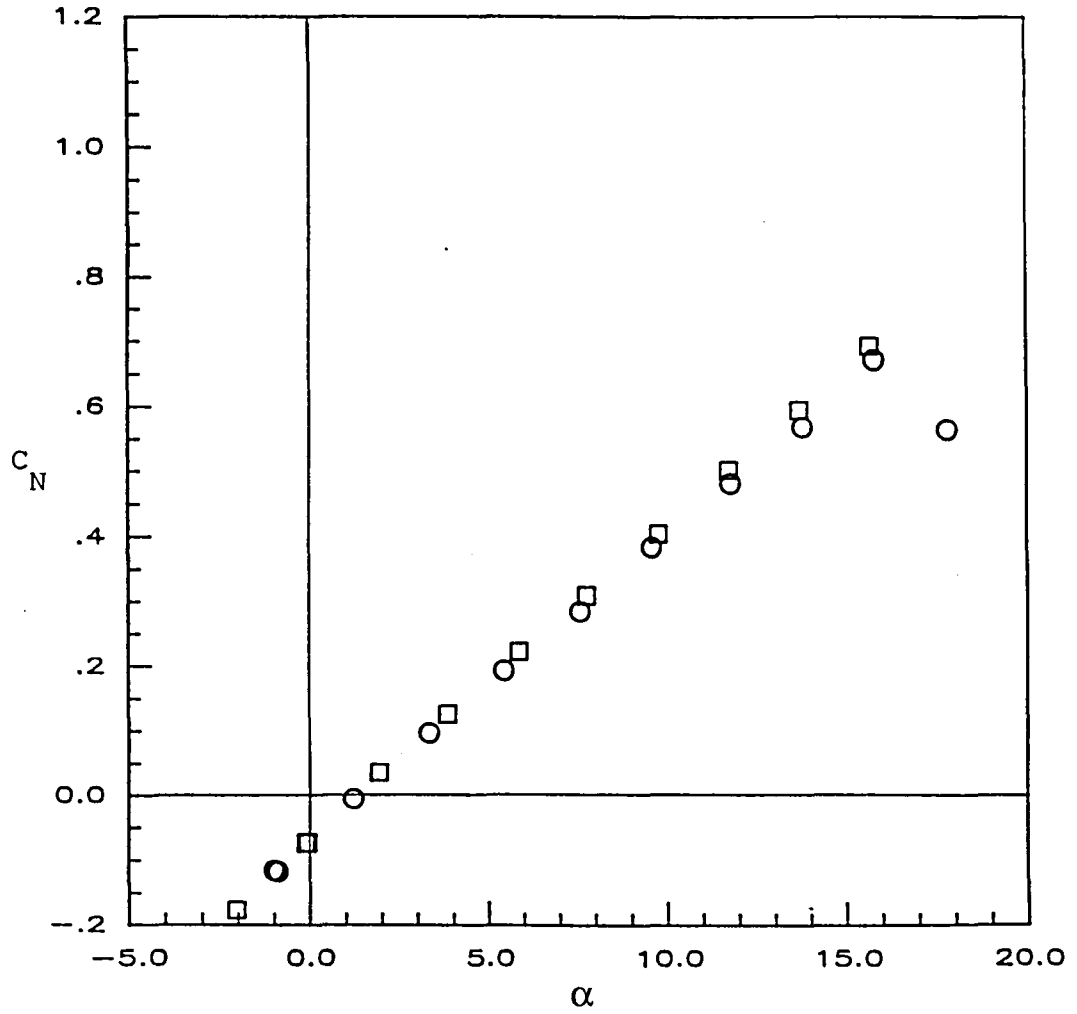


B. Trailing edge flaps only

Figure 6. continued

FLAP SETTINGS			
LEI	LEO	TEI	TEO
15	20	0	0

WIND TUNNEL	
○	GLENN MARTIN
□	LANGLEY 7 X 10

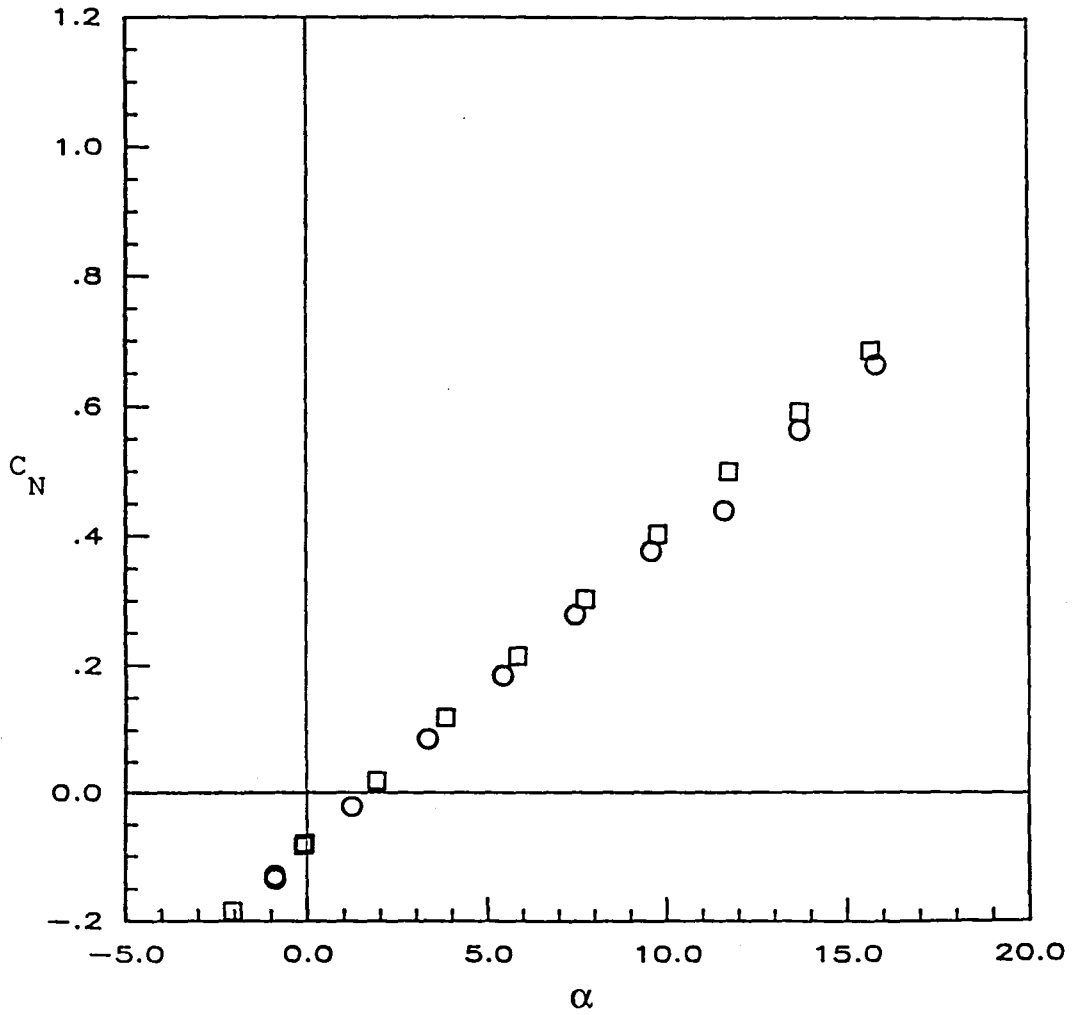


C. Leading edge flap only

Figure 6. continued

FLAP SETTINGS			
LEI	LEO	TEI	TEO
20	20	0	0

WIND TUNNEL	
○	GLENN MARTIN
□	LANGLEY 7 X 10

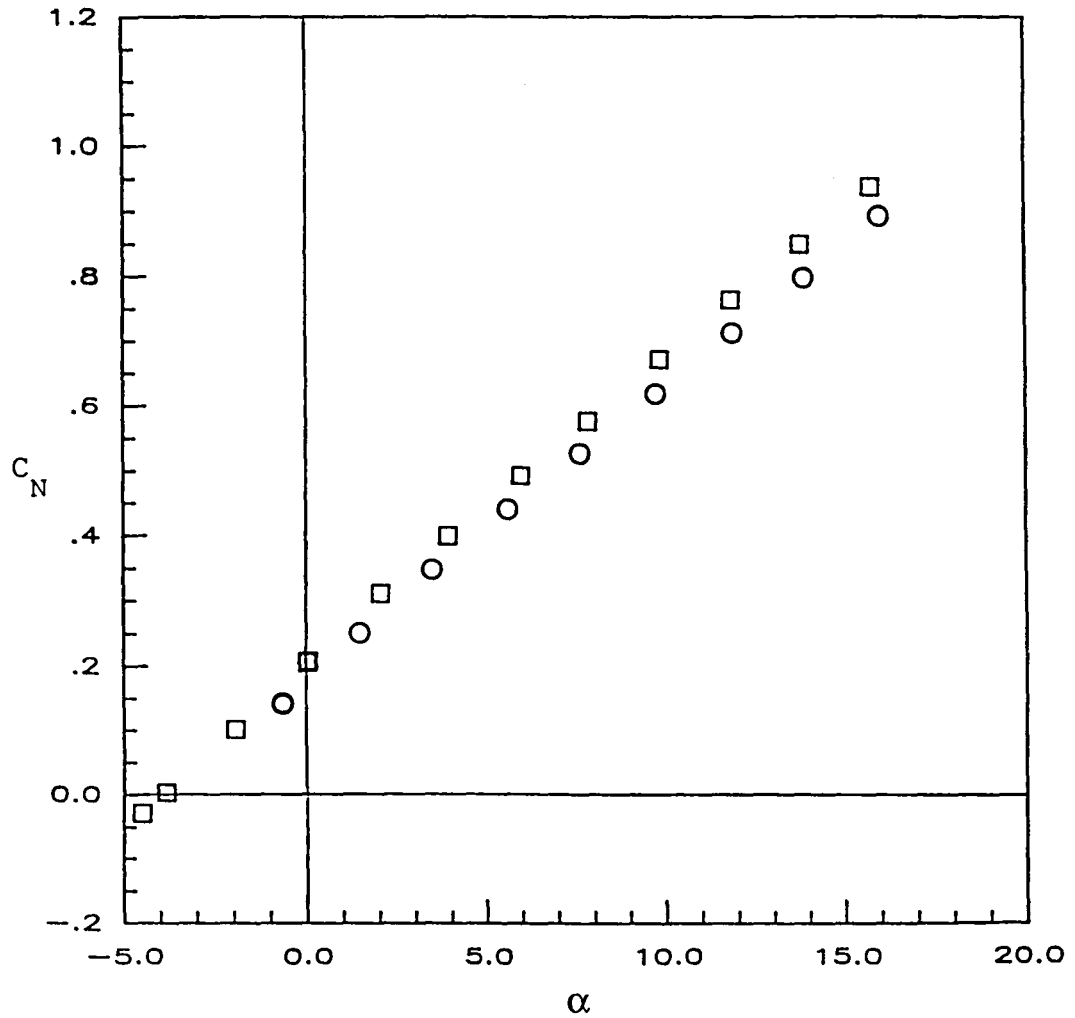


D. Leading edge flaps only

Figure 6. continued

FLAP SETTINGS			
LEI	LEO	TEI	TEO
15	20	15	12

WIND TUNNEL	
○	GLENN MARTIN
□	LANGLEY 7 X 10

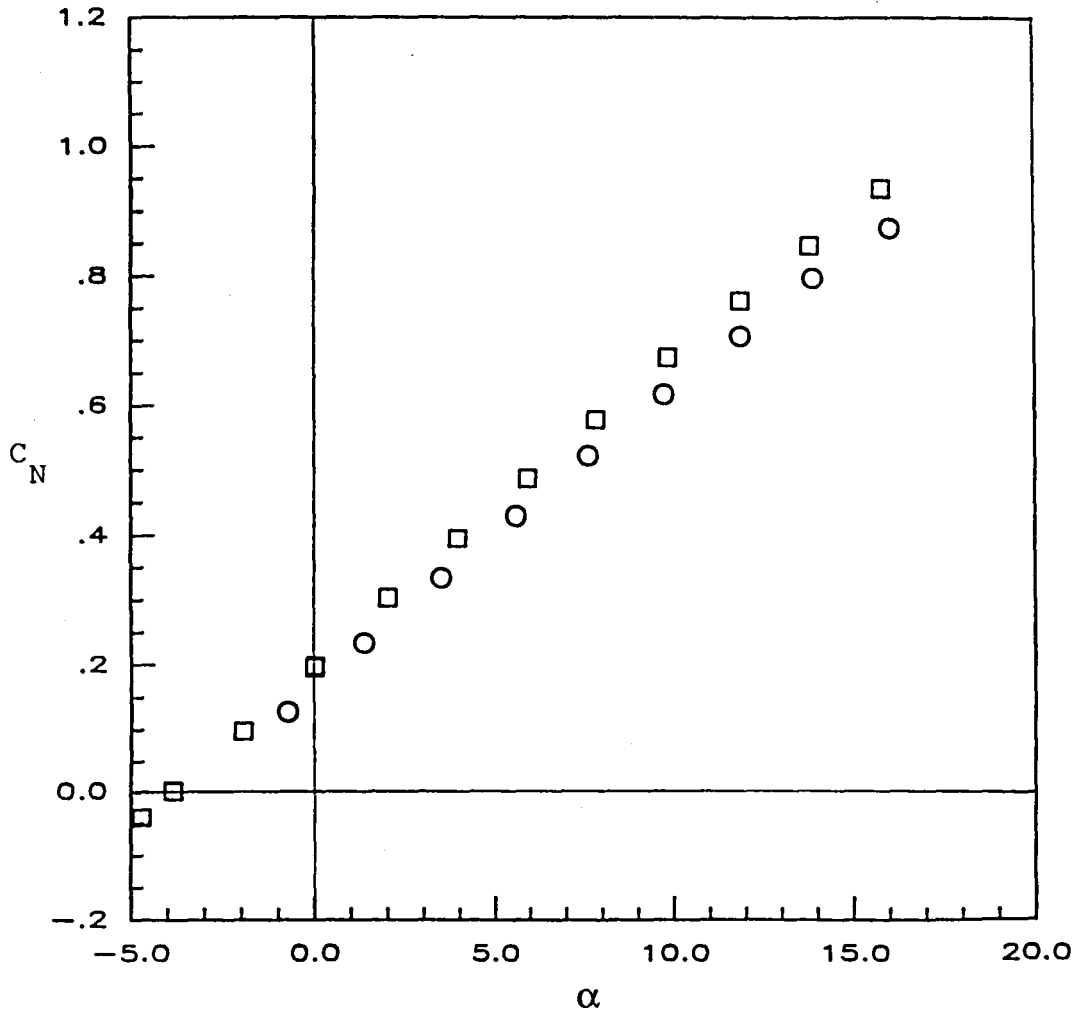


E. All flaps deflected

Figure 6. continued

FLAP SETTINGS			
LEI	LEO	TEI	TEO
20	20	15	12

WIND TUNNEL	
○	GLENN MARTIN
□	LANGLEY 7 X 10

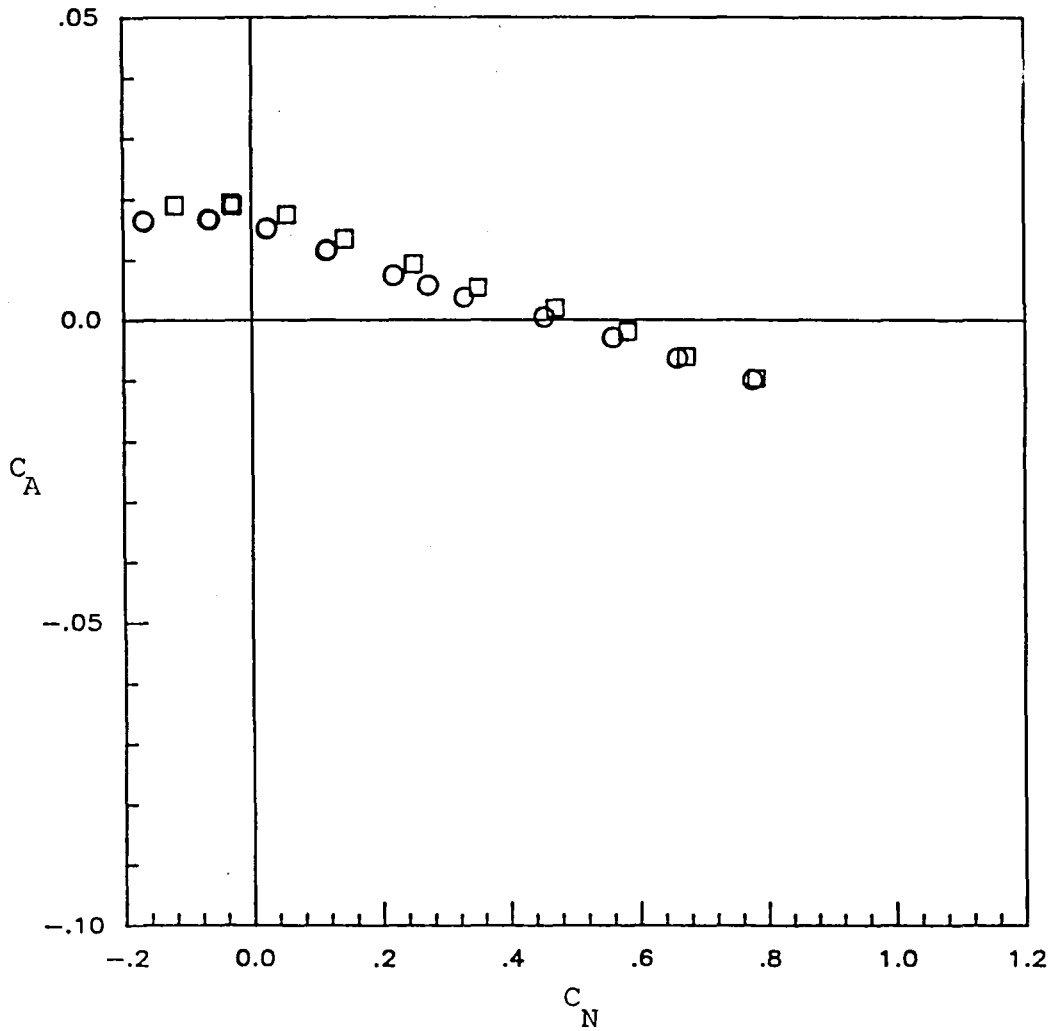


F. All flaps deflected

Figure 6. concluded

FLAP SETTINGS			
LEI	LEO	TEI	TEO
0	0	0	0

WIND TUNNEL	
○	GLENN MARTIN
□	LANGLEY 7 X 10

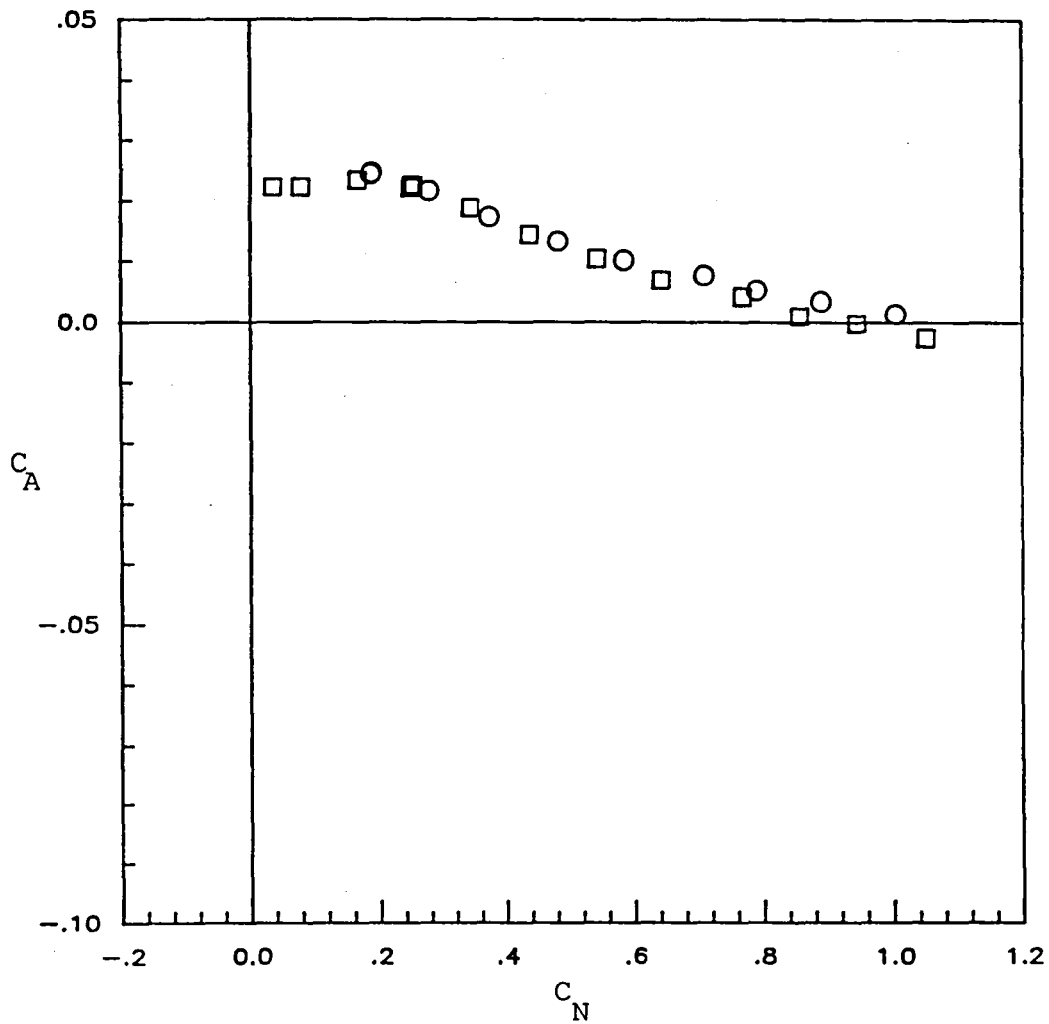


A. Flaps undeflected (basic configuration)

Figure 7. Axial force versus normal force characteristics compared with NASA Langley data at  $Rn_{mac} = 1.6 \times 10^6$ .

FLAP SETTINGS			
LEI	LEO	TEI	TEO
0	0	15	12

WIND TUNNEL	
○	GLENN MARTIN
□	LANGLEY 7 X 10

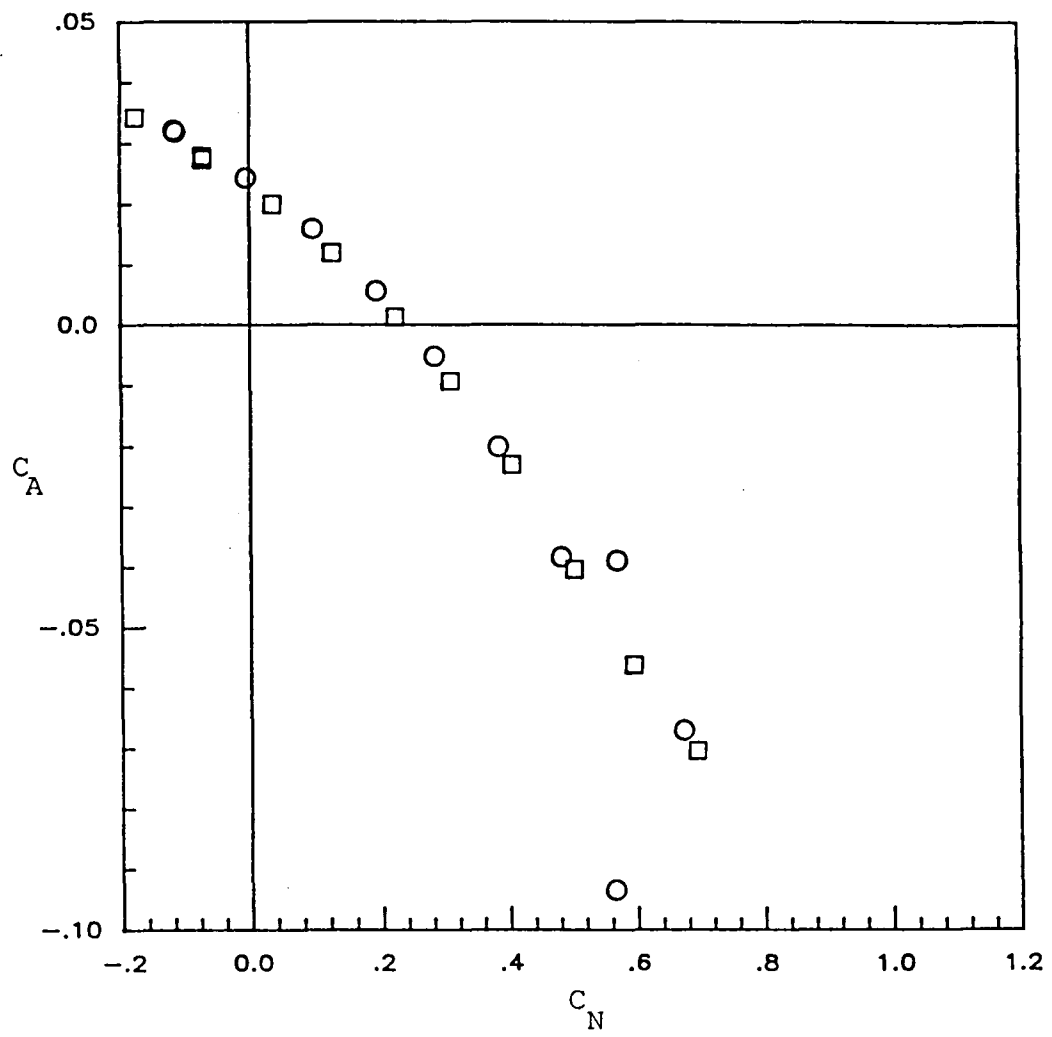


B. Trailing edge flaps only

Figure 7. continued

FLAP SETTINGS			
LEI	LEO	TEI	TEO
15	20	0	0

WIND TUNNEL	
○	GLENN MARTIN
□	LANGLEY 7 X 10



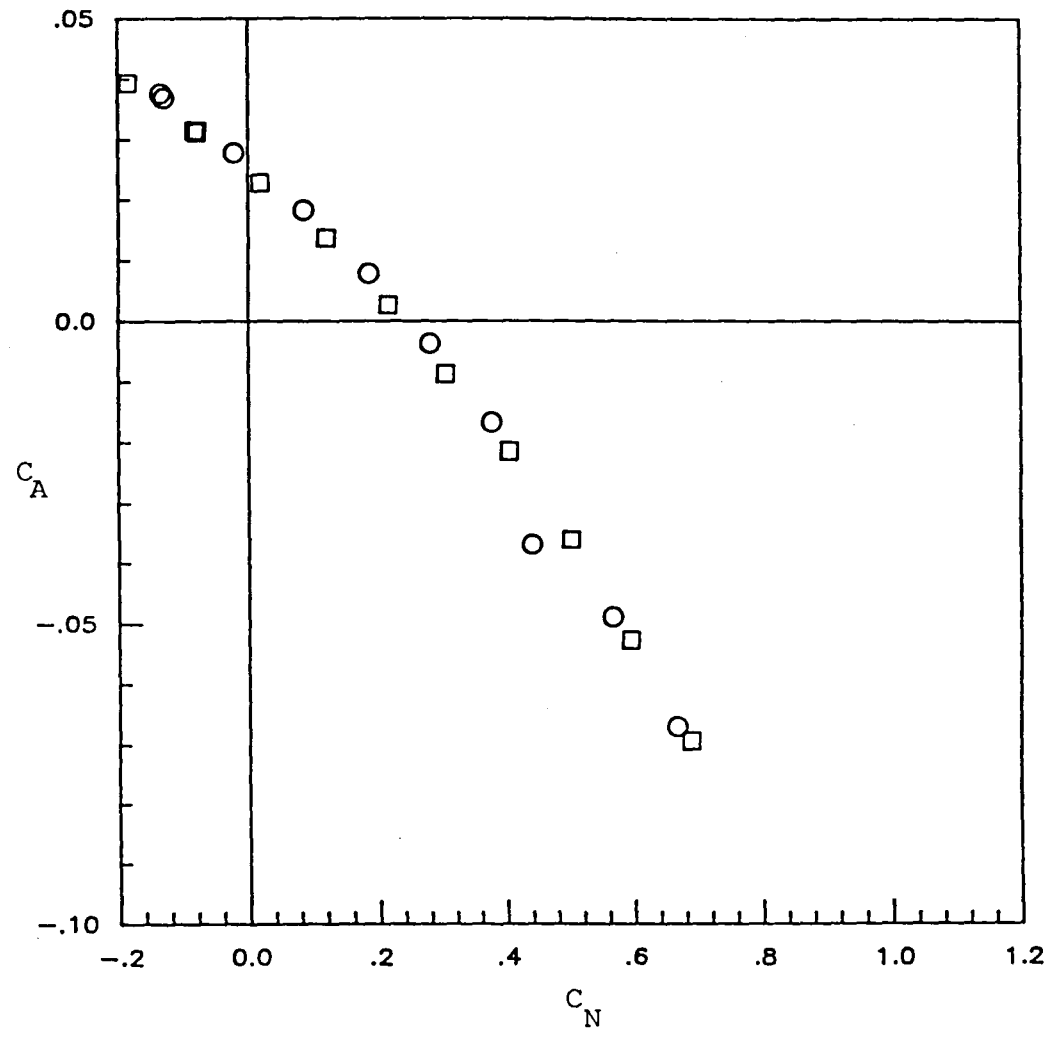
C. Leading edge flaps only

Figure 7. continued



FLAP SETTINGS			
LEI	LEO	TEI	TEO
20	20	0	0

WIND TUNNEL	
○	GLENN MARTIN
□	LANGLEY 7 X 10

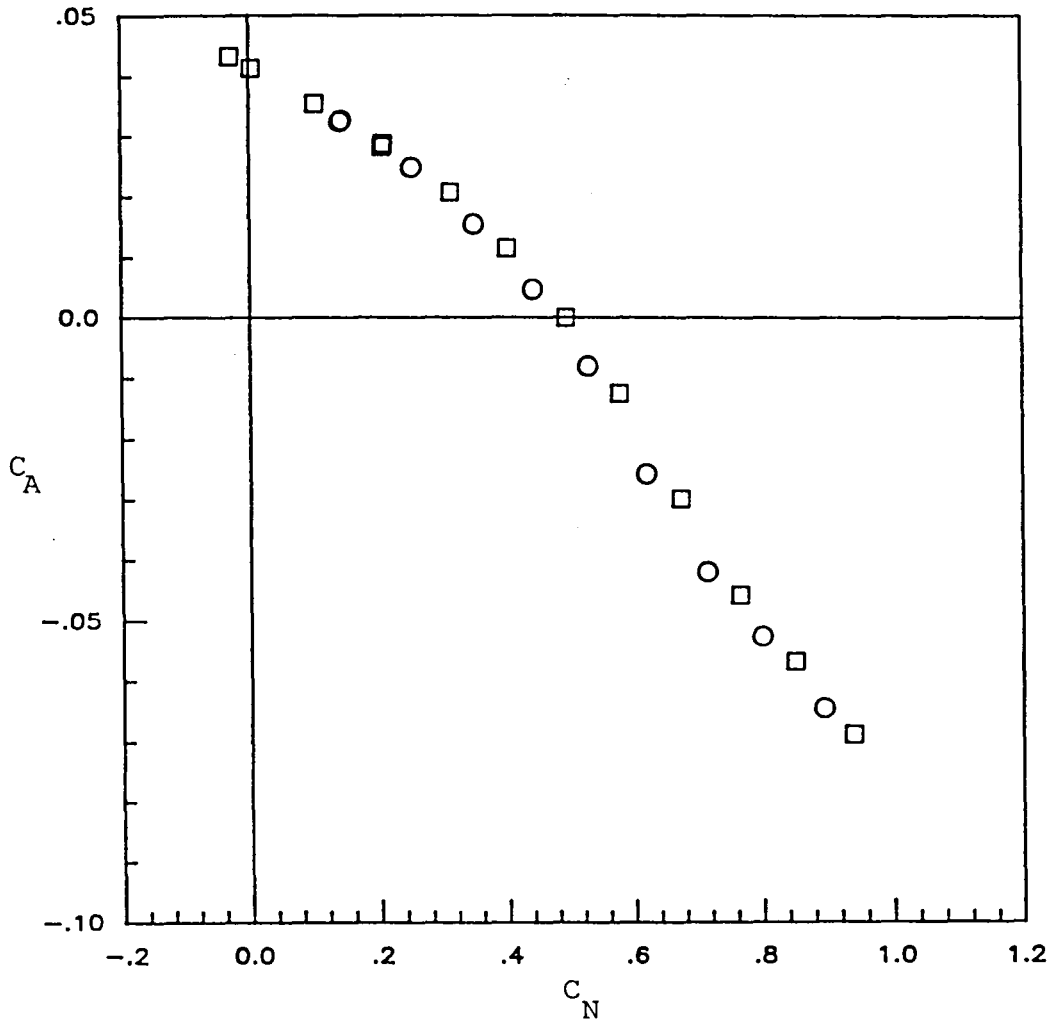


D. Leading edge flaps only

Figure 7. continued

FLAP SETTINGS			
LEI	LEO	TEI	TEO
15	20	15	12

WIND TUNNEL	
○	GLENN MARTIN
□	LANGLEY 7 X 10

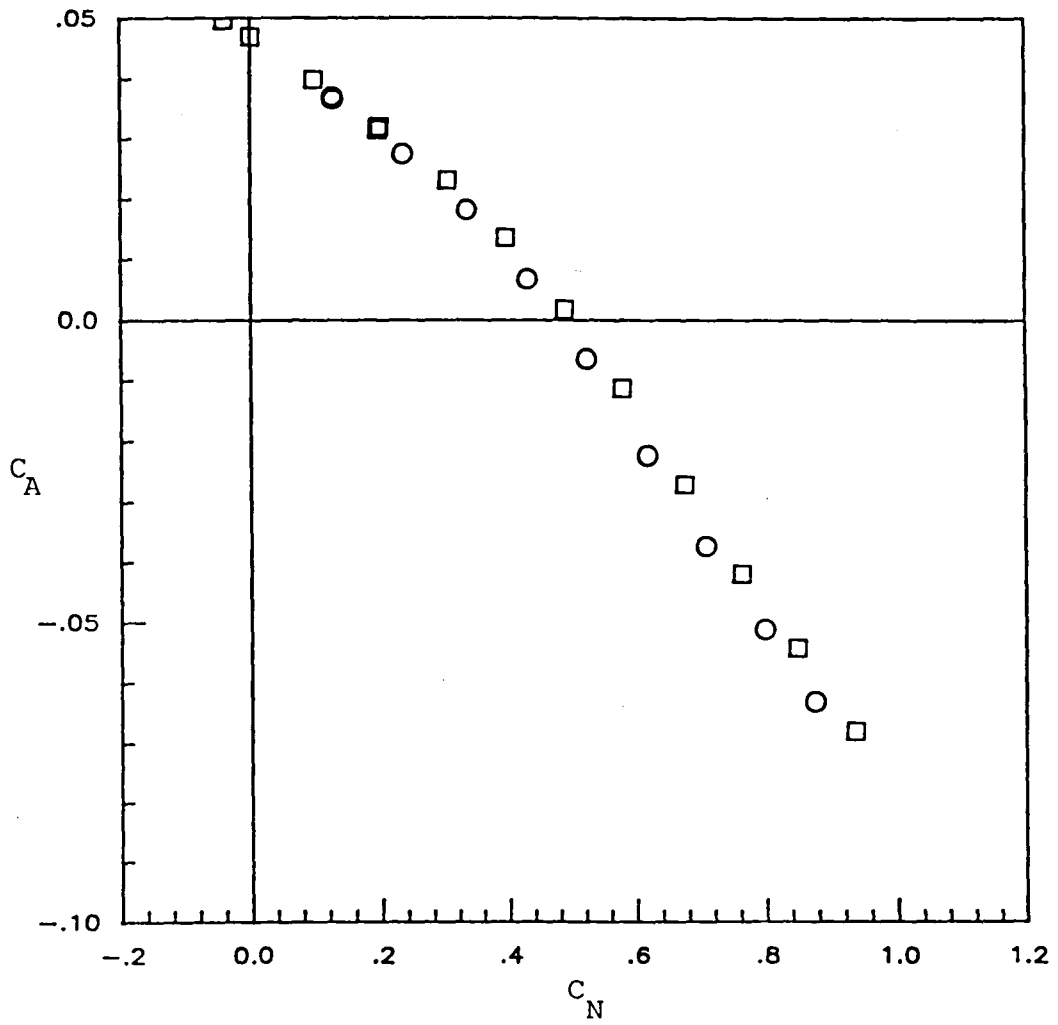


E. All flaps deflected

Figure 7. continued

FLAP SETTINGS			
LEI	LEO	TEI	TEO
20	20	15	12

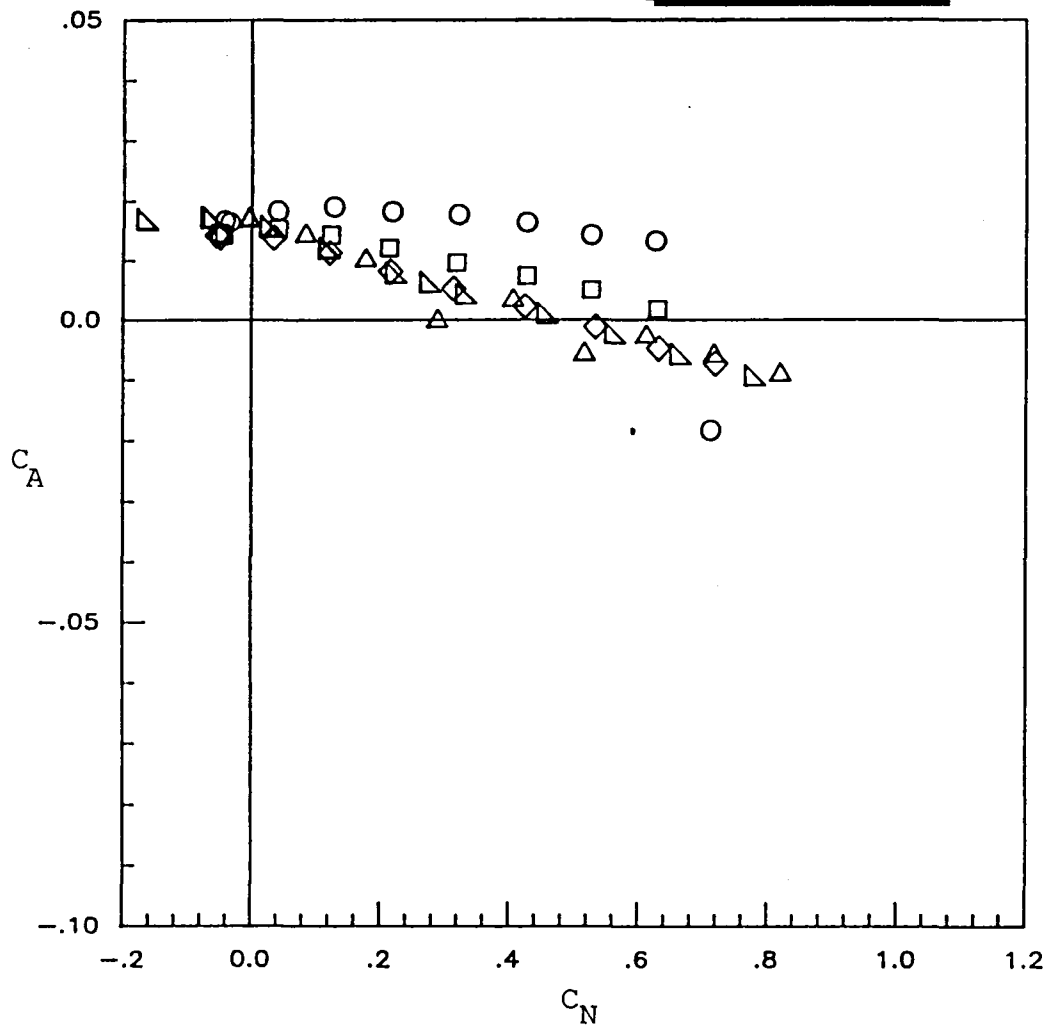
WIND TUNNEL	
○	GLENN MARTIN
□	LANGLEY 7 X 10



F. All flaps deflected  
 Figure 7. concluded

FLAP SETTINGS			
LEI	LEO	TEI	TEO
0	0	0	0

$Rn_{mac}$
○ 0.30 MILLION
□ 0.43 MILLION
◇ 0.60 MILLION
△ 1.17 MILLION
▴ 1.60 MILLION

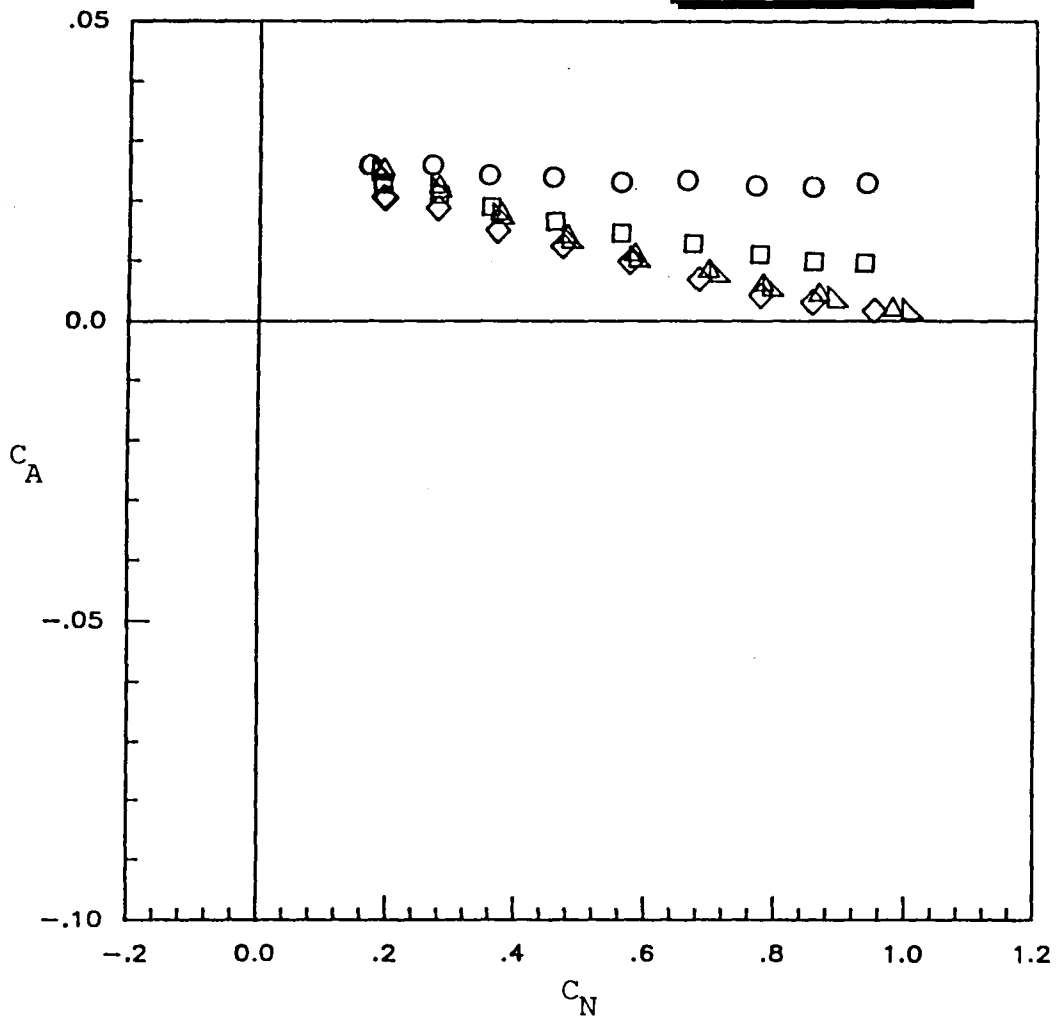


A. Flaps undeflected (basic configuration)

Figure 8. Axial force versus normal force characteristics at various Reynolds numbers.

FLAP SETTINGS			
LEI	LEO	TEI	TEO
0	0	15	12

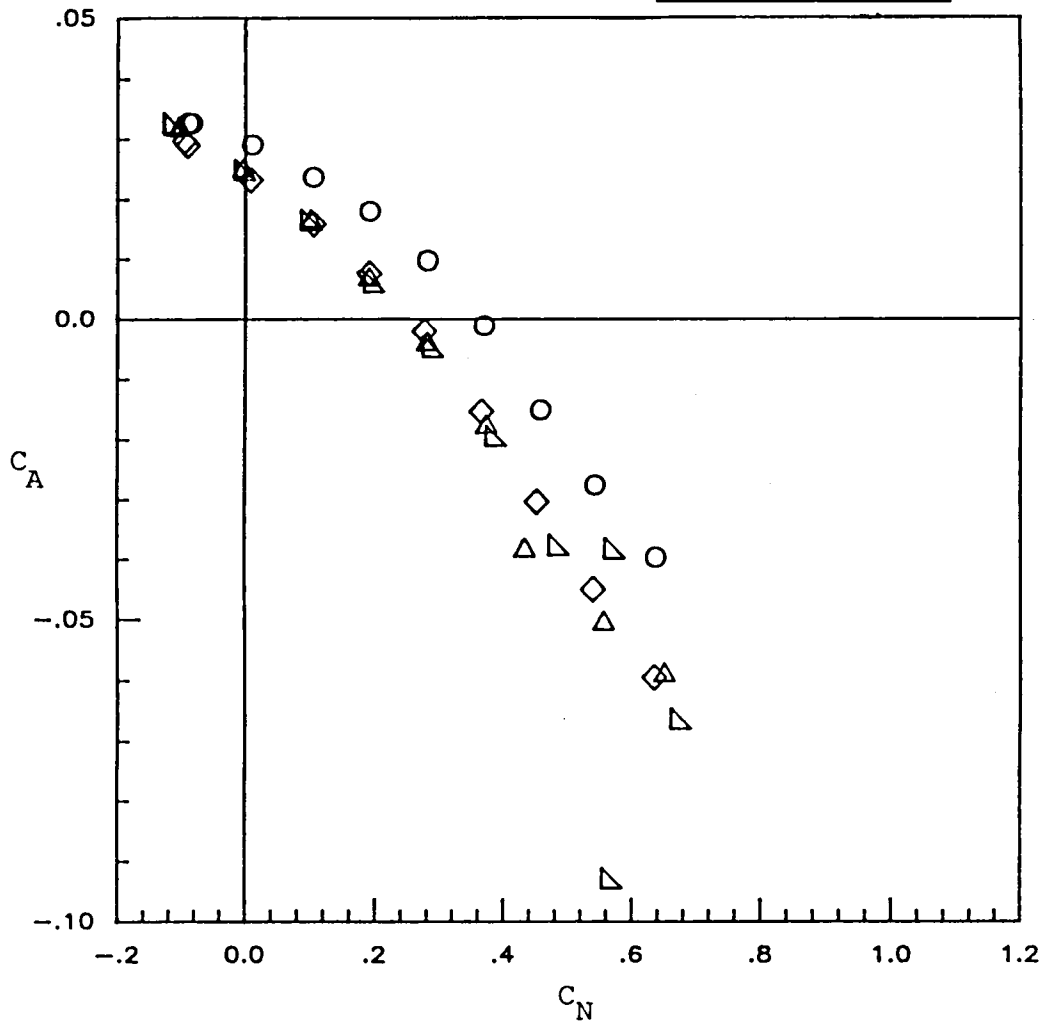
Rn <sub>mac</sub>	
○	0.30 MILLION
□	0.43 MILLION
◇	0.60 MILLION
△	1.17 MILLION
▴	1.60 MILLION



B. Trailing edge flap only  
 Figure 8. continued

FLAP SETTINGS			
LEI	LEO	TEI	TEO
15	20	0	0

$Rn_{mac}$	
○	0.30 MILLION
□	0.43 MILLION
◇	0.60 MILLION
△	1.17 MILLION
▽	1.60 MILLION

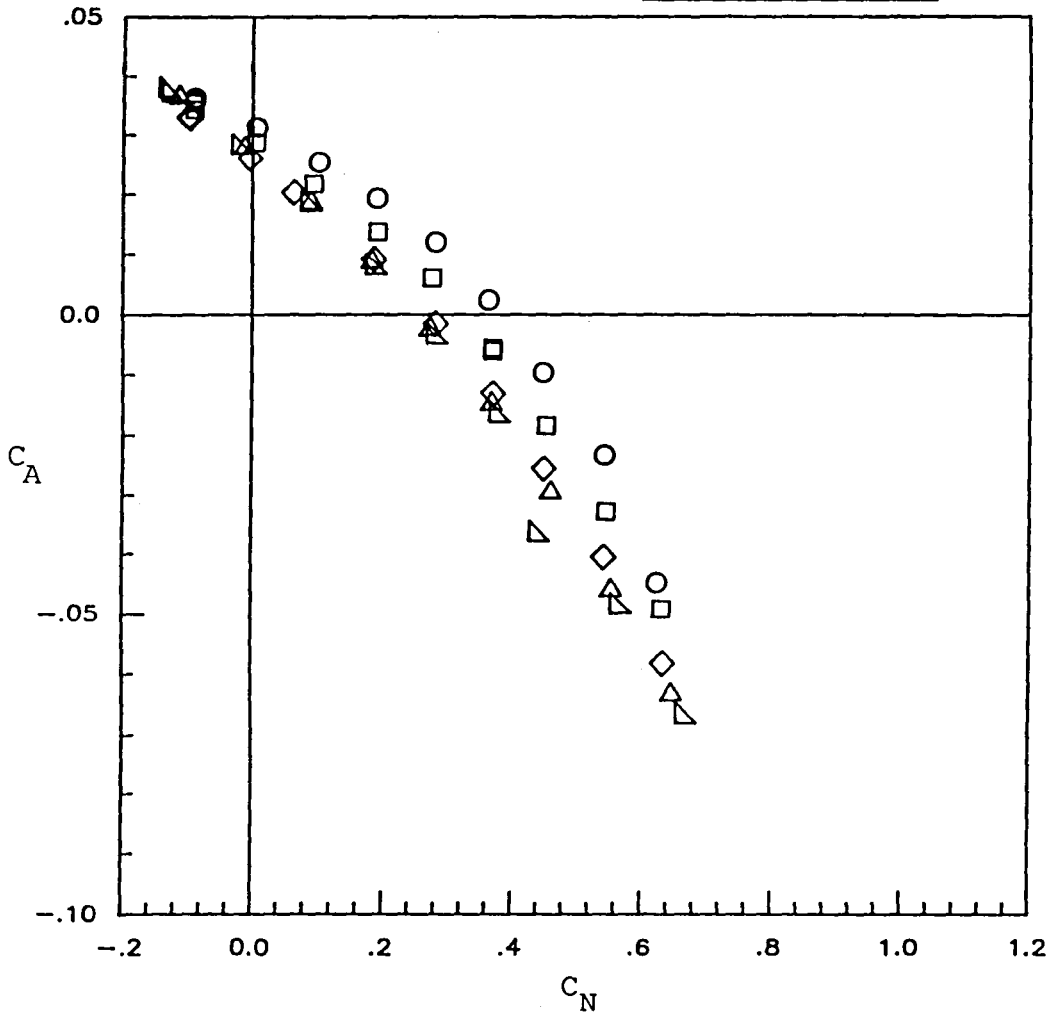


C. Leading edge flaps only

Figure 8. continued

FLAP SETTINGS			
LEI	LEO	TEI	TEO
20	20	0	0

$Rn_{mac}$
○ 0.30 MILLION
□ 0.43 MILLION
◇ 0.60 MILLION
△ 1.17 MILLION
▽ 1.60 MILLION

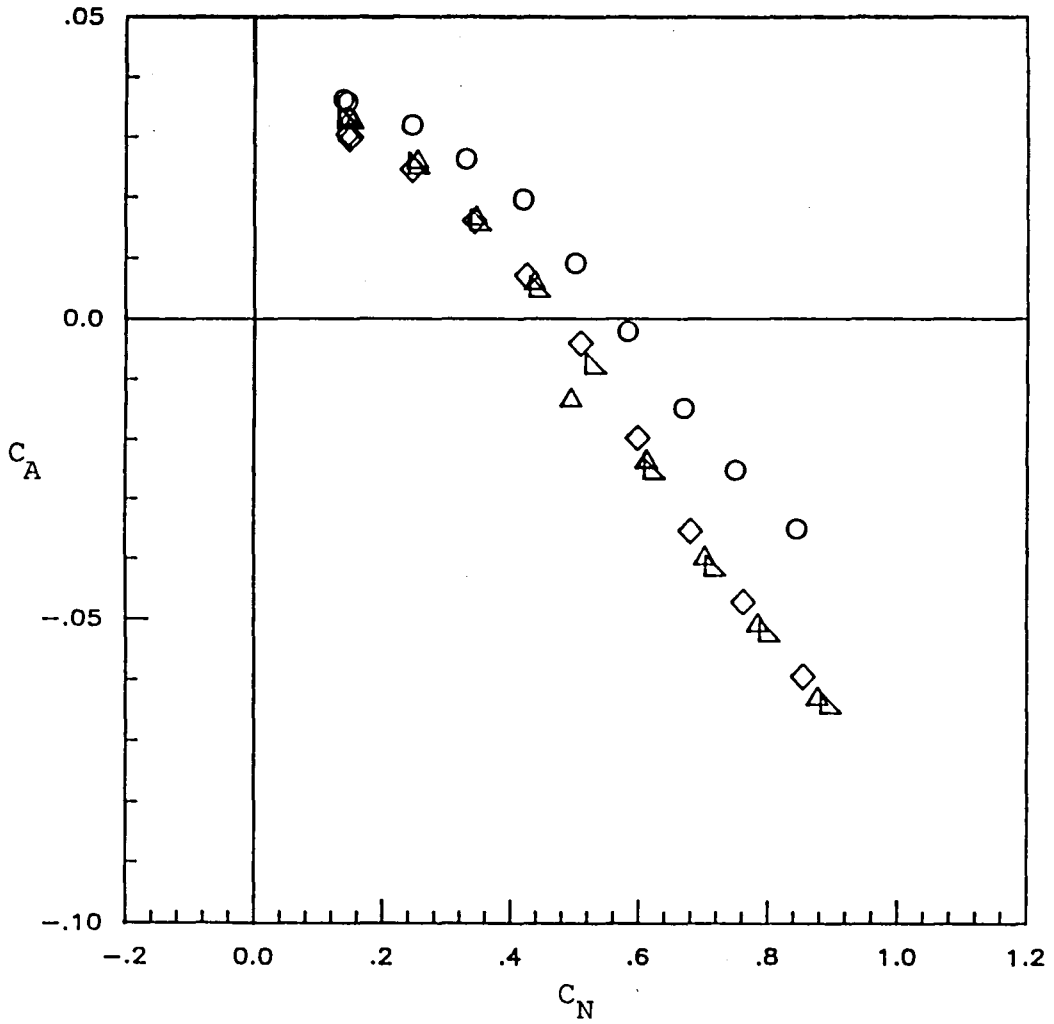


D. Leading edge flaps only

Figure 8. continued

FLAP SETTINGS			
LEI	LEO	TEI	TEO
15	20	15	12

$Rn_{mac}$	
○	0.30 MILLION
□	0.43 MILLION
◇	0.60 MILLION
△	1.17 MILLION
▴	1.60 MILLION



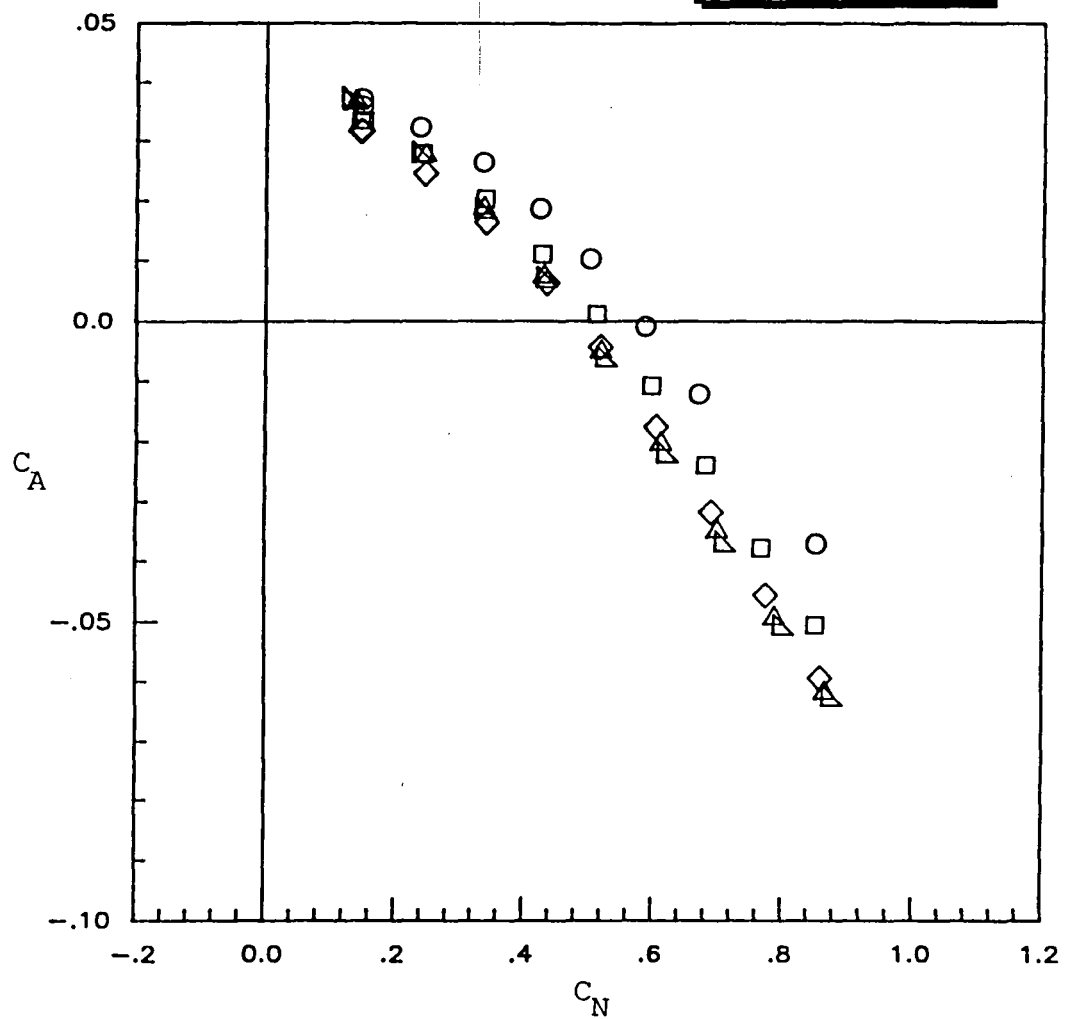
E. All flaps deflected

Figure 8. continued



FLAP SETTINGS			
LEI	LEO	TEI	TEO
20	20	15	12

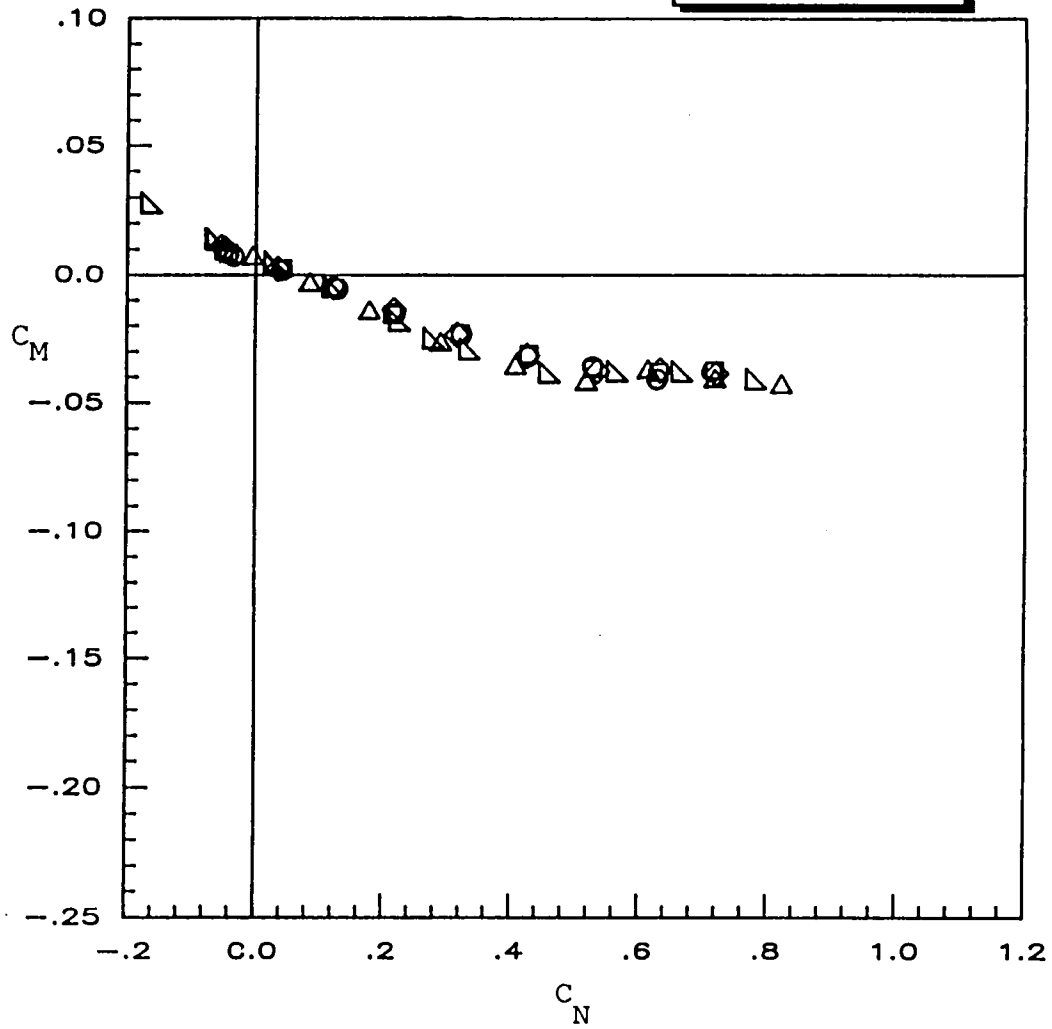
$Rn_{mac}$	
○	0.30 MILLION
□	0.43 MILLION
◇	0.60 MILLION
△	1.17 MILLION
▴	1.60 MILLION



F. All flaps deflected  
 Figure 8. Concluded

FLAP SETTINGS			
LEI	LEO	TEI	TEO
0	0	0	0

$Rn_{mac}$
○ 0.30 MILLION
□ 0.43 MILLION
◇ 0.60 MILLION
△ 1.17 MILLION
▽ 1.60 MILLION

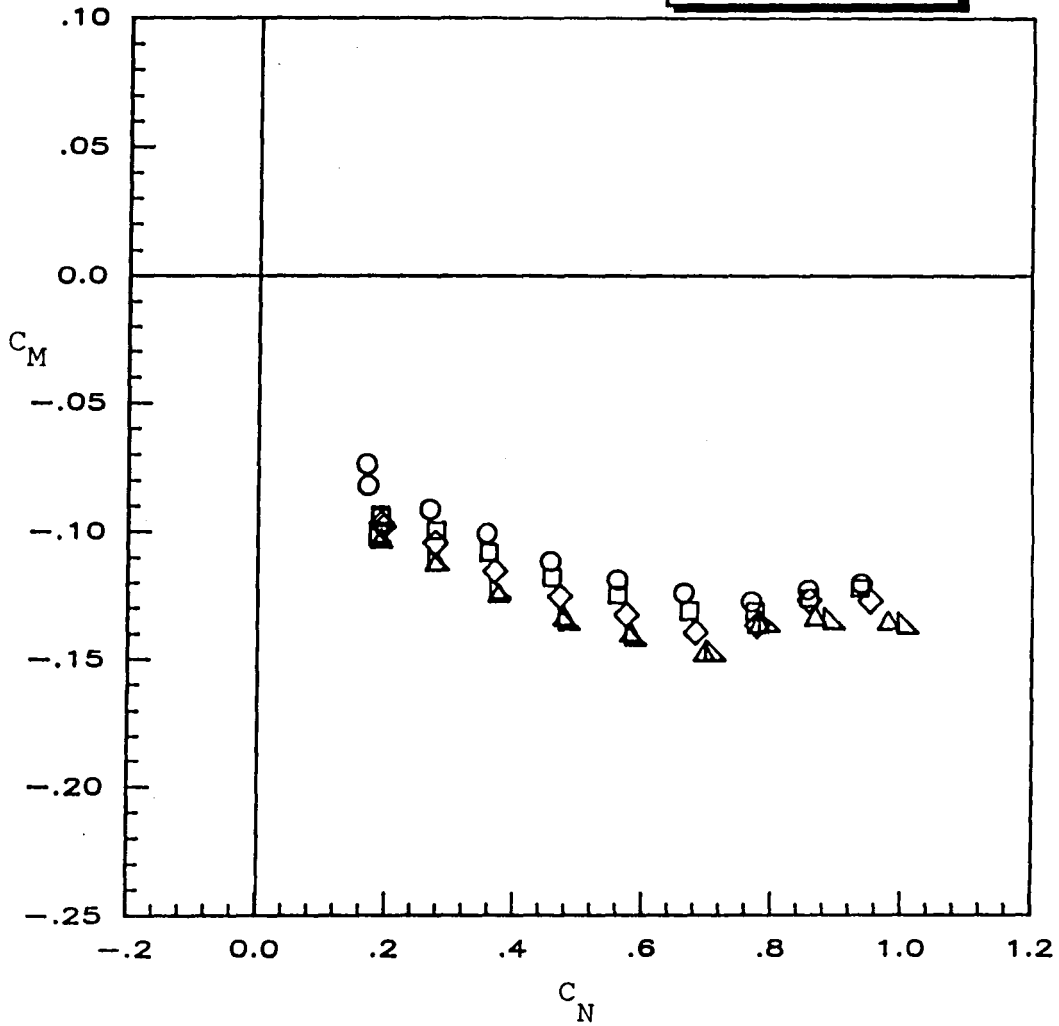


A. Flaps undeflected (basic configuration)

Figure 9. Pitching moment versus normal force characteristics at various Reynolds numbers.

FLAP SETTINGS			
LEI	LEO	TEI	TEO
0	0	15	12

$Rn_{mac}$	
○	0.30 MILLION
□	0.43 MILLION
◇	0.60 MILLION
△	1.17 MILLION
▽	1.60 MILLION

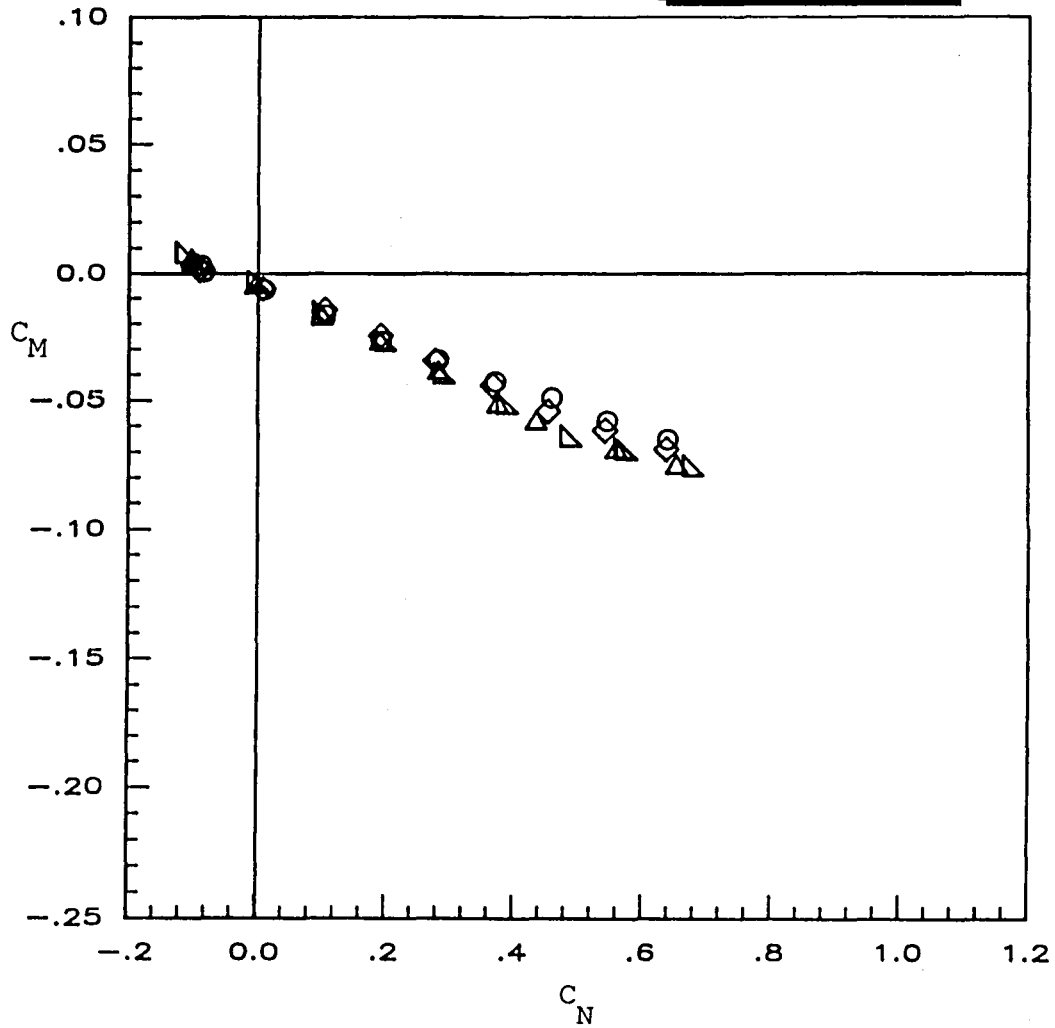


B. Trailing edge flaps only

Figure 9. continued

FLAP SETTINGS			
LEI	LEO	TEI	TEO
15	20	0	0

$Rn_{mac}$	
○	0.30 MILLION
□	0.43 MILLION
◇	0.60 MILLION
△	1.17 MILLION
▽	1.60 MILLION

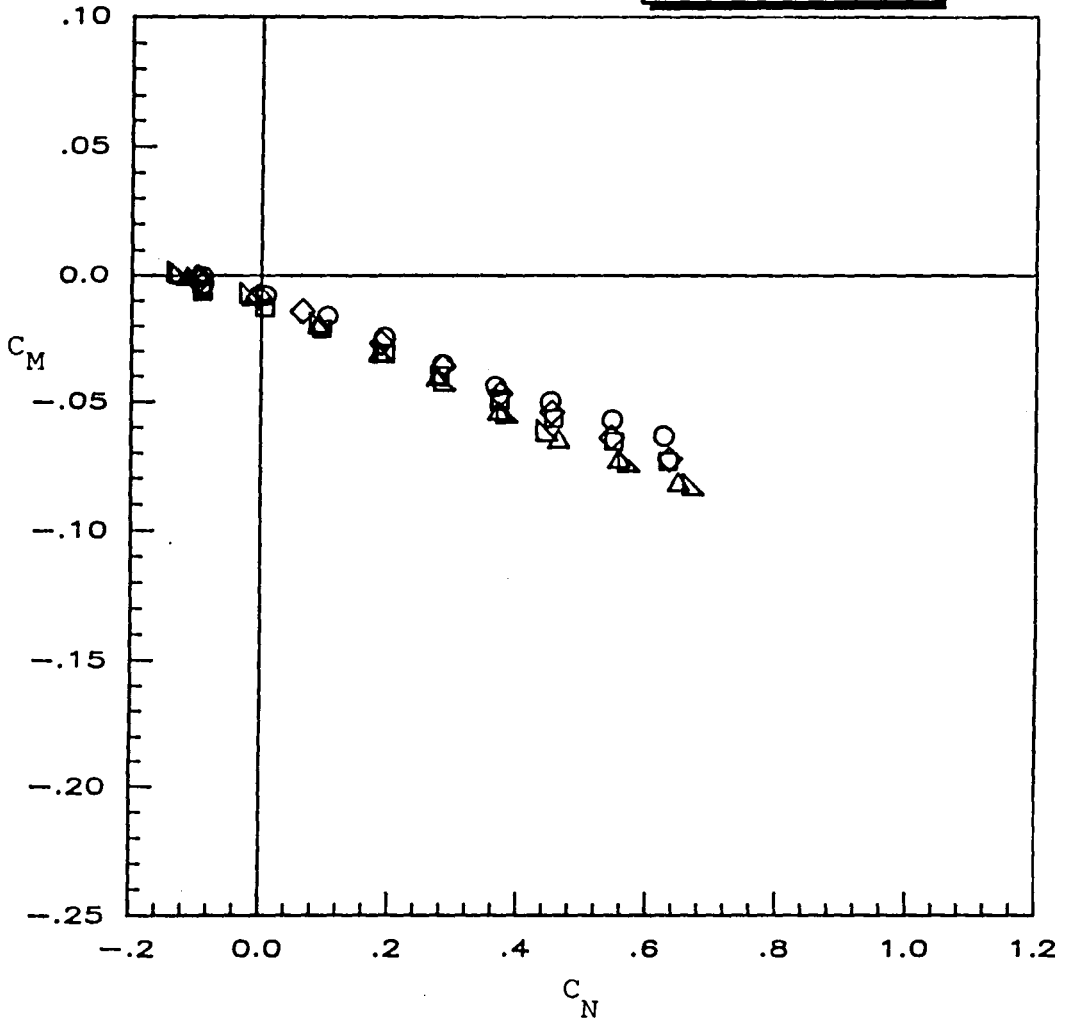


C. Leading edge flaps only

Figure 9. continued

FLAP SETTINGS			
LEI	LEO	TEI	TEO
20	20	0	0

$Rn_{mac}$	
○	0.30 MILLION
□	0.43 MILLION
◇	0.60 MILLION
△	1.17 MILLION
▽	1.60 MILLION

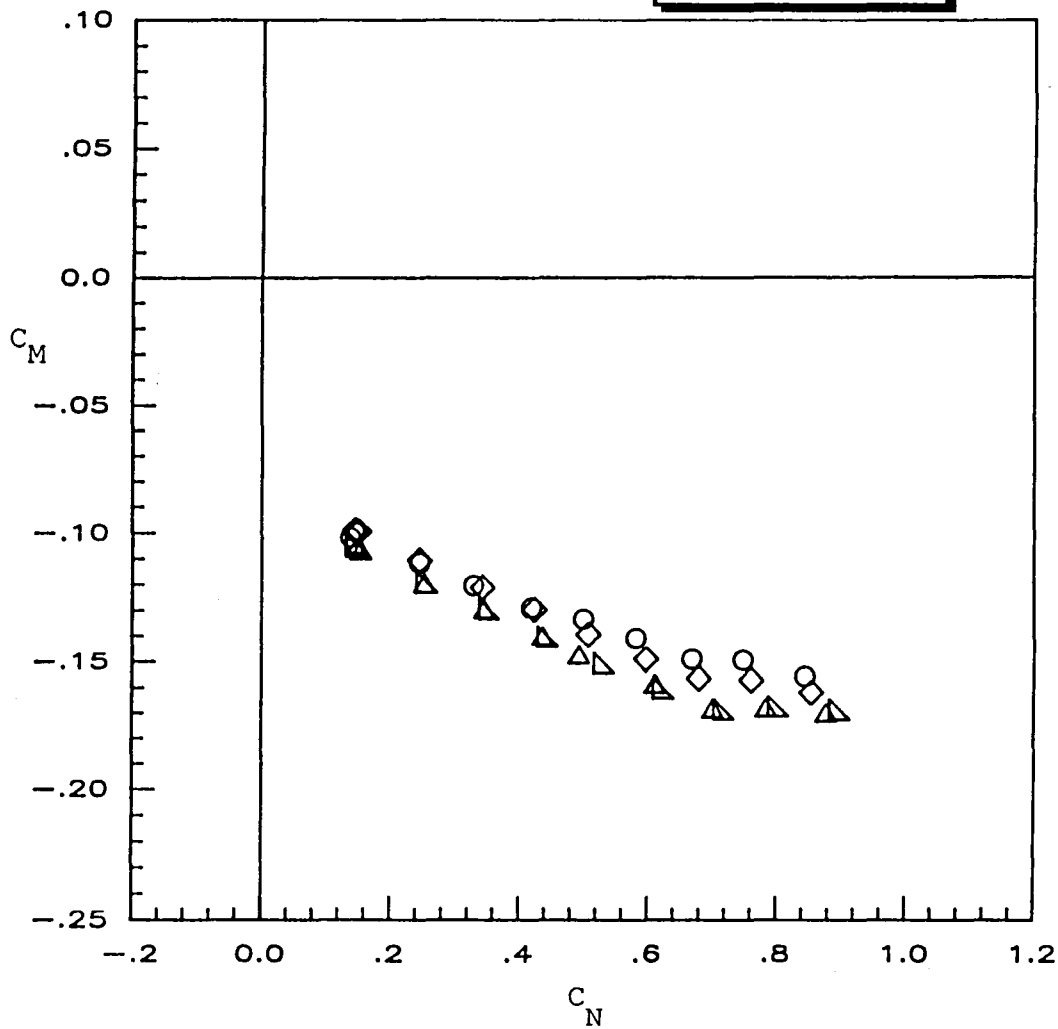


D. Leading edge flaps only

Figure 9. Continued

FLAP SETTINGS			
LEI	LEO	TEI	TEO
15	20	15	12

$Rn_{mac}$	
○	0.30 MILLION
□	0.43 MILLION
◇	0.60 MILLION
△	1.17 MILLION
▽	1.60 MILLION

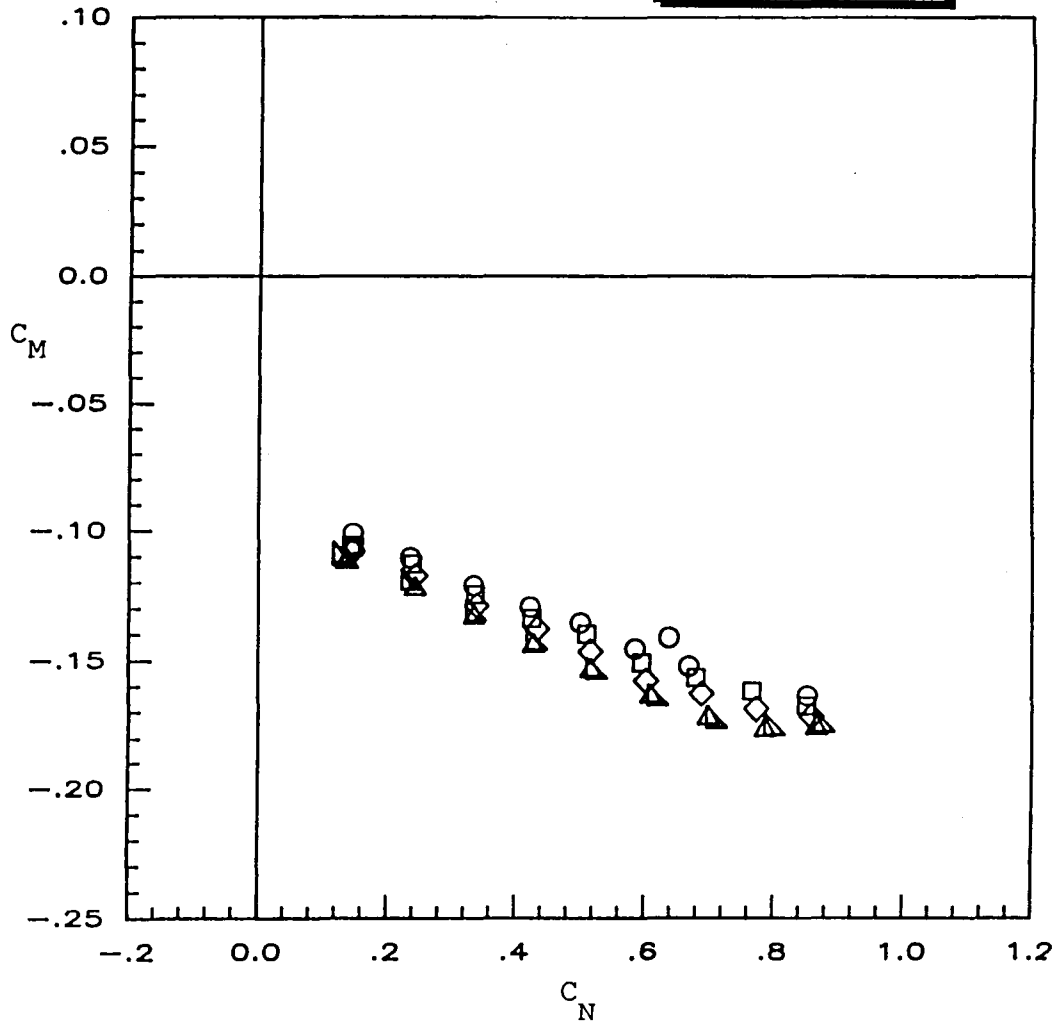


E. All flaps deflected

Figure 9. continued

FLAP SETTINGS			
LEI	LEO	TEI	TEO
20	20	15	12

$Rn_{mac}$
○ 0.30 MILLION
□ 0.43 MILLION
◇ 0.60 MILLION
△ 1.17 MILLION
▽ 1.60 MILLION

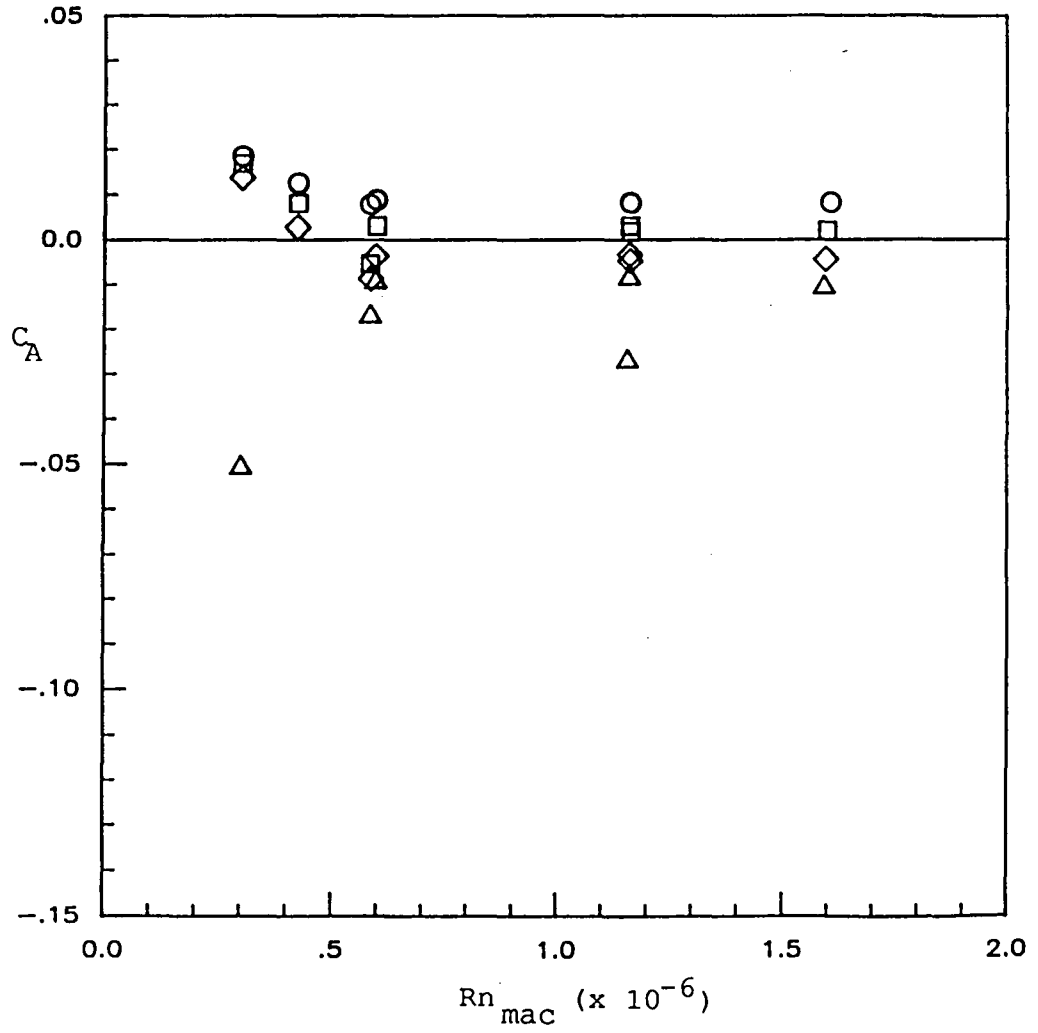


F. All flaps deflected

Figure 9. concluded

FLAP SETTINGS			
LEI	LEO	TEI	TEO
0	0	0	0

$C_N$	
○	0.2
□	0.4
◇	0.6
△	0.8



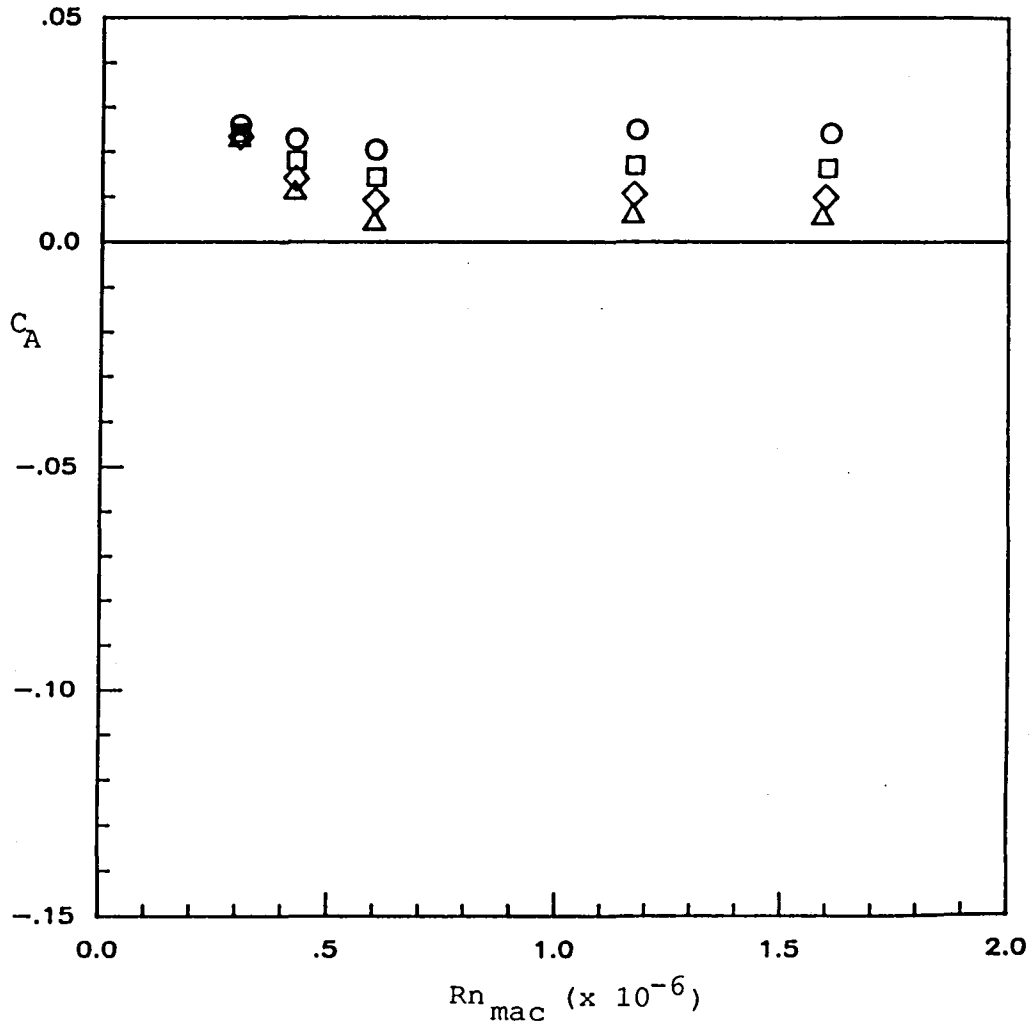
A. Flaps undeflected (basic configuration)

Figure 10. Axial force trends with Reynolds number.



FLAP SETTINGS			
LEI	LEO	TEI	TEO
0	0	15	12

$C_N$	
○	0.2
□	0.4
◇	0.6
△	0.8

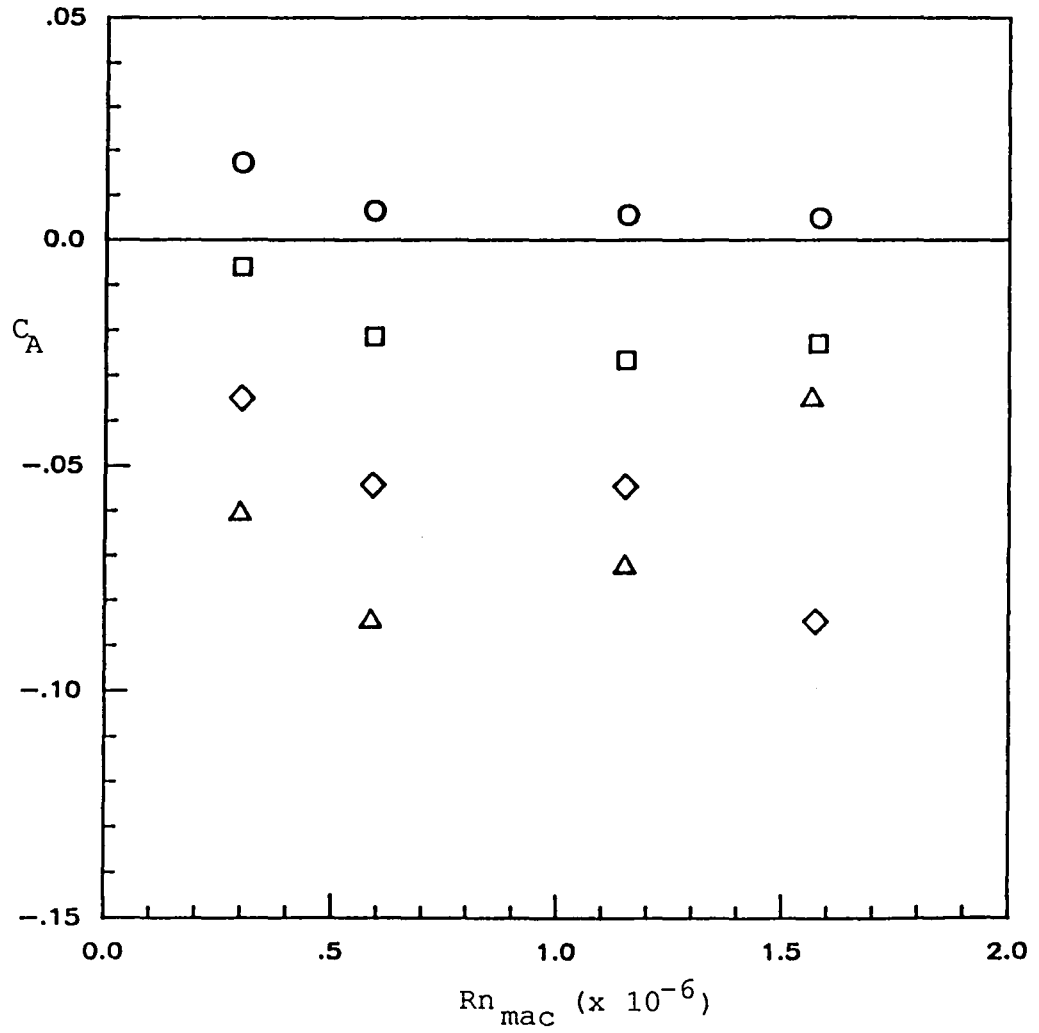


B. Trailing edge flaps only

Figure 10. continued

FLAP SETTINGS			
LEI	LEO	TEI	TEO
15	20	0	0

$C_N$	
○	0.2
□	0.4
◇	0.6
△	0.8

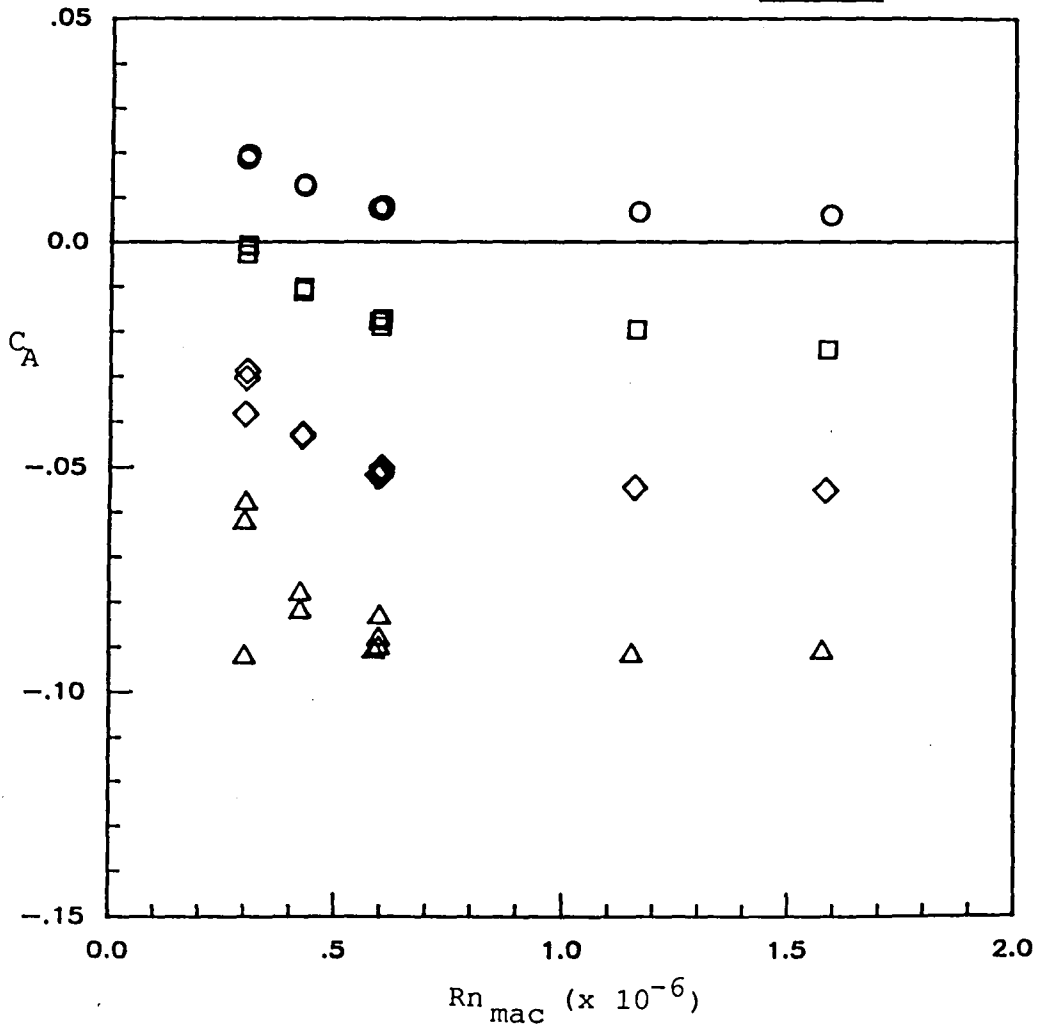


C. Leading edge flaps only

Figure 10. continued

FLAP SETTINGS			
LEI	LEO	TEI	TEO
20	20	0	0

$C_N$	
○	0.2
□	0.4
◇	0.6
△	0.8

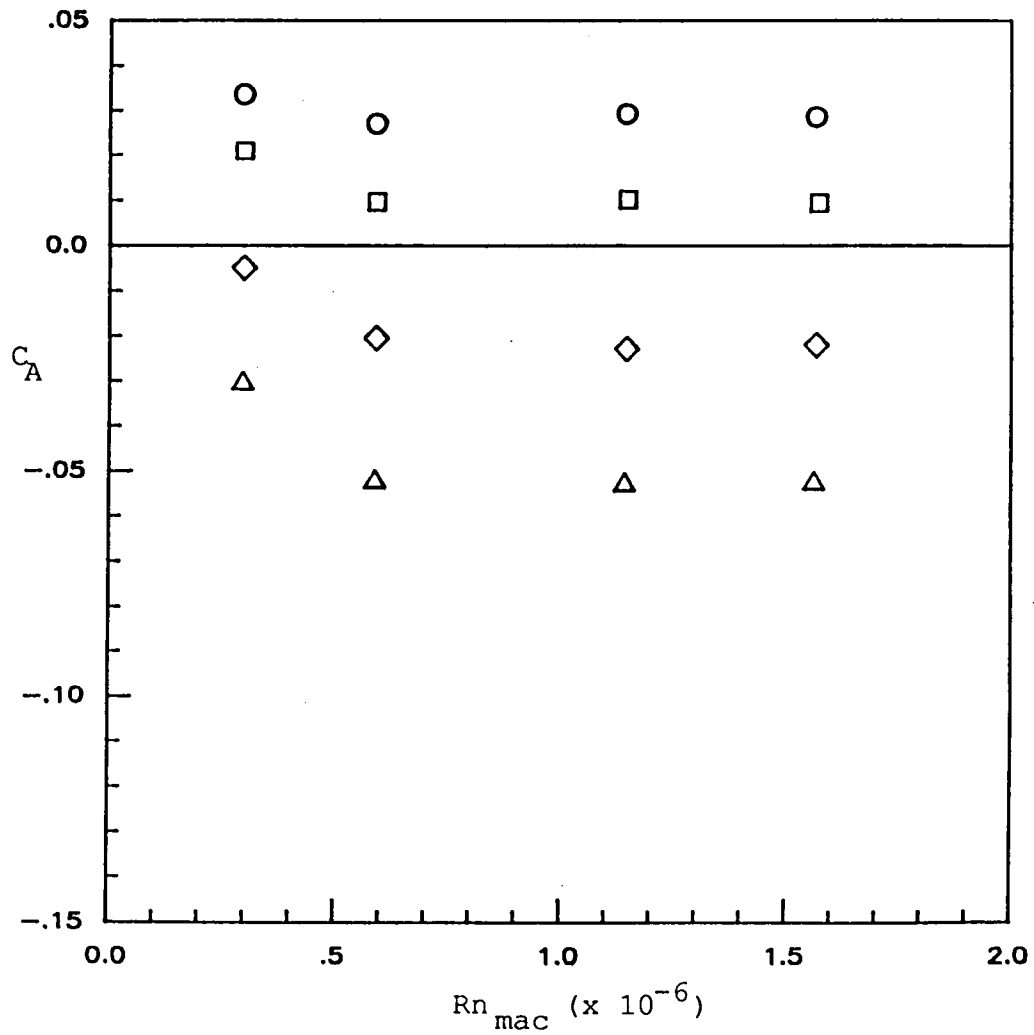


D. Leading edge flaps only

Figure 10. continued

FLAP SETTINGS			
LEI	LEO	TEI	TEO
15	20	15	12

$C_N$	
○	0.2
□	0.4
◇	0.6
△	0.8

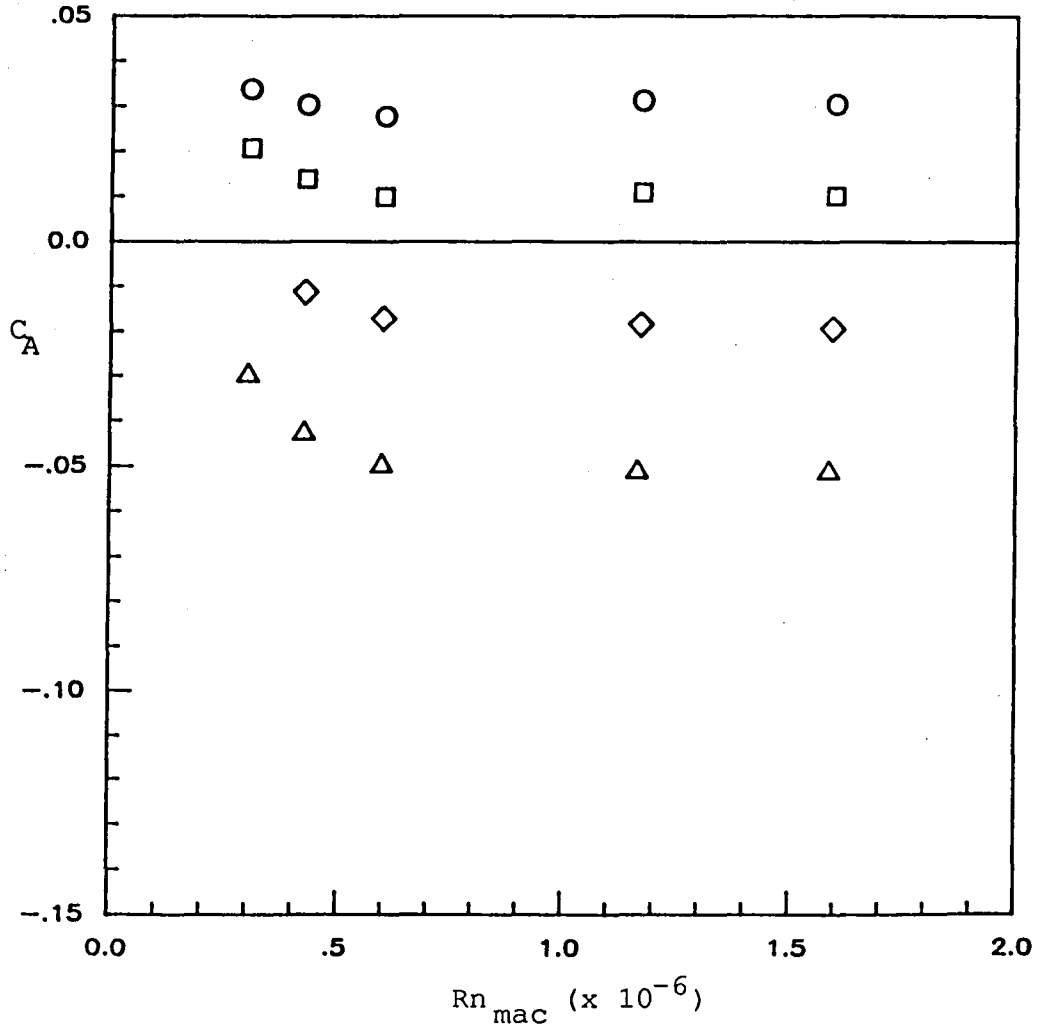


E. All flaps deflected

Figure 10. continued

FLAP SETTINGS			
LEI	LEO	TEI	TEO
20	20	15	12

$C_N$	
○	0.2
□	0.4
◇	0.6
△	0.8



F. All flaps deflected

Figure 10. concluded

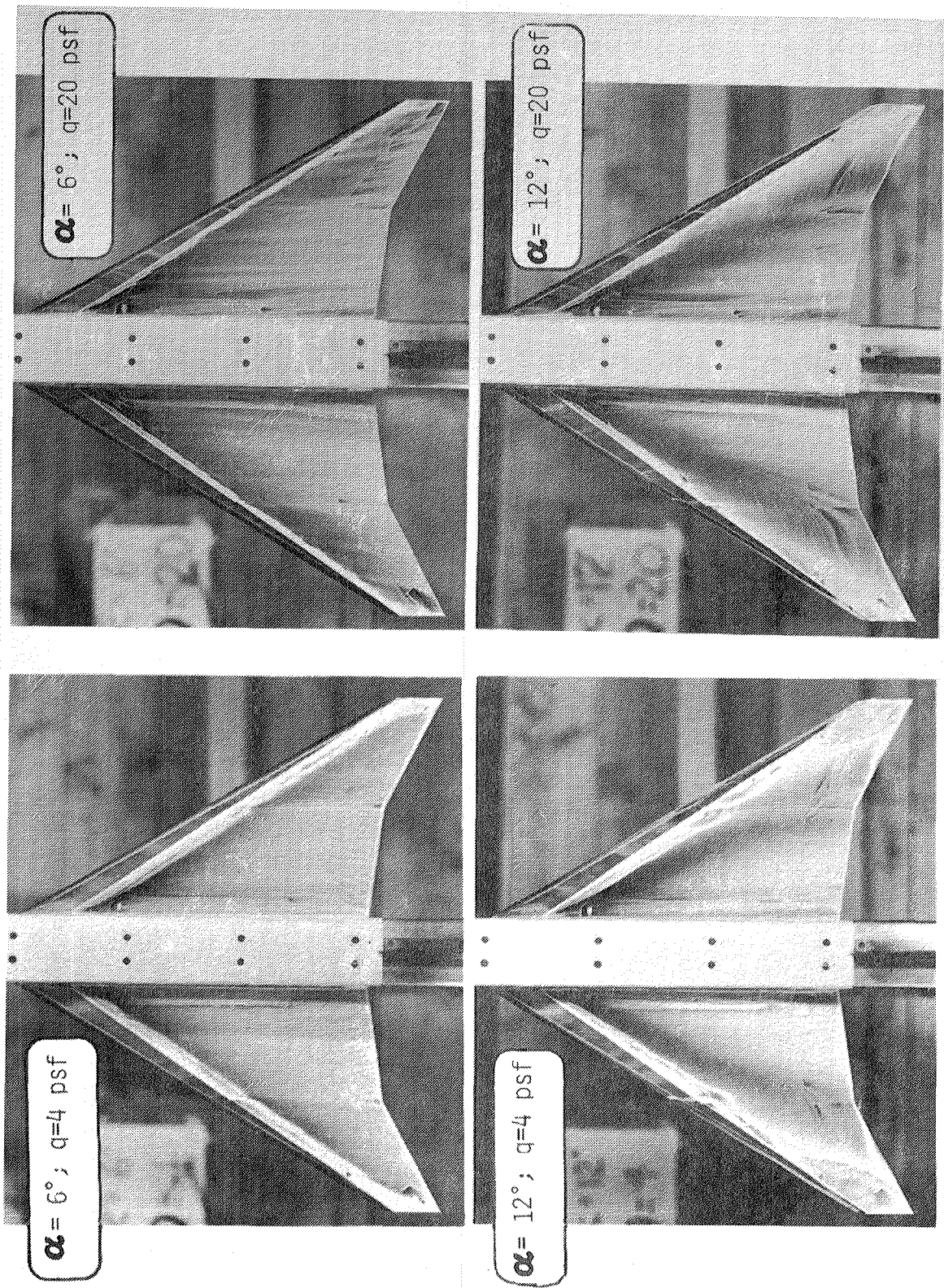


Figure 11. Oil flow visualization obtained in Vigyan low speed tunnel. (configuration 20/20/0/0)

APPENDIX

TABULATED BALANCE DATA  
FROM GLENN MARTIN TUNNEL TEST

RUN	TEST POINT	$\alpha$	$q$	MACH	$Rn_{mac}$ ( $\times 10^{-6}$ )	$C_N$	$C_A$	$C_M$	$C_n$	$C_l$	$C_y$
5.	69.	-3.0	125.05	.2910	1.6305	-.1670	.0163	.0265	.0022	.0015	-.0040
5.	70.	-.9	125.08	.2910	1.6219	-.0660	.0166	.0125	.0019	.0008	-.0040
5.	71.	1.3	124.72	.2900	1.6136	.0240	.0151	.0039	.0018	.0011	-.0040
5.	72.	3.5	124.70	.2900	1.6099	.1160	.0115	-.0060	.0017	.0012	-.0030
5.	73.	5.6	124.64	.2900	1.6067	.2200	.0074	-.0194	.0017	.0010	-.0040
5.	74.	6.7	124.74	.2900	1.6042	.2730	.0058	-.0262	.0017	.0018	-.0050
5.	75.	7.8	124.73	.2900	1.6023	.3290	.0038	-.0304	.0017	.0017	-.0050
5.	76.	10.1	124.46	.2900	1.5990	.4540	.0005	-.0396	.0014	.0003	-.0010
5.	77.	12.2	124.57	.2900	1.5967	.5590	-.0029	-.0391	.0013	.0018	-.0020
5.	78.	14.4	124.60	.2900	1.5947	.6600	-.0063	-.0391	.0014	.0016	-.0020
5.	79.	16.6	124.92	.2900	1.5937	.7760	-.0099	-.0421	.0011	.0010	-.0010
5.	80.	-3.0	124.64	.2900	1.5900	-.1680	.0165	.0267	.0022	.0017	-.0040
5.	81.	-.9	124.63	.2900	1.5886	-.0680	.0168	.0128	.0019	.0012	-.0040
5.	82.	-.9	124.76	.2900	1.5876	-.0650	.0167	.0124	.0019	.0012	-.0030
5.	83.	1.3	124.67	.2900	1.5856	.0250	.0153	.0028	.0019	.0017	-.0050
5.	84.	3.5	124.74	.2900	1.5848	.1170	.0117	-.0061	.0017	.0015	-.0040
6.	85.	-.8	15.67	.1030	.5793	-.0560	.0177	.0112	.0015	.0011	-.0020
6.	86.	1.3	15.80	.1030	.5823	.0280	.0156	.0034	.0012	.0003	-.0020
6.	87.	3.3	15.81	.1030	.5827	.0570	.0138	-.0004	.0011	.0002	-.0030
6.	88.	5.3	15.90	.1040	.5847	.2100	.0073	-.0171	.0002	-.0023	-.0020
6.	89.	7.3	15.87	.1040	.5843	.3070	-.0002	-.0276	-.0003	-.0023	-.0030
6.	90.	9.3	15.87	.1040	.5843	.3430	-.0054	-.0302	-.0009	-.0038	-.0010
6.	91.	11.4	15.93	.1040	.5855	.5210	-.0053	-.0402	-.0019	-.0044	-.0020
6.	92.	13.4	15.93	.1040	.5859	.5250	-.0237	-.0407	-.0019	-.0039	-.0030
6.	93.	15.4	15.91	.1040	.5858	.7110	-.0134	-.0377	-.0031	-.0071	.0030
6.	94.	-.8	16.01	.1040	.5879	-.0570	.0171	.0114	.0016	.0011	-.0020
7.	95.	-.8	63.74	.2070	1.1635	-.0590	.0171	.0116	.0017	.0011	-.0030
7.	96.	1.4	63.90	.2080	1.1647	.0350	.0152	.0015	.0017	.0008	-.0030
7.	97.	3.4	63.85	.2080	1.1633	.1170	.0117	-.0061	.0016	.0011	-.0040
7.	98.	5.4	63.87	.2080	1.1622	.2140	.0076	-.0166	.0014	.0011	-.0030
7.	99.	7.5	64.13	.2080	1.1638	.3220	.0039	-.0295	.0014	.0018	-.0040
7.	100.	9.7	64.11	.2080	1.1638	.4420	.0006	-.0390	.0010	.0003	-.0020
7.	101.	11.8	64.08	.2080	1.1628	.5460	-.0028	-.0404	.0009	.0016	-.0010



RUN	TEST POINT	$\alpha$	$q$	MACH	$Rn_{mac}$ ( $\times 10^{-6}$ )	$C_N$	$C_A$	$C_M$	$C_n$	$C_l$	$C_y$
7.	102.	13.8	63.94	.2080	1.1605	.6370	-.0060	-.0382	.0007	.0007	-.0020
7.	103.	16.7	63.80	.2080	1.1592	.7420	-.0197	-.0407	.0005	.0002	-.0010
7.	104.	-.8	64.02	.2080	1.1604	-.0570	.0170	.0114	.0018	.0013	-.0030
8.	105.	.7	63.69	.2070	1.1655	-.0030	.0169	.0064	-.0007	.0025	-.0010
8.	106.	2.8	63.66	.2070	1.1643	.0860	.0142	-.0041	-.0006	.0019	-.0020
8.	107.	4.9	63.64	.2070	1.1629	.1790	.0100	-.0151	-.0007	.0028	-.0020
8.	108.	7.0	63.65	.2070	1.1624	.2900	-.0003	-.0274	-.0007	.0028	-.0030
8.	109.	9.1	63.79	.2080	1.1621	.4070	.0032	-.0365	-.0009	.0015	-.0030
8.	110.	11.2	63.80	.2080	1.1620	.5170	-.0059	-.0427	-.0011	.0037	-.0060
8.	111.	13.3	63.88	.2080	1.1608	.6130	-.0029	-.0381	-.0012	.0033	-.0050
8.	112.	15.4	64.06	.2080	1.1625	.7180	-.0061	-.0416	-.0014	.0033	-.0070
8.	113.	17.5	63.93	.2080	1.1614	.8210	-.0093	-.0439	-.0012	.0037	-.0070
8.	114.	.7	63.89	.2080	1.1599	-.0030	.0166	.0064	-.0006	.0022	-.0030
9.	115.	-.6	64.05	.2080	1.1764	.1930	.0251	-.1039	.0020	.0023	-.0050
9.	116.	1.5	63.94	.2080	1.1727	.2790	.0223	-.1130	.0019	.0025	-.0060
9.	117.	3.6	64.06	.2080	1.1718	.3760	.0178	-.1255	.0017	.0020	-.0060
9.	118.	5.7	64.03	.2080	1.1710	.4780	.0140	-.1347	.0016	.0018	-.0060
9.	119.	7.8	64.03	.2080	1.1687	.5810	.0110	-.1409	.0015	.0004	-.0050
9.	120.	9.9	63.97	.2080	1.1681	.6960	.0083	-.1488	.0011	.0015	-.0050
9.	121.	11.9	64.03	.2080	1.1673	.7790	.0060	-.1375	.0011	.0021	-.0070
9.	122.	14.0	63.98	.2080	1.1661	.8660	.0043	-.1347	.0008	.0015	-.0060
9.	123.	16.1	63.85	.2080	1.1642	.9790	.0019	-.1363	.0006	.0013	-.0050
9.	124.	-.6	63.77	.2080	1.1630	.1930	.0250	-.1039	.0020	.0026	-.0050
10.	125.	-.5	124.66	.2900	1.6068	.1850	.0245	-.1019	.0026	.0026	-.0060
10.	126.	1.7	124.76	.2900	1.6031	.2760	.0217	-.1126	.0025	.0017	-.0060
10.	127.	3.9	124.82	.2900	1.6004	.3730	.0173	-.1241	.0023	.0026	-.0060
10.	128.	6.1	125.04	.2910	1.5970	.4800	.0133	-.1359	.0022	.0018	-.0060
10.	129.	8.3	125.06	.2910	1.5945	.5830	.0102	-.1422	.0021	.0021	-.0060
10.	130.	10.5	124.64	.2900	1.5900	.7070	.0077	-.1482	.0016	.0026	-.0070
10.	131.	12.6	124.71	.2900	1.5883	.7890	.0054	-.1368	.0015	.0026	-.0060
10.	132.	14.8	124.82	.2900	1.5859	.8890	.0035	-.1357	.0012	.0020	-.0060
10.	133.	17.0	125.12	.2910	1.5852	1.0040	.0015	-.1375	.0011	.0021	-.0070

RUN	TEST POINT	$\alpha$	$q$	MACH	$Rn_{mac}$ ( $\times 10^{-6}$ )	$C_N$	$C_A$	$C_M$	$C_n$	$C_l$	$C_y$
10.	134.	- .5	124.71	.2900	1.5804	.1860	.0247	-.1030	.0026	.0022	-.0060
11.	135.	- .6	64.05	.2080	1.1781	.1380	.0366	-.1118	.0023	.0019	-.0060
11.	136.	1.5	64.04	.2080	1.1752	.2450	.0275	-.1226	.0020	.0020	-.0050
11.	137.	3.5	64.00	.2080	1.1723	.3370	.0187	-.1335	.0018	.0023	-.0050
11.	138.	5.6	64.05	.2080	1.1714	.4300	.0073	-.1445	.0017	.0017	-.0060
11.	139.	7.7	64.02	.2080	1.1693	.5190	-.0051	-.1540	.0016	.0019	-.0060
11.	140.	9.8	64.05	.2080	1.1684	.6120	-.0204	-.1639	.0016	.0005	-.0050
11.	141.	11.9	63.92	.2080	1.1662	.7000	-.0352	-.1723	.0010	.0002	-.0050
11.	142.	13.9	63.91	.2080	1.1651	.7880	-.0495	-.1767	.0008	.0008	-.0050
11.	143.	16.0	63.87	.2080	1.1635	.8680	-.0620	-.1760	.0012	.0024	-.0040
11.	144.	- .6	63.93	.2080	1.1635	.1400	.0364	-.1121	.0022	.0016	-.0040
12.	145.	- .6	124.91	.2900	1.6141	.1280	.0365	-.1095	.0032	.0015	-.0070
12.	146.	1.6	124.71	.2900	1.6068	.2340	.0275	-.1202	.0029	.0022	-.0070
12.	147.	3.8	124.85	.2900	1.6028	.3340	.0182	-.1321	.0026	.0028	-.0070
12.	148.	6.0	124.91	.2900	1.5978	.4290	.0067	-.1433	.0026	.0019	-.0080
12.	149.	8.1	124.68	.2900	1.5941	.5220	-.0064	-.1543	.0026	.0022	-.0070
12.	150.	10.3	124.83	.2900	1.5929	.6170	-.0223	-.1646	.0024	.0007	-.0060
12.	151.	12.5	124.92	.2900	1.5902	.7070	-.0373	-.1732	.0019	.0012	-.0050
12.	152.	14.6	124.81	.2900	1.5880	.7970	-.0511	-.1758	.0017	.0021	-.0050
12.	153.	16.8	124.89	.2900	1.5859	.8740	-.0630	-.1747	.0017	.0027	-.0070
12.	154.	- .6	124.74	.2900	1.5825	.1270	.0370	-.1104	.0030	.0017	-.0070
13.	155.	- .9	63.78	.2080	1.1682	-.1130	.0365	-.0014	.0019	-.0006	-.0030
13.	156.	1.2	63.86	.2080	1.1650	-.0110	.0277	-.0096	.0017	.0001	-.0030
13.	157.	3.3	63.76	.2080	1.1619	.0910	.0185	-.0207	.0014	.0003	-.0020
13.	158.	5.4	64.01	.2080	1.1631	.1840	.0087	-.0317	.0014	.0004	-.0030
13.	159.	7.5	63.98	.2080	1.1619	.2740	-.0025	-.0413	.0012	.0002	-.0020
13.	160.	9.6	63.91	.2080	1.1605	.3700	-.0149	-.0547	.0010	.0003	-.0020
13.	161.	11.7	63.87	.2080	1.1594	.4630	-.0297	-.0657	.0009	-.0015	-.0030
13.	162.	13.8	63.85	.2080	1.1589	.5560	-.0462	-.0737	.0007	-.0005	-.0010
13.	163.	15.8	63.74	.2070	1.1567	.6480	-.0635	-.0826	.0006	-.0008	-.0020
13.	164.	- .9	63.97	.2080	1.1585	-.1120	.0363	-.0016	.0019	.0006	-.0030

RUN	TEST POINT	$\alpha$	$q$	MACH	$Rn_{mac}$ ( $\times 10^{-6}$ )	$C_N$	$C_A$	$C_M$	$C_n$	$C_l$	$C_y$
14.	165.	-1.0	124.82	.2900	1.6027	-.1290	.0369	-.0004	.0020	-.0003	-.0020
14.	166.	1.2	124.81	.2900	1.5989	-.0210	.0278	-.0083	.0016	.0004	-.0030
14.	167.	3.4	124.89	.2900	1.5953	.0860	.0183	-.0201	.0016	.0008	-.0030
14.	168.	5.6	124.90	.2900	1.5927	.1850	.0078	-.0319	.0017	.0004	-.0040
14.	169.	7.7	125.02	.2910	1.5896	.2790	-.0037	-.0430	.0016	.0005	-.0030
14.	170.	9.9	124.95	.2900	1.5872	.3770	-.0167	-.0556	.0014	.0003	-.0030
14.	171.	12.0	124.77	.2900	1.5859	.4390	-.0369	-.0626	.0013	-.0007	-.0020
14.	172.	14.2	124.90	.2900	1.5835	.5650	-.0489	-.0749	.0013	0.0000	-.0010
14.	173.	16.4	124.93	.2900	1.5811	.6650	-.0670	-.0838	.0014	-.0004	-.0010
14.	174.	-1.0	125.20	.2910	1.5805	-.1340	.0376	.0003	.0020	.0003	-.0030
15.	175.	-.8	63.67	.2070	1.1614	-.1020	.0318	.0052	.0017	.0001	-.0030
15.	176.	1.2	63.73	.2070	1.1562	-.0020	.0247	-.0057	.0015	.0007	-.0030
15.	177.	3.3	63.93	.2070	1.1568	.1020	.0162	-.0182	.0013	.0007	-.0040
15.	178.	5.4	63.94	.2070	1.1553	.1920	.0066	-.0278	.0013	.0007	-.0030
15.	179.	7.5	63.76	.2070	1.1531	.2820	-.0043	-.0394	.0012	.0004	-.0030
15.	180.	9.6	63.87	.2070	1.1533	.3750	-.0180	-.0524	.0010	.0006	-.0030
15.	181.	11.6	63.80	.2070	1.1525	.4350	-.0387	-.0591	.0012	.0005	-.0030
15.	182.	13.8	63.89	.2070	1.1516	.5580	-.0508	-.0700	.0011	.0003	-.0050
15.	183.	15.8	63.88	.2070	1.1518	.6520	-.0593	-.0761	.0007	-.0006	-.0040
15.	184.	-.8	63.97	.2070	1.1516	-.1000	.0315	.0039	.0018	.0008	-.0020
16.	185.	-1.1	124.78	.2900	1.5935	-.1150	.0319	.0068	.0019	.0004	-.0030
16.	186.	1.2	125.13	.2900	1.5915	-.0050	.0243	-.0044	.0017	.0003	-.0020
16.	187.	3.4	125.00	.2900	1.5874	.0970	.0159	-.0165	.0016	0.0000	-.0030
16.	188.	5.6	124.81	.2900	1.5844	.1940	.0056	-.0280	.0017	.0007	-.0040
16.	189.	7.8	124.74	.2900	1.5800	.2850	-.0052	-.0408	.0018	.0011	-.0050
16.	190.	9.9	124.79	.2900	1.5787	.3840	-.0200	-.0525	.0016	.0011	-.0040
16.	191.	12.2	125.00	.2900	1.5774	.4820	-.0383	-.0652	.0018	.0004	-.0040
16.	192.	18.3	125.00	.2900	1.5758	.5650	-.0934	-.0699	.0019	.0005	-.0030
16.	193.	14.3	124.82	.2900	1.5738	.5690	-.0389	-.0704	.0015	.0002	-.0050
16.	194.	16.4	124.92	.2900	1.5716	.6720	-.0670	-.0767	.0014	-.0002	-.0040
16.	195.	-1.0	124.99	.2900	1.5697	-.1170	.0322	.0071	.0019	-.0002	-.0030
17.	196.	-.6	64.06	.2070	1.1516	.1480	.0329	-.1071	.0021	.0018	-.0050

RUN	TEST POINT	$\alpha$	$q$	MACH	$Rn_{mac}$ ( $\times 10^{-6}$ )	CN	CA	CM	Cn	Cl	Cy
17.	197.	1.5	64.09	.2080	1.1517	.2540	.0256	-.1208	.0019	.0013	-.0050
17.	198.	3.5	64.05	.2070	1.1502	.3470	.0164	-.1308	.0018	.0021	-.0040
17.	199.	5.6	64.05	.2070	1.1493	.4380	.0058	-.1415	.0016	.0018	-.0040
17.	200.	7.7	64.00	.2070	1.1486	.4940	-.0137	-.1487	.0017	.0019	-.0050
17.	201.	9.8	63.92	.2070	1.1471	.6120	-.0239	-.1599	.0016	.0001	-.0040
17.	202.	9.8	63.96	.2070	1.1471	.6130	-.0241	-.1601	.0015	.0007	-.0040
17.	203.	11.9	63.87	.2070	1.1460	.7020	-.0402	-.1696	.0014	.0012	-.0050
17.	204.	13.9	63.78	.2070	1.1444	.7850	-.0512	-.1693	.0012	.0001	-.0050
17.	205.	16.0	64.01	.2070	1.1460	.8780	-.0633	-.1713	.0011	0.0000	-.0030
17.	206.	-.6	63.91	.2070	1.1446	.1550	.0323	-.1080	.0022	.0017	-.0040
18.	207.	-.5	124.67	.2890	1.5831	.1410	.0325	-.1052	.0029	.0009	-.0060
18.	208.	1.7	124.77	.2900	1.5795	.2510	.0249	-.1204	.0028	.0019	-.0070
18.	209.	3.8	124.71	.2900	1.5748	.3480	.0156	-.1309	.0025	.0021	-.0060
18.	210.	6.0	124.83	.2900	1.5733	.4400	.0047	-.1418	.0025	.0019	-.0070
18.	211.	8.1	124.76	.2900	1.5703	.5270	-.0080	-.1520	.0026	.0024	-.0060
18.	212.	10.3	124.67	.2890	1.5677	.6190	-.0257	-.1619	.0027	.0013	-.0070
18.	213.	12.5	124.73	.2900	1.5659	.7130	-.0419	-.1700	.0022	.0016	-.0070
18.	214.	14.6	124.91	.2900	1.5646	.7980	-.0526	-.1689	.0019	.0007	-.0050
18.	215.	16.8	124.87	.2900	1.5616	.8930	-.0645	-.1702	.0017	.0008	-.0070
18.	216.	-.5	124.46	.2890	1.5579	.1430	.0327	-.1054	.0028	.0010	-.0050
19.	217.	-.8	16.05	.1030	.5934	.1480	.0295	-.0991	0.0000	.0004	.0020
19.	218.	-.8	16.08	.1040	.5928	.1450	.0303	-.0987	0.0000	.0008	.0010
19.	219.	1.2	16.08	.1040	.5924	.2450	.0245	-.1106	-.0004	-.0013	.0020
19.	220.	3.2	16.06	.1040	.5921	.3430	.0161	-.1212	-.0009	-.0024	.0020
19.	221.	5.2	16.07	.1040	.5920	.4240	.0070	-.1297	-.0011	-.0037	.0020
19.	222.	7.3	16.05	.1030	.5919	.5080	-.0041	-.1395	-.0015	-.0053	.0010
19.	223.	9.3	16.06	.1040	.5918	.5970	-.0199	-.1490	-.0022	-.0082	.0010
19.	224.	11.3	16.04	.1030	.5912	.6790	-.0356	-.1566	-.0024	-.0089	0.0000
19.	226.	13.3	16.06	.1040	.5912	.7610	-.0473	-.1572	-.0033	-.0111	-.0020
19.	227.	15.3	16.03	.1030	.5905	.8540	-.0596	-.1622	-.0042	-.0129	0.0000
19.	228.	-.8	16.07	.1040	.5916	.1510	.0299	-.0995	.0004	.0007	.0010
20.	229.	-.8	4.07	.0520	.2984	.1380	.0362	-.1018	.0014	.0008	-.0060

RUN	TEST POINT	$\alpha$	q	MACH	Rn <sub>mac</sub> ( $\times 10^{-6}$ )	CN	CA	CM	Cn	Ci	Cy
20.	230.	1.2	4.06	.0520	.2978	.2450	.0319	-.1116	-.0007	-.0062	-.0030
20.	231.	3.2	4.07	.0520	.2986	.3290	.0262	-.1204	-.0030	-.0126	-.0020
20.	232.	5.2	4.05	.0520	.2981	.4190	.0195	-.1291	-.0054	-.0200	-.0030
20.	233.	7.3	4.07	.0520	.2977	.5000	.0091	-.1335	-.0076	-.0265	-.0020
20.	234.	9.3	4.06	.0520	.2980	.5810	-.0021	-.1409	-.0099	-.0330	-.0020
20.	235.	11.3	4.05	.0520	.2977	.6680	-.0149	-.1492	-.0128	-.0399	-.0050
20.	236.	13.3	4.05	.0520	.2980	.7480	-.0253	-.1495	-.0154	-.0465	-.0030
20.	237.	15.3	4.05	.0520	.2977	.8440	-.0353	-.1559	-.0190	-.0526	-.0020
20.	238.	-.8	4.06	.0520	.2976	.1440	.0358	-.0996	.0022	.0006	-.0070
21.	239.	-.8	4.12	.0520	.3001	-.0880	.0328	.0034	.0027	0.0000	-.0060
21.	240.	1.2	4.12	.0520	.3009	.0110	.0291	-.0064	.0014	-.0062	-.0070
21.	241.	3.3	4.10	.0520	.3002	.1050	.0237	-.0165	-.0011	-.0130	-.0040
21.	242.	5.3	4.12	.0520	.3006	.1920	.0180	-.0268	-.0035	-.0199	-.0040
21.	243.	7.3	4.11	.0520	.3002	.2810	.0098	-.0342	-.0060	-.0265	.0020
21.	244.	9.3	4.11	.0520	.3004	.3700	-.0011	-.0427	-.0086	-.0337	.0010
21.	245.	11.3	4.09	.0520	.3001	.4580	-.0151	-.0491	-.0116	-.0405	.0010
21.	246.	13.3	4.10	.0520	.2999	.5430	-.0277	-.0580	-.0143	-.0467	.0020
21.	247.	15.3	4.11	.0520	.2999	.6370	-.0398	-.0652	-.0172	-.0524	-.0010
21.	248.	-.8	4.12	.0520	.3005	-.0830	.0327	.0007	.0041	.0009	-.0080
22.	249.	-.8	16.08	.1040	.5933	-.0950	.0297	.0033	.0026	-.0001	-.0040
22.	250.	1.2	16.12	.1040	.5929	.0080	.0232	-.0060	.0020	-.0008	-.0040
22.	251.	3.3	16.15	.1040	.5936	.1050	.0158	-.0145	.0011	-.0027	-.0020
22.	252.	5.3	16.10	.1040	.5926	.1910	.0076	-.0246	.0002	-.0050	-.0020
22.	253.	7.3	16.11	.1040	.5926	.2760	-.0021	-.0346	-.0006	-.0063	-.0020
22.	254.	9.3	16.13	.1040	.5929	.3660	-.0154	-.0442	-.0015	-.0075	0.0000
22.	255.	11.3	16.11	.1040	.5921	.4520	-.0305	-.0543	-.0020	-.0090	0.0000
22.	256.	13.3	16.10	.1040	.5921	.5400	-.0451	-.0617	-.0024	-.0107	-.0020
22.	257.	15.3	16.05	.1030	.5911	.6350	-.0596	-.0689	-.0036	-.0127	-.0010
22.	258.	-.8	16.14	.1040	.5929	-.0900	.0290	.0016	.0039	-.0001	-.0080
23.	259.	-.8	4.13	.0520	.3006	-.0900	.0357	-.0004	.0025	.0006	-.0050
23.	260.	1.2	4.11	.0520	.3003	.0070	.0313	-.0079	.0007	-.0062	-.0040
23.	261.	3.3	4.10	.0520	.3002	.1020	.0253	-.0162	-.0017	-.0125	-.0030

RUN	TEST POINT	$\alpha$	q	MACH	Rn <sub>mac</sub> (x 10 <sup>-6</sup> )	C <sub>N</sub>	C <sub>A</sub>	C <sub>M</sub>	C <sub>n</sub>	C <sub>l</sub>	C <sub>y</sub>
23.	262.	5.3	4.10	.0520	.3002	.1910	.0193	-.0246	-.0040	-.0196	0.0000
23.	263.	7.3	4.13	.0520	.3011	.2810	.0120	-.0352	-.0065	-.0261	.0030
23.	264.	9.3	4.12	.0520	.3005	.3640	.0024	-.0440	-.0093	-.0331	.0020
23.	265.	11.3	4.12	.0520	.3005	.4490	-.0097	-.0499	-.0122	-.0408	.0020
23.	266.	13.3	4.09	.0520	.2995	.5440	-.0233	-.0572	-.0152	-.0458	.0030
23.	267.	15.3	4.11	.0520	.3002	.6240	-.0449	-.0635	-.0175	-.0496	.0020
23.	268.	-.8	4.09	.0520	.2998	-.0890	.0363	-.0035	.0031	.0010	-.0050
24.	269.	-.8	15.94	.1030	.5904	-.0980	.0331	-.0004	.0023	.0006	-.0030
24.	270.	1.2	15.99	.1030	.5907	-.0040	.0260	-.0085	.0013	-.0013	-.0020
24.	271.	3.3	16.05	.1030	.5917	.0640	.0203	-.0143	.0009	-.0022	-.0030
24.	272.	5.3	16.08	.1040	.5917	.1860	.0092	-.0270	-.0002	-.0044	.0010
24.	273.	7.3	16.08	.1040	.5923	.2810	-.0015	-.0362	-.0010	-.0058	.0010
24.	274.	9.3	16.05	.1030	.5915	.3710	-.0132	-.0469	-.0018	-.0074	.0010
24.	275.	11.3	16.04	.1030	.5914	.4510	-.0256	-.0542	-.0020	-.0091	.0020
24.	276.	13.3	16.05	.1030	.5913	.5430	-.0406	-.0640	-.0032	-.0109	.0010
24.	277.	15.3	16.00	.1030	.5906	.6330	-.0583	-.0727	-.0037	-.0129	.0020
24.	278.	-.8	16.05	.1030	.5911	-.0970	.0328	-.0025	.0029	.0006	-.0050
25.	279.	-.8	16.05	.1040	.6009	-.0980	.0332	-.0014	.0026	0.0000	-.0040
25.	280.	1.2	16.07	.1040	.6017	.0030	.0261	-.0114	.0016	-.0013	-.0040
25.	281.	3.3	16.06	.1040	.6010	.0970	.0180	-.0195	.0009	-.0035	-.0020
25.	282.	5.3	16.06	.1040	.6010	.1840	.0099	-.0277	.0004	-.0039	-.0040
25.	283.	7.3	16.06	.1040	.6005	.2730	-.0001	-.0392	-.0005	-.0062	-.0020
25.	284.	9.3	16.04	.1040	.6002	.3710	-.0126	-.0489	-.0010	-.0079	-.0020
25.	285.	11.3	16.03	.1040	.5996	.4560	-.0256	-.0568	-.0015	-.0092	-.0020
25.	286.	13.3	16.03	.1040	.5997	.5460	-.0404	-.0674	-.0024	-.0109	-.0020
25.	287.	15.3	16.04	.1040	.5995	.6340	-.0577	-.0758	-.0027	-.0127	0.0000
25.	288.	-.8	16.06	.1040	.6001	-.0980	.0332	-.0034	.0031	.0007	-.0060
26.	289.	-.8	8.08	.0740	.4258	-.0910	.0354	-.0053	.0034	.0004	-.0070
26.	290.	1.2	8.06	.0740	.4256	.0060	.0287	-.0128	.0021	-.0024	-.0050
26.	291.	3.3	8.06	.0740	.4252	.0940	.0217	-.0211	.0008	-.0062	-.0040
26.	292.	5.3	8.06	.0740	.4254	.1920	.0137	-.0308	-.0006	-.0096	-.0040
26.	293.	7.3	8.06	.0740	.4250	.2760	.0060	-.0396	-.0020	-.0128	-.0030

RUN	TEST POINT	$\alpha$	q	MACH	Rn <sub>mac</sub> (x 10 <sup>-6</sup> )	C <sub>N</sub>	C <sub>A</sub>	C <sub>M</sub>	C <sub>n</sub>	C <sub>l</sub>	C <sub>y</sub>
26.	294.	9.3	8.05	.0740	.4251	.3700	-.0056	-.0487	-.0033	-.0164	-.0030
26.	295.	9.3	8.08	.0740	.4259	.3710	-.0061	-.0499	-.0029	-.0161	-.0010
26.	296.	11.3	8.06	.0740	.4257	.4540	-.0184	-.0566	-.0049	-.0203	-.0030
26.	297.	13.3	8.04	.0740	.4249	.5470	-.0329	-.0656	-.0063	-.0227	0.0000
26.	298.	15.3	8.05	.0740	.4249	.6310	-.0493	-.0734	-.0083	-.0260	-.0020
26.	299.	-.8	8.07	.0740	.4254	-.0900	.0343	-.0064	.0042	.0001	-.0080
27.	300.	-.8	16.05	.1040	.5996	-.1020	.0332	-.0018	.0027	.0007	-.0060
27.	301.	1.2	16.06	.1040	.5997	.0050	.0254	-.0106	.0021	-.0007	-.0040
27.	302.	3.3	16.10	.1050	.6001	.0910	.0181	-.0187	.0011	-.0029	-.0020
27.	303.	5.3	16.10	.1050	.6008	.1870	.0091	-.0291	.0005	-.0040	-.0040
27.	304.	7.3	16.12	.1050	.6004	.2780	-.0010	-.0389	-.0003	-.0060	-.0030
27.	305.	9.3	16.10	.1050	.6004	.3690	-.0127	-.0496	-.0008	-.0075	-.0020
27.	306.	11.3	16.07	.1040	.5995	.4560	-.0259	-.0568	-.0014	-.0096	-.0020
27.	307.	13.3	16.09	.1050	.5996	.5480	-.0413	-.0677	-.0021	-.0107	-.0020
27.	309.	-.8	16.07	.1040	.5992	-.0920	.0325	.0109	.0003	.0001	-.0080
28.	310.	-.8	4.08	.0530	.3025	-.0870	.0370	-.0118	.0053	.0010	-.0150
28.	311.	1.2	4.09	.0530	.3027	.0130	.0316	-.0187	.0034	-.0060	-.0130
28.	312.	3.3	4.10	.0530	.3032	.1090	.0253	-.0261	.0012	-.0125	-.0100
28.	313.	5.3	4.08	.0530	.3025	.2010	.0195	-.0359	-.0013	-.0197	-.0120
28.	314.	7.3	4.07	.0530	.3026	.2920	.0119	-.0457	-.0042	-.0259	-.0080
28.	315.	9.3	4.08	.0530	.3027	.3760	.0030	-.0525	-.0065	-.0332	-.0080
28.	316.	11.3	4.09	.0530	.3030	.4480	-.0080	-.0578	-.0092	-.0402	-.0080
28.	317.	13.3	4.07	.0530	.3027	.5440	-.0215	-.0672	-.0126	-.0457	-.0050
28.	318.	15.3	4.08	.0530	.3021	.6290	-.0351	-.0751	-.0163	-.0523	-.0080
28.	319.	-.8	4.09	.0530	.3030	-.0880	.0359	-.0126	.0054	.0009	-.0130
29.	320.	-.8	4.09	.0530	.3032	.1470	.0360	-.1010	-.0003	.0007	0.0000
29.	321.	1.2	4.10	.0530	.3037	.2360	.0323	-.1104	-.0020	-.0064	-.0010
29.	322.	3.2	4.08	.0530	.3032	.3350	.0264	-.1212	-.0038	-.0125	-.0010
29.	323.	5.2	4.11	.0530	.3043	.4230	.0187	-.1296	-.0058	-.0193	0.0000
29.	324.	7.3	4.10	.0530	.3043	.5010	.0103	-.1356	-.0076	-.0261	-.0020
29.	325.	9.3	4.10	.0530	.3036	.5860	-.0008	-.1456	-.0096	-.0322	-.0010
29.	326.	11.3	4.10	.0530	.3038	.6690	-.0121	-.1523	-.0131	-.0401	0.0000

RUN	TEST POINT	$\alpha$	$q$	MACH	$Rn_{mac}$ ( $\times 10^{-6}$ )	$C_N$	$C_A$	$C_M$	$C_n$	$C_l$	$C_y$
29.	327.	13.3	4.09	.0530	.3032	.6380	.2239	-.1413	.0056	-.1100	.0020
29.	328.	15.3	4.09	.0530	.3033	.8520	-.0372	-.1639	-.0187	-.0507	-.0010
29.	329.	-.8	4.09	.0530	.3034	.1470	.0372	-.1070	.0013	.0005	-.0030
30.	330.	-.8	8.05	.0740	.4254	.1440	.0335	-.1056	.0007	.0013	-.0020
30.	331.	1.2	8.08	.0740	.4263	.2390	.0279	-.1128	-.0006	-.0030	0.0000
30.	332.	3.2	8.08	.0740	.4261	.3380	.0203	-.1246	-.0014	-.0049	0.0000
30.	333.	5.2	8.08	.0740	.4261	.4260	.0111	-.1340	-.0023	-.0089	-.0020
30.	334.	7.3	8.08	.0740	.4260	.5110	.0012	-.1399	-.0034	-.0121	0.0000
30.	335.	9.3	8.08	.0740	.4258	.5960	-.0107	-.1509	-.0045	-.0154	0.0000
30.	336.	11.3	8.06	.0740	.4256	.6800	-.0239	-.1567	-.0058	-.0189	-.0020
30.	337.	13.3	8.07	.0740	.4258	.7660	-.0379	-.1618	-.0072	-.0214	-.0010
30.	338.	15.3	8.06	.0740	.4254	.8510	-.0506	-.1678	-.0088	-.0244	-.0040
30.	339.	-.8	8.08	.0740	.4255	.1490	.0335	-.1062	.0009	.0008	-.0020
31.	340.	-.8	16.11	.1050	.6005	.1440	.0317	-.1076	.0016	.0008	-.0020
31.	341.	1.2	16.12	.1050	.6005	.2440	.0245	-.1175	.0009	-.0005	-.0020
31.	342.	3.2	16.11	.1050	.6005	.3400	.0164	-.1289	.0003	-.0018	-.0020
31.	343.	5.2	16.12	.1050	.6004	.4340	.0063	-.1380	.0001	-.0037	-.0030
31.	344.	7.3	16.09	.1050	.6000	.5170	-.0043	-.1467	-.0003	-.0053	-.0040
31.	345.	9.3	16.11	.1050	.6001	.6030	-.0176	-.1578	-.0004	-.0070	-.0040
31.	346.	11.3	16.08	.1050	.5994	.6890	-.0319	-.1629	-.0013	-.0085	-.0040
31.	347.	13.3	16.05	.1040	.5988	.7730	-.0457	-.1687	-.0022	-.0102	-.0010
31.	348.	15.3	16.03	.1040	.5985	.8590	-.0595	-.1718	-.0026	-.0114	-.0060
31.	349.	-.8	16.10	.1050	.5995	.1470	.0317	-.1080	.0013	.0006	-.0020
32.	350.	-.8	4.09	.0530	.3022	.1690	.0260	-.0738	-.0022	.0015	.0090
32.	351.	1.2	4.12	.0530	.3041	.2670	.0260	-.0914	-.0041	-.0054	.0080
32.	352.	3.3	4.12	.0530	.3048	.3560	.0243	-.1009	-.0058	-.0115	.0090
32.	353.	5.3	4.11	.0530	.3043	.4550	.0239	-.1117	-.0080	-.0183	.0080
32.	354.	7.3	4.09	.0530	.3038	.5590	.0232	-.1191	-.0098	-.0256	.0090
32.	355.	9.3	4.10	.0530	.3039	.6610	.0235	-.1243	-.0121	-.0336	.0070
32.	356.	11.3	4.09	.0530	.3037	.7660	.0226	-.1278	-.0148	-.0367	.0090
32.	357.	13.3	4.09	.0530	.3039	.8530	.0224	-.1230	-.0171	-.0428	.0050
32.	358.	15.3	4.09	.0530	.3036	.9360	.0231	-.1207	-.0200	-.0500	.0040



RUN	TEST POINT	$\alpha$	q	MACH	$Rn_{mac}$ ( $\times 10^{-6}$ )	$C_N$	$C_A$	$C_M$	$C_n$	$C_l$	$C_y$
32.	359.	-.8	4.11	.0530	.3039	.1710	.0260	-.0821	-.0003	.0015	.0050
33.	360.	-.8	8.09	.0740	.4263	.1900	.0230	-.0935	-.0007	.0012	.0040
33.	361.	1.2	8.11	.0740	.4272	.2770	.0211	-.0997	-.0016	-.0016	.0050
33.	362.	3.2	8.11	.0740	.4268	.3590	.0190	-.1083	-.0028	-.0058	.0030
33.	363.	5.3	8.11	.0740	.4265	.4580	.0166	-.1181	-.0035	-.0086	.0030
33.	364.	7.3	8.10	.0740	.4263	.5590	.0147	-.1251	-.0047	-.0129	.0040
33.	365.	9.3	8.08	.0740	.4260	.6700	.0130	-.1314	-.0061	-.0174	.0040
33.	366.	11.3	8.06	.0740	.4254	.7720	.0112	-.1316	-.0071	-.0173	.0040
33.	367.	13.3	8.05	.0740	.4251	.8550	.0100	-.1263	-.0085	-.0204	.0010
33.	368.	15.3	8.05	.0740	.4249	.9340	.0098	-.1225	-.0099	-.0236	.0020
33.	369.	-.8	8.11	.0740	.4262	.1910	.0227	-.0946	-.0005	.0016	.0030
34.	370.	-.8	16.09	.1050	.6003	.1920	.0206	-.0968	.0007	.0010	.0010
34.	371.	1.2	16.12	.1050	.6006	.2760	.0188	-.1046	0.0000	-.0003	.0010
34.	372.	3.2	16.14	.1050	.6009	.3690	.0151	-.1156	.0002	-.0020	-.0020
34.	373.	5.3	16.14	.1050	.6000	.4700	.0125	-.1256	-.0002	-.0038	-.0030
34.	374.	7.3	16.10	.1050	.5996	.5730	.0099	-.1329	-.0011	-.0065	0.0000
34.	375.	9.3	16.08	.1050	.5987	.6800	.0070	-.1397	-.0019	-.0082	-.0010
34.	376.	11.3	16.07	.1040	.5988	.7750	.0043	-.1370	-.0023	-.0064	0.0000
34.	377.	13.3	16.06	.1040	.5982	.8550	.0032	-.1273	-.0029	-.0089	0.0000
34.	378.	15.4	16.02	.1040	.5977	.9500	.0018	-.1276	-.0042	-.0115	0.0000
34.	379.	-.8	16.12	.1050	.5998	.1950	.0205	-.0982	.0004	.0013	0.0000
35.	380.	-.8	4.10	.0530	.3031	-.0340	.0165	.0074	.0032	.0012	-.0070
35.	381.	1.3	4.14	.0530	.3044	.0410	.0184	.0017	.0013	-.0067	-.0060
35.	382.	3.3	4.12	.0530	.3045	.1280	.0191	-.0055	-.0007	-.0123	-.0060
35.	383.	5.3	4.12	.0530	.3044	.2180	.0183	-.0151	-.0031	-.0193	-.0040
35.	384.	7.3	4.10	.0530	.3038	.3210	.0178	-.0234	-.0060	-.0258	-.0040
35.	385.	9.3	4.11	.0530	.3037	.4260	.0165	-.0320	-.0086	-.0336	-.0010
35.	386.	11.3	4.11	.0530	.3039	.5260	.0144	-.0359	-.0112	-.0379	-.0020
35.	387.	13.3	4.10	.0530	.3034	.6260	.0134	-.0408	-.0144	-.0439	-.0040
35.	388.	15.3	4.11	.0530	.3037	.7120	-.0184	-.0378	-.0151	-.0431	-.0060
35.	389.	-.8	4.10	.0530	.3036	-.0420	.0168	.0084	.0038	.0011	-.0070

RUN	TEST POINT	$\alpha$	$q$	MACH	$Rn_{mac}$ ( $\times 10^{-6}$ )	CN	$C_A$	$C_M$	$C_n$	$C_l$	$C_y$
36.	390.	- .8	8.09	.0740	.4263	-.0500	.0147	.0095	.0031	.0006	-.0060
36.	391.	1.3	8.11	.0740	.4263	.0420	.0154	.0026	.0020	-.0027	-.0050
36.	392.	3.3	8.10	.0740	.4261	.1240	.0144	-.0050	.0007	-.0059	-.0050
36.	393.	5.3	8.09	.0740	.4262	.2140	.0122	-.0156	-.0007	-.0094	-.0040
36.	394.	7.3	8.10	.0740	.4264	.3190	.0097	-.0232	-.0020	-.0118	-.0030
36.	395.	9.3	8.09	.0740	.4259	.4270	.0075	-.0311	-.0034	-.0174	0.0000
36.	396.	11.3	8.09	.0740	.4258	.5260	.0051	-.0369	-.0051	-.0188	-.0030
36.	397.	13.3	8.06	.0740	.4249	.6290	.0018	-.0381	-.0062	-.0213	-.0030
36.	398.	15.3	8.06	.0740	.4248	.7160	.0510	-.0374	-.0086	-.0315	-.0040
36.	399.	- .8	8.09	.0740	.4260	-.0430	.0143	.0085	.0037	.0008	-.0060
37.	400.	- .8	16.04	.1040	.5987	-.0540	.0143	.0110	.0032	.0008	-.0060
37.	401.	1.3	16.07	.1040	.5988	.0350	.0139	.0025	.0023	-.0011	-.0050
37.	402.	3.3	16.06	.1040	.5989	.1220	.0114	-.0047	.0017	-.0026	-.0040
37.	403.	5.3	16.05	.1040	.5983	.2160	.0082	-.0139	.0007	-.0048	-.0040
37.	404.	7.3	16.06	.1040	.5985	.3140	.0053	-.0235	0.0000	-.0054	-.0020
37.	405.	9.3	16.06	.1040	.5984	.4240	.0023	-.0317	-.0010	-.0084	-.0030
37.	406.	11.3	16.02	.1040	.5975	.5330	-.0012	-.0378	-.0017	-.0095	-.0040
37.	407.	13.4	16.01	.1040	.5973	.6310	-.0048	-.0374	-.0019	-.0100	-.0040
37.	408.	15.4	16.01	.1040	.5976	.7190	-.0073	-.0388	-.0027	-.0125	-.0060
37.	409.	- .8	16.05	.1040	.5977	-.0480	.0140	.0102	.0036	.0004	-.0080
38.	410.	- .8	4.08	.0530	.3017	-.0890	.0346	-.0015	.0015	-.0002	-.0030
38.	411.	1.2	4.10	.0530	.3027	-.0010	.0322	-.0079	0.0000	-.0065	0.0000
38.	412.	3.3	4.10	.0530	.3034	.1030	.0253	-.0173	-.0020	-.0125	0.0000
38.	413.	5.3	4.10	.0530	.3033	.1920	.0200	-.0268	-.0048	-.0196	.0020
38.	414.	7.3	4.11	.0530	.3035	.2770	.0134	-.0347	-.0071	-.0254	.0020
38.	415.	9.3	4.11	.0530	.3038	.3660	.0039	-.0432	-.0100	-.0328	.0030
38.	416.	11.3	4.11	.0530	.3034	.4480	-.0078	-.0498	-.0121	-.0391	.0040
38.	417.	13.3	4.10	.0530	.3031	.5400	-.0201	-.0597	-.0156	-.0446	.0060
38.	418.	15.3	4.10	.0530	.3034	.6220	-.0321	-.0652	-.0186	-.0508	.0020
38.	419.	- .8	4.09	.0530	.3029	-.0920	.0357	-.0031	.0031	.0004	-.0030
39.	420.	- .8	8.08	.0740	.4254	-.0980	.0343	-.0014	.0022	.0005	-.0030
39.	421.	1.2	8.09	.0740	.4259	0.0000	.0282	-.0090	.0013	-.0027	-.0020

RUN	TEST POINT	$\alpha$	q	MACH	Rn <sub>mac</sub> (x 10 <sup>-6</sup> )	C <sub>N</sub>	C <sub>A</sub>	C <sub>M</sub>	C <sub>n</sub>	C <sub>l</sub>	C <sub>y</sub>
39.	422.	3.3	8.09	.0740	.4256	.0980	.0209	-.0176	-.0002	-.0057	-.0020
39.	423.	5.3	8.08	.0740	.4257	.1870	.0138	-.0261	-.0017	-.0094	.0020
39.	424.	7.3	8.10	.0740	.4260	.2730	.0054	-.0352	-.0033	-.0118	.0010
39.	425.	9.3	8.06	.0740	.4250	.3650	-.0059	-.0441	-.0052	-.0161	.0030
39.	426.	11.3	8.07	.0740	.4253	.4490	-.0181	-.0519	-.0064	-.0202	.0040
39.	427.	13.3	8.08	.0740	.4253	.5430	-.0326	-.0610	-.0081	-.0220	.0020
39.	428.	15.3	8.06	.0740	.4251	.6250	-.0472	-.0676	-.0095	-.0263	.0020
39.	429.	-.8	8.09	.0740	.4257	-.0990	.0345	-.0032	.0028	.0004	-.0050
40.	430.	-.8	16.06	.1040	.5986	-.1050	.0332	-.0005	.0022	.0007	-.0030
40.	431.	1.2	16.06	.1040	.5988	-.0010	.0257	-.0089	.0016	-.0012	-.0020
40.	432.	3.3	16.05	.1040	.5985	.0930	.0179	-.0180	.0008	-.0024	-.0030
40.	433.	5.3	16.06	.1040	.5983	.1820	.0094	-.0265	0.0000	-.0039	-.0010
40.	434.	7.3	16.09	.1050	.5985	.2730	-.0014	-.0362	-.0010	-.0058	-.0010
40.	435.	9.3	16.08	.1040	.5984	.3610	-.0128	-.0466	-.0020	-.0074	-.0020
40.	436.	11.3	16.09	.1050	.5984	.4450	-.0257	-.0554	-.0029	-.0099	.0010
40.	437.	13.3	16.02	.1040	.5972	.5440	-.0416	-.0642	-.0034	-.0113	.0020
40.	438.	15.3	16.04	.1040	.5977	.6300	-.0573	-.0703	-.0038	-.0133	.0020
40.	439.	-.8	16.05	.1040	.5978	-.1010	.0329	-.0020	.0029	.0008	-.0050



# Report Documentation Page

1. Report No. NASA CR-181684		2. Government Accession No.		3. Recipient's Catalog No.	
4. Title and Subtitle A Low Speed Wind Tunnel Investigation of Reynolds Number Effects on a 60-Deg. Swept Wing Configuration with Leading and Trailing Edge Flaps			5. Report Date August 1988		
			6. Performing Organization Code		
7. Author(s) Dhanvada M. Rao and Keith D. Hoffler			8. Performing Organization Report No.		
			10. Work Unit No. 505-61-71-05		
9. Performing Organization Name and Address Vigyan Research Associates, Inc. 30 Research Drive Hampton, VA 23666-1325			11. Contract or Grant No. NAS1-17919		
			13. Type of Report and Period Covered Contractor Report		
12. Sponsoring Agency Name and Address National Aeronautics and Space Administration Langley Research Center Hampton, VA 23665-5225			14. Sponsoring Agency Code		
			15. Supplementary Notes Langley Technical Monitor - William J. Small		
16. Abstract <p>A low-speed wind tunnel test was performed to investigate Reynolds number effects on the aerodynamic characteristics of a supersonic cruise wing concept model with a 60 deg. swept wing incorporating leading-edge and trailing edge flap deflections. The Reynolds number ranged from <math>0.3 \times 10^6</math> to <math>1.6 \times 10^6</math>, and corresponding Mach numbers from .05 to 0.3. The objective was to define a threshold Reynolds number above which the flap aerodynamics basically remained unchanged, and also to generate a data base useful for validating theoretical predictions of the Reynolds number effects on flap performance. This report documents the test procedures used and the basic data acquired in the investigation.</p>					
17. Key Words (Suggested by Author(s)) Reynolds number effects Wing flap effectiveness Flow separation Low speed aerodynamics			18. Distribution Statement Unclassified - Unlimited  Subject Category 02		
19. Security Classif. (of this report) Unclassified		20. Security Classif. (of this page) Unclassified		21. No. of pages 67	22. Price A04

**End of Document**